Universitat de Girona

ANALYSIS OF CREEP CRACK GROWTH IN ADHESIVELY BONDED JOINTS UNDER MODE I LOADING

Edwin Meulman

Universitat de Girona

Doctoral Thesis

Analysis of Creep Crack Growth in Adhesively Bonded Joints under Mode I Loading

Edwin Meulman

2023

Universitat de Girona

Doctoral Thesis

Analysis of Creep Crack Growth in Adhesively Bonded Joints under Mode I Loading

Edwin Meulman

2023
Doctoral Program in Technology

Supervised by:

Dr. Jordi Renart Canalias

Dr. Laura Carreras Blasco

Dr. Javier Zurbitu González

Tutor:

Josep Costa Balanzat

Thesis submitted to the University of Girona for the degree of Doctor

Publications

The presented thesis is a compendium of articles listed below:

Peer-reviewed journal articles

- Article 1:

  E. Meulman, J. Renart, L. Carreras, and J. Zurbitu, “Analysis of mode I fracture toughness of adhesively bonded joints by a low friction roller wedge driven quasi-static test” *Engineering Fracture Mechanics*, vol. 271, no. May, 108619, 2022, doi: 10.1016/j.engfracmech.2022.108619

  ISSN: 0013-7944, Impact Factor: 4.898, ranked 19/138 in the category of Mechanics (1st quartile)[1]

- Article 2:

  E. Meulman, J. Renart, L. Carreras, and J. Zurbitu, “A methodology for the experimental characterization of energy release rate-controlled creep crack growth under mode I loading” *Engineering Fracture Mechanics*, vol. 283, no. April, 109222, 2023, doi: 10.1016/j.engfracmech.2023.109222

  ISSN: 0013-7944, Impact Factor: 4.898, ranked 19/138 in the category of Mechanics (1st quartile)[1]

- Article 3:

  E. Meulman, J. Renart, L. Carreras, and J. Zurbitu, “Analysis of creep crack growth in bonded joints based on a Paris' law-like approach” Submitted to Engineering Fracture Mechanics, 2023. ISSN: 0013-7944, Impact Factor: 4.898, ranked 19/138 in the category of Mechanics (1st quartile)[1]

[1]According to the 2021 Journal Citation Reports

Conference proceedings and training schools

- **E. Meulman**, J. Renart, L. Carreras, J. Zurbitu, Design of a low friction roller wedge driven quasi-static test, oral presentation, XXI Congreso Internacional de Adhesión y Adhesivos online, 16-17th of November 2021.
- **E. Meulman**, J. Renart, L. Carreras, J. Zurbitu, Design of test methods for mode I testing of adhesively bonded joints, oral presentation, 3-day training school, COST Action CA18120 Reliable roadmap for certification of bonded primary structures, October 17-19, 2022, University of Minho – Guimarães, Portugal.
- **E. Meulman**, J. Renart, L. Carreras, J. Zurbitu, Design of an energy release rate-controlled mode I creep crack growth rate test method for adhesively bonded joints, 14th Adhesion Conference (EURADH) combined with 7th World Congress on Adhesion and Related Phenomena (WCARP). 10-13 September 2023, Garmisch-Partenkirchen/ (Germany). Accepted oral communication.

List of abbreviations

a	crack length
a_0	initial crack length
a_c	corrected crack length
a_e	crack length with exact contact point
B	width of specimen
c	Empirical parameter for the creep crack growth model
C	compliance
d	distance from the initial location of the bonded section
da/dt	crack growth rate
Δ	correction by taking the intercept of $C^{1/3}$ against a
d_{ini}	initial wedge displacement for fracture toughness calculation
d_{lim}	wedge displacement limit
D_w	diameter of the wedge
E_f	back-calculated modulus of the substrate
E_x	longitudinal Young´s modulus
E_y	transversal Young´s modulus
F_{push}	force to push the wedge
$F_{Push\|s}$	force to push the wedge simplified data reduction method
G	energy release rate
G_c	critical energy release rate
G_e	energy release rate with exact contact point
G_{xy}	in-plane shear modulus
h	thickness of the adherend
J	energy release rate with J-integral method
L	specimen length
m	Specimen geometry factor
N	correction to compensate for the stiffness of the DCB bonding blocks
P	opening force
r_w	radius of the wedge
s	Empirical parameter for the creep crack growth model describing the slope
t_a	bondline thickness
T_g	glass transition temperature
w	wedge displacement
δ_y	opening displacement
θ	adherend tip rotation angle
θ_c	adherend tip rotation angle at critical energy release rate
θ_{ini}	adherend initial rotation angle
µ	friction coefficient
χ	crack length correction factor
BK	Benzeggagh and Kenane fracture criterion
CBBM	Compliance Based Beam Method
CZM	Cohesive Zone Model
CBT	Corrected Beam Theory

COF	Coefficient of Friction
DC	Direct Cyclic
DCB	Double Cantilever Beam
ECM	Experimental Compliance Method
FEM	Finite Element Method
LVDT	Linear Variable Displacement Transducer
MMA	Methyl Methacrylate
RWD	Roller Wedge Driven
RWDC	RWD creep crack growth
TDCB	Tapered Double Cantilever Beam
VCCT	Virtual Crack Closure Technique
WDT	Wedge Driven Test
WDT+	Wedge Driven Test simplified data reduction method

Acknowledgements

First, I would like to express my deepest gratitude to Jordi Renart, Laura Carreras and Javier Zurbitu for their support during the PhD project. A team can achieve more than an individual and I always felt that I was part of a great team. I am very grateful for the time and energy they have spent to guide me through the project and sharing their knowledge and expertise with me.

Secondly, I would like to thank to the staff members of the AMADE laboratory for their support with all the experimental tests of this project. A special thanks to Daniel Piedrafita and Ivan Recio, who always did whatever they could to fulfil my requests and, if something was not possible, then helping me to find a good alternative.

Thirdly, I am grateful for AMADE giving me the opportunity to do this interesting PhD project in such a nice work environment. The main part of the great work environment is created by all colleagues of AMADE. I want to thank them for the good and enjoyable time I had during the PhD project.

And last but not least, I would like to thank all my friends and family for their unconditional support during the last years. Talking with them about the common struggles of the PhD life helped me a lot to pass through some challenging moments and to always stay positive.

Universitat de Girona

Dr. Jordi Renart Canalias, of University of Girona, Dr. Laura Carreras Blasco, of the University of Girona, and Dr. Javier Zurbitu González, of Ikerlan Technology Research Centre, Basque Research and Technology Alliance (BRTA).

I/we declare:

That the thesis titles Analysis of Creep Crack Growth in Adhesively Bonded Joints under Mode I Loading, presented by Edwin Meulman to obtain a doctoral degree, has been completed under my supervision.

For all intents and purposes, I hereby sign this document.

Girona, 24-07-2023

Jordi Renart Canalias

Laura Carreras Blasco

Javier Zurbitu González

Contents

1. Introduction 1
   1.1. Background 1
   1.2. Literature review 2
      1.2.1. Durability of bonded joints 2
      1.2.2. Creep crack growth 4
      1.2.3. Creep crack growth test methods 5
      1.2.4. Creep crack growth numerical models 9
   1.3. Motivation 10
   1.4. Objectives 12
   1.5. Thesis layout 12
2. Analysis of mode I fracture toughness of adhesively bonded joints by a low friction roller wedge driven quasi-static test 14
3. A methodology for the experimental characterization of energy release rate-controlled creep crack growth under mode I loading 36
4. Analysis of creep crack growth in bonded joints based on a Paris' law-like approach 50
5. General results and discussion 87
   5.1. A Low friction roller wedge test 87
   5.2. Creep crack growth 91
   5.3. Creep crack growth models 94
6. Concluding remarks 100
   6.1. Conclusions 100
   6.2. Perspectives and future work 102

References 106

List of Figures

Figure 1-1: example of bonded parts in Airbus A380 (left) and a car (right) [4], [5] 2

Figure 1-2. DCB test on a bonded joint with two inclinometers attached to the loading block of each adherend [43]. 6

Figure 1-3. Left: wedge driven test (WDT) [43]. Right: schematic view of WDT [46]. 7

Figure 1-4: Wedge test ASTM D-3762 [50]. 8

Figure 2-1: Top left: RWD test setup. Top right: Roller wedge inserted in specimen. Bottom left: Sketch of roller wedge design with three rollers. Bottom right: Side view sketch of wedge where the middle roller and the two outer rollers have an offset of 0.5 mm (solid red line) from the wedge centre line (black dashed line). 18

Figure 2-2: RWD manual test setup configuration with a threaded bar that pushes the loading beam of the wedge down when rotated with a spanner. 19

Figure 2-3: Specimen geometry, top: for RWD test, bottom: for DCB test including two blocks with holes to attach the specimen to the test machine. Only the two holes in the block closest to the adherends are used to make the block function as a hinge. The second hole is only there so the blocks can be re-used for another DCB test. 21

Figure 2-4: Force-displacement curves of DCB specimens. 23

Figure 2-5: Energy release rate vs. opening displacement of DCB specimens determined with the DCB J-integral method. 23

Figure 2-6: Energy release rate vs. opening displacement of DCB specimens determined with the CBT method. 23

Figure 2-7: Comparison of DCB J-integral and CBT method. Specimens on the left were tested at the AMADE laboratory and those on the right at the Ikerlan Technology Research Centre. 24

Figure 2-8: Cohesive fracture surface of specimen DCB_03, to the right of the red line the adhesive fractured during the DCB test, to the left the specimen fractured during the process of splitting the adherends with lab tools to be able to inspect the fracture surface (later not part of the test). 24
Figure 2-9: Force-displacement and G-displacement curves of RWD specimens. 25
Figure 2-10: Specimen RWD_04 as an example of how the d_{ini} and d_{lim} cut-offs determine the range over which the average energy release rate is calculated and is considered as the fracture toughness of the specimen. 26
Figure 2-11: Resistance curves (R-curves) of RWD specimens. 26
Figure 2-12: Energy release rate vs. roller wedge displacement of RWD specimens determined with the RWD J-integral data reduction method. 26
Figure 2-13: Cohesive fracture surface of specimen RWD_01. To the right of the red line the adhesive is fractured with the roller wedge, while to the left of the red line the specimen was fractured post-test by splitting the adherends completely with lab tools to be able to inspect the fracture surface (later not part of the test). 27
Figure 2-14: Force and energy release rate vs. wedge displacement curves of manually loaded RWD specimens. 28
Figure 2-15: Resistance curves (R-curves) of RWD manually loaded specimens. 28
Figure 2-16: Energy release rate vs. roller wedge displacement of RWD manually loaded specimens determined with the RWD J-integral method. 29
Figure 2-17: Displacement-time plot of RWD manual test with the slope indicated, which equals the displacement rate. 29
Figure 2-18: Overview of average fracture toughness (and minimum and maximum values) results for the DCB, RWD and RWD Manual tests when using different data reduction methods (CBT, RWD J-int and RWD force). 30
Figure 2-19: Left: Specimen RWD_02 showing the difference between using the simplified and exact contact point for the RWD force data reduction method. Right: specimen RWD_01 plot of the

numerically solved crack length with the simplified contact point a, for the exact contact point a_e and the corrected crack length a_c. 30

Figure 2-20: Effect of friction parameter μ on the energy release rate G, results from specimen RWD_01 where the RWD J-integral functions as a reference value. 31

Figure 2-21: Sensitivity of RWD J-integral data reduction method compared to RWD force data reduction method with the normalized average angle Θ and force F_{push} plotted against the normalized average calculated J and G..... 32

Figure 2-22: Specimen RWD_03. Left: adherend rotation angle plot with d_{ini} and d_{lim} cut-off displacements indicated with dashed lines. Right: force-displacement plot showing multiple peaks at maximum force before the force declines..... 32

Figure 2-23: Force-displacement curve comparison between the RWD test (RWD_01 to RWD_04) and RWD manual test (RWD-M_01 to RWDM_03) specimens. 33

Figure 2-24: R-curves of the RWD test (RWD_01 to RWD_04) and RWD manual test (RWD-M_01 to RWD-M_03) specimens. 33

Figure 3-1: Left: RWD creep crack growth test where the roller wedge was loaded with a weight. (The Logitech C920 camera for visual measurement is behind Canon 550D camera and not visible in the picture). Right: Sketch of the roller wedge design with three rollers and the offset of the rollers indicated. 40

Figure 3-2: DCB-like specimen geometry for the RWD creep crack growth test with L the specimen length, a_0 the initial crack length and t_a the bondline thickness..... 41

Figure 3-3: Wedge displacement (w) in millimeters against time (t) in hours of specimen RWD-C_03 measured with the visual measurement method. 42

Figure 3-4: Wedge displacement (w) in millimeters against time (t) in hours of specimen RWD-C_02 measured with the visual measurement method and the LVDT. 42

Figure 3-5: Average crack growth rate (da/dt) against normalised energy release rate (G/Gc) on a log–log scale of the visual and LVDT measurement method. Specimens RWD-C_06 to RWD-C_09 are considered to have a da/dt of 0 mm/h and cannot be plotted on the log scale. 44
Figure 3-6: Specimen RWD-C_03, 0: Teflon insert region, 1: Pre-crack region, 2: Creep crack propagation region, 3: Lab tool specimen opening region. 44
Figure 3-7: Fracture surface of specimens RWD-C_01 to 05. With region 1 indicating the fracture surface created with the pre-crack, region 2 the RWD creep crack growth test and region 3 opening the specimen with lab tools to be able to inspect the fracture surface of the specimen. Scratches on the adherends are caused by the lab tools, after the tests were already finished. 45
Figure 3-8: Specimen RWD-C_05 with whitened adhesive ahead of the crack tip. The yellow arrow indicates the distance the whitened area had passed through the adhesive and the red arrow the crack tip. 45
Figure 3-9: Specimen RWD-C_05 pre-cracked visual measurement data of the craze front and the crack tip distance from the initial location of the bonded section (d). 46
Figure 3-10: Specimen RWD-C_05 creep crack growth phase with progressing craze front and crack tip in the adhesive, data normalized with the crack tip distance from the initial location of the bonded section (d). 46
Figure 3-11: Applied normalised energy release rate against the transitory time in hours found for specimens RWD-C_01 to RWD-C_05. 46
Figure 4-1: Test setup of the RWDC test method. The specimen is vertically clamped and loaded with a weight on top of the wedge. 59
Figure 4-2: Example of creep crack growth curve obtained with the RWDC test method in previous work. 60
Figure 4-3: Required input cycle in the DC module of Abaqus to simulate creep crack growth in a bonded joint. 61

Figure 4-4: TDCB constant load test frame and canon cameras to capture the crack propagation over time. The two cardboard boxes below the weights are just there to provide a soft landing for the weights when the specimens fail. 63
Figure 4-5: Example of TDCB specimen with the blue arrow indicating the measurement distance for the calibration of the pixels in the photos and the red arrow the crack length measurement from the tip of the pre-crack. 64
Figure 4-6: TDCB specimen geometry with mm =278 mm-1. 64
Figure 4-7: Energy release rate vs crack length of the three quasi-static TDCB tests. Energy release rate determined with the ECM data reduction method. 66
Figure 4-8: The cohesive fracture surface of specimen TDCB_01. 67
Figure 4-9: Crack length (a) measured in the photos taken during the test of TDCB_CL_02 and plotted against time (t) in hours. The slope of the blue trendline is considered the propagation slope and provides the average creep crack growth rate. 69
Figure 4-10: Crack growth rate (da/dt) against normalised energy release rate (G/Gc) on a log-log scale with the data of the RWDC tests and the results found for the constant load TDCB tests. 70
Figure 4-11: Fracture surface of the TDCB constant load specimens with from left to right increasing load applied 71
Figure 4-12: Creep crack growth rate against normalised energy release rate on a log-log scale with the data of the RWDC tests, constant load TDCB tests and the TDCB FEM model. 72
Figure 4-13: RWDC curve corrected by assuming a friction coefficient of 0.02 in the roller wedge instead of assuming a friction coefficient of zero. 74
Figure 5-1. A roller wedge entered in a specimen with the real and simplified contact points indicated. For a smaller diameter roller, the simplified and real contact point can be considered equal and therefore crack length a can be assumed from the centre of the roller (the simplified contact point). 90

Figure 5-2. example of crazing in Specimen RWD-C_05 with whitened adhesive ahead of the crack tip. The yellow arrow indicates the distance the whitened area had passed through the adhesive and the red arrow the crack tip. [95] (Figure 8 in article of chapter 3). 92

Figure 5-3. Transitory time in hours found for specimens RWD-C_01 to RWD-C_05 against the normalized applied energy release rate [95](Figure 11 in article of chapter 3). 93

Figure 5-4. Wedge displacement (w) in millimeters against time (t) in hours of specimen RWD-C_02 measured with the visual measurement method and the LVDT [95](Figure 4 in article of chapter 3). 94

Figure 5-5: Friction coefficient correction of 0.02 for the roller compared to the zero friction roller wedge results and the TDCB [96] (Figure 13 in article of chapter 4). 96

Figure 5-6. Example from literature where the threshold energy release rate (G_{th}) describes a vertical asymptote, where below no crack growth takes place [15]. 97

Figure 5-7. Creep crack growth rate against normalised energy release rate on a log-log scale with the data of the RWDC tests, constant load TDCB tests and the TDCB FEM model [96] (Figure 12 in article of chapter 4). 99

List of Tables

Table 2-1: Overview of tested specimens. 22

Table 2-2: Overview of average DCB test results. The standard deviations in the column are the standard deviations found for the result of one specimen. The standard deviation in the last row is the standard deviation found when taking the average value for all specimens tested. 25

Table 2-3: Overview of average RWD test results. The standard deviations in the column are the standard deviations found for the result of one specimen. The standard deviation in the last row is the standard deviation found when taking the average value for all specimens tested. 28

Table 2-4: Overview of average RWD manually loaded specimen test results. The standard deviations in the column are the standard deviations found for the result of one specimen. The standard deviation in the last row is the standard deviation found when taking the average value for all specimens tested. 29

Table 3-1: Overview table of tested specimens. 42

Table 3-2: Overview of specimen test data. 43

Table 4-1: Tested specimen overview. 65

Table 4-2: Overview of the three TDCB specimens that are tested quasi-static. 67

Table 4-3: Overview of the four TDCB specimens that are tested with a constant applied load 68

Table 4-4: Overview of the data from the four TDCB FEM simulations. 71

Abstract

Adhesive bonds could replace more traditional mechanical joints, making structures lighter and smoother. Stresses are distributed over a larger area, and dissimilar materials can be bonded, accommodating differences in expansion. These advantages of bonded joints are valuable in industries like automotive and aeronautics, where lightweight and aerodynamic design reduces fuel consumption and service costs.

These days structural designs need to be durable. It is crucial to comprehend the long-term performance of bonded joints to create durable ones and establish proper maintenance protocols. A vital aspect that must be considered in designing a durable bonded joint is viscoelastic creep crack growth and how it impacts the structural integrity. Creep crack growth is one of the factors that could impact the longevity of a bonded joint. However, there is a limited availability of test methods and numerical tools to assess the effects of creep crack growth in bonded joints.

In this work, a method is developed to obtain the average crack growth rate (da/dt) in mode I as a function of the applied energy release rate (G). The method is based on the wedge test, because it has been found as a good candidate to obtain creep crack growth curves of a bonded joint in mode I. Although, the friction between the wedge and the specimen should be considered and reduced to a minimum. A low friction roller wedge is proposed to achieve that, called the Roller Wedge Driven (RWD) test method. Results have shown that the friction of the roller is indeed significantly lower compared to a sliding wedge but cannot be completely neglected in the data reduction to determine the energy release rate.

Making use of the designed roller wedge test setup, a RWD creep crack growth (RWDC) method is developed. The roller wedge is loaded with a deadweight which result in a constant energy release rate at the crack tip of the bonded joint. Applying for each specimen a different energy release rate results in different creep crack growth rates. Plotting the results on a log-log scale will produce creep crack growth curves that can be described by a Paris´ law-like expression.

Based on the obtained creep crack growth curve the Creep Crack Growth Model (CCGM) is proposed and describes the relationship between an applied energy release rate and the expected creep crack growth in a bonded joint. The materials parameters that describe the CCGM are derived directly from the RWDC test results. The proposed model is validated against Tapered DCB (TDCB) specimens that are loaded with a weight. Similar results are obtained for both the RWDC and TDCB constant load methods which confirms that the model indeed describes the relationship between the applied energy release rate and the creep crack growth rate.

It is also demonstrated that the creep crack growth model can be implemented in an existing commercially available finite element method (FEM). A virtual TDCB specimen is defined in Abaqus and the results of the RWDC tests are used to simulate the creep crack growth behaviour of the adhesive. The Direct Cyclic (DC) plus Virtual Crack Closure Technique (VCCT) modules are used to simulate the creep crack growth in the TDCB specimen. FEM results show that the model follows the relationship as described before and that it does so regardless of the geometry of the bonded joint.

When designing durable bonded joints, it is shown that it is essential to keep in mind that relying solely on data from quasi-static testing will likely lead to an overestimation of the bond's durability. Therefore, testing bonded joints for creep crack growth is essential for accurately predicting the durability of a bonded joint. For more complex structures the analysis of bonded joints requires numerical tools. Accurate and reliable creep crack growth experimental methodologies and models are crucial for the development of numerical tools. This is the objective of the present document.

Resum

Les unions adhesives tenen un gran potencial per a substituir les unions mecàniques tradicionals, permetent obtenir estructures continues i reduint-ne el seu pes. En una unió adhesiva, les tensions es reparteixen en una àrea més gran i es poden unir materials dissimilars amb diferents coeficients d'expansió tèrmica. Aquests avantatges tenen un alt valor en indústries com la de l'automoció i l'aeronàutica, on disposar de dissenys més lleugers i aerodinàmics permet reduir el consum de combustible i els costos d'operació.

Actualment, els dissenys estructurals han de ser duradors. Per tant, és crucial comprendre el rendiment de les unions adhesives a llarg termini per crear-ne de més duradores i establir protocols de manteniment adequats. Un aspecte vital per tal que el disseny d'una unió adhesiva sigui duradora és la predicció del creixement d'esquerdes degudes a la fluència del material i quin efecte té en la integritat estructural. El creixement d'esquerdes degudes a la fluència del material és un dels factors que tenen un efecte important en la vida de la unió adhesiva. No obstant, fins ara s'han desenvolupat molt poques eines numèriques i mètodes d'assaig per analitzar la fractura d'unions adhesives per fluència.

En aquest treball s'ha desenvolupat un mètode per obtenir la velocitat de creixement d'esquerda (da/dt) en funció de l'energia disponible per a la fractura (G). El mètode utilitzat és un assaig de propagació d'esquerda mitjançant una cunya, doncs s'ha observat que aquest assaig és un bon candidat per obtenir corbes de creixement d'esquerda en assaigs de fluència en mode I d'unions adhesives. No obstant, cal tenir en compte la fricció entre la cunya i la mostra i reduir-la al mínim. Per fer-ho, es proposa utilitzar un rodament de baixa fricció com a cunya. A aquest assaig se l'ha anomenat assaig d'avanç de cunya amb rodaments forçat, en anglès "roller wedge driven test" i que porta per sigles RWD. Els resultats de l'assaig s'han comparat amb els del mètode estàndard de doble biga en voladís ("double cantilever beam") o DCB. Els resultats han demostrat que la fricció del rodament és significativament menor en comparació amb l'obtingut amb una cunya que llisqui directament sobre

la superfície de l'adherent, tot i que no es pot ignorar completament l'efecte de la fricció en els resultats.

A partir de l'utillatge de cunya amb rodaments ("roller wedge driven", RWD) s'ha desenvolupat un assaig de propagació d'esquerda per càrregues de fluència ("roller wedge driven creep, RWDC). La cunya amb rodaments està carregada amb un pes mort, de manera que s'aplica una energia disponible per a la fractura constant a la punta de l'esquerda de la unió adhesiva. Al repetir l'assaig per varis nivells de carrega, i per tant varis nivells d'energia disponible per a la fractura, s'obtenen diferents valors de velocitat de creixement de l'esquerda. Al representar els resultats en una escala logarítmica s'obtindran corbes de creixement d'esquerda que es poden descriure amb una expressió similar a la llei de Paris. Aquest model de creixement d'esquerdes per fluència ("creep crack growth model", CCGM) s'obté a partir dels resultats dels assajos RWDC. El model s'ha validat amb resultats d'un altre assaig alternatiu de fluència, l'assaig de doble biga en voladís amb proveta de secció variable, ("tappered double cantilever beam", TDCB). S'han obtingut resultats similars per a ambdós mètodes d'assaig, RWDC i TDCB, el que indica que el model proposat descriu correctament la relació entre la taxa d'alliberament d'energia aplicada i la taxa de creixement d'esquerda per fluència.

Es demostra que el model de creixement d'esquerda per càrregues a fluència es pot implementar en un model d'elements finits ("finite element method", FEM) comercial. Per validar la implementació del model s'ha creat un assaig TDCB virtual en el programa Abaqus, i s'ha fet servir la corba de creixement d'esquerda obtinguda dels resultats de l'assaig RWDC. La propagació de l'esquerda s'ha simulat mitjançant el mòdul Direct Cyclic (DC) i el mètode VCCT ("virtual crack closure technique"). Els resultats del model d'elements finits concorden amb les evidències experimentals, i per tant, indiquen que el creixement d'esquerda segueix el model de CCGM, i que ho fa independentment de la geometria de la proveta. Cal esmentar, que el mòdul DC no està dissenyat per a la simulació de fractura

degut a càrregues de fluència i que té algunes petites limitacions pràctiques que probablement es podrien modificar mitjançant la utilització d'un subrutina d'usuari específica.

Pel disseny d'unions adhesives duradores, si es tenen en compte únicament les dades dels assaigs quasi-estàtics s'obtindrà amb tota probabilitat una sobreestimació de la durabilitat de la junta. Per tant, és imprescindible realitzar assaigs de fluència per a poder determinar amb exactitud la durabilitat de la unió. Per al disseny durador d'unions adhesives més complexes cal utilitzar eines numèriques, i per tant, cal desenvolupar models de creixement d'esquerda amb dades de fluència precises i fiables.

Resumen

Las uniones adhesivas tienen un gran potencial para sustituir las uniones mecánicas tradicionales, permitiendo obtener estructuras continuas y de menor peso. Las tensiones se distribuyen sobre una superficie mayor y se pueden unir distintos materiales con diferentes coeficientes de dilatación. Estas ventajas son especialmente valiosas en sectores como la automoción y la aeronáutica, donde un diseño ligero y aerodinámico reduce el consumo de combustible y los costes de mantenimiento.

Hoy en día, los diseños estructurales deben ser duraderos. Por consiguiente, es crucial poder comprender el rendimiento a largo plazo de las uniones adhesivas, y así poder crear uniones duraderas y establecer protocolos de mantenimiento adecuados. Un aspecto muy importante que debe tenerse en cuenta para que el diseño de una unión adhesivas sea duradero es la predicción del crecimiento de grieta debido a la fluencia del material, y que efecto tiene sobre la integridad de la estructura. El crecimiento de grieta por fluencia es uno de los factores que tienen un efecto importante en la vida de la unión adhesiva. Sin embargo, la disponibilidad de herramientas numéricas y métodos de ensayo para evaluar el crecimiento de grietas en uniones adhesivas sometidas a cargas de fluencia es muy limitada.

En este trabajo, se ha desarrollado un método para obtener la velocidad de crecimiento de grieta (da⁄dt) en una unión adhesiva en función de la tasa de liberación de energía (G). El método utilizado es un ensayo de propagación de grieta por cuña, siendo este tipo de ensayo un buen candidato para obtener curvas de crecimiento en ensayos de fluencia en modo I de uniones adhesivas. Sin embargo, en el ensayo de cuña se debe tener en cuenta la fricción entre la cuña y la probeta, y a ser posible reducirla al mínimo. Para conseguirlo, se propone una cuña hecha a partir de rodamientos de baja fricción. A este ensayo se lo ha denominado ensayo de avance forzado de cuña con rodamientos, en inglés “Roller Wedge Driven” (RWD). Los resultados de este ensayo se han comparado con los del ensayo de doble viga en voladizo (“double cantilever beam”, o DCB). Dichos resultados han demostrado que la cuña con rodamientos presenta una fricción significativamente menor que el de

una cuña deslizante. Sin embargo, no puede despreciarse por completo en la reducción de datos para determinar la tasa de liberación de energía.

A partir del utillaje de cuña con rodamientos, se ha desarrollado un ensayo de propagación de grieta por cargas a fluencia ("roller wedge driven creep", RWDC). En este caso, se aplica un peso muerto sobre la cuña, teniendo así una energía disponible para la fractura constante en la punta de la grieta de la unión adhesiva. Al repetir el ensayo para varios niveles de carga, y por consiguiente varios niveles de energía disponible para la fractura, se obtienen diferentes velocidades de crecimiento de grieta por fluencia. Al representar los resultados en una escala logarítmica, se obtienen curvas de crecimiento de grieta por fluencia que se pueden describir mediante una expresión similar a la ley de París. A partir de los resultados del ensayo RWDC se ha obtenido un modelo de crecimiento de grieta por fluencia (CCGM). El modelo se ha validado con resultados de otro ensayo alternativo de fluencia, el ensayo de doble viga en voladizo con probetas de sección variable o "Tapered DCB" (TDCB). Al realizar la comparación, se han obtenido resultados similares para ambos métodos de carga constante RWDC y TDCB, lo que indica que el modelo describe realmente la relación entre la tasa de liberación de energía aplicada y la velocidad de crecimiento de la grieta de fluencia.

Se demuestra que el modelo de crecimiento de grieta por fluencia puede implementarse en un modelo de método de elementos finitos (MEF) comercial. Para validar la implementación, se ha creado un ensayo TDCB virtual mediante el programa de elementos finitos Abaqus, y se ha utilizado la curva de crecimiento de grieta obtenida de los resultados del ensayo RWDC. La propagación de la grieta se ha simulado mediante los módulos Direct Cyclic (DC) y Virtual Crack Closure Technique (VCCT). Los resultados del modelo de elementos finitos muestran también que, efectivamente, el modelo sigue la relación descrita anteriormente y que lo hace independientemente de la geometría de la unión. Debe mencionarse que el módulo DC no está diseñado para la simulación del crecimiento de grietas por fluencia y tiene algunas pequeñas limitaciones prácticas que probablemente podrían modificarse utilizando una subrutina de usuario.

En el diseño de uniones adhesivas duraderas es importante no confiar únicamente en los datos de los ensayos cuasiestáticos, puesto que esto conlleva a una sobreestimación de la durabilidad de la unión. Por lo tanto, para predecir con exactitud la durabilidad de una unión adherida es esencial realizar ensayos de crecimiento de grieta por fluencia. Para el diseño duradero de uniones adheridas más complejas, se deben utilizar herramientas numéricas, lo que requiere el desarrollo de modelos de crecimiento de grieta por fluencia precisos y fiables.

1. Introduction

1.1. Background

An adhesive is a material that is capable to bond two surfaces. One could refer to adhesion as a state in which two bodies are in contact and can transfer load and work. A definition of adhesion can be given by considering the condition where two bodies adhere (macroscopic) or where two phases adhere to each other(microscopic), see for a more profound description “On the Definition of Adhesion” by Good [1]. Adhesives can bond structural and non-structural parts. An adhesive which bonds structural parts should be able to withstand a relatively high stress up to the design limit and needs to be reliable within the designed service life. The main types of synthetic adhesives used in industry for structural bonds are acrylics, epoxies and silicones. The best adhesion is achieved if a chemical bond mechanism like covalent bonds, hydrogen bonds, van der Waals forces or acid-base interactions are present in the adhesive bond [2].

Bonded joints

Structural adhesive bonds are increasingly used in industry as an alternative to mechanical joints [3]. Structural adhesive bonds make the necessity of more traditional fasteners obsolete which, makes the structure lighter, smoother and distributes stresses over a larger area (i.e., stress concentrations are limited). In addition, adhesives make it possible to bond dissimilar materials and accommodate the difference in expansion between the two substrates. Advantages like these are valuable in for instance the aeronautic and automotive industry. Lightness and smoothness related to aerodynamics can significantly reduce the fuel consumption, which will be beneficial for service cost reduction and the climate. Two examples from the aeronautic and automotive industry that use bonded joints are shown in Figure 1-1. The Airbus A380 contains bonded joints, although, bonded joints are still not widespread in the aeronautic industry due to lack of reliability [4].

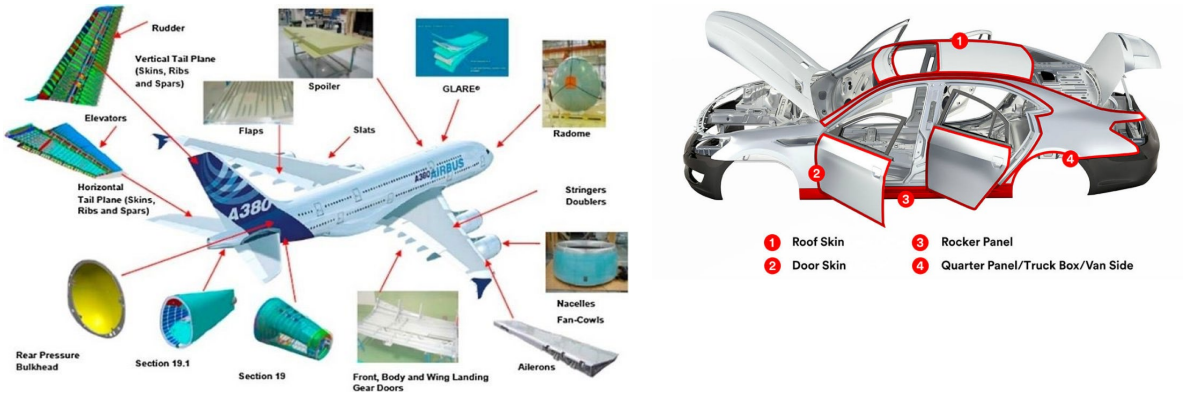

Figure 1-1: example of bonded parts in Airbus A380 (left) and a car (right) [4], [5]

Some disadvantages of using adhesives for structural bonding are limited visual inspection, high-quality surface preparation is required, controlling process parameters is important, characterizing the mechanical properties of the bonded joint is challenging and adhesives are in general environment sensitive. The latter indicates that environmental factors like temperature and humidity have a detrimental effect on the mechanical properties of a bonded joint. Another durability factor is time [3], [6], [7]. Even if the bonded joint is not negatively affected by increased temperature and humidity it can still degrade over time. Doing experimental tests in a quasi-static way to characterize the mechanical properties of a bonded joint can overestimate the structural capacity when a long period of service life is considered. In addition to structural reliability, the durability of structures is becoming increasingly important.

1.2. Literature review

1.2.1. Durability of bonded joints

Durability of an adhesively bonded joint is affected by load, time and environmental conditions like temperature and humidity. One form of durability that has been researched extensively is fatigue. Due to the adoption of fibre reinforced plastics (FRP) in structures subjected to random load spectre, fatigue testing has been done extensively on those materials. Some examples involve testing of fatigue behaviour and identification of failure mechanisms [8], accelerated testing of long-term fatigue [9], effect of temperature on fatigue [10], strength degradation [11] and nonlinear damage accumulation

due to fatigue [12]. Some examples of fatigue testing research to specifically characterize bonded joints under cyclic loading are done by Pirondi et al. [13], Campos et al. [14] and Ashcroft et al. [15].

Environmental effects on bonded joints

However, the long-term time dependent loads (like creep) and environmental effects on the mechanical properties of a structural adhesive have not yet been studied extensively [16]. Standard environmental tests for bonded joints are ASTM 1151-00 [17] and ASTM 1183-03 [18], but do not include testing of stressed specimens. In these standards, different possible temperatures and relative humidity combinations are proposed, for example, temperature ranging from -57 to +316°C and relative humidity of 95-100%, but they do not consider the application of a constant load during the test or conditioning. More recently, Manterola et al. [19] tested the specimens in a climate chamber at 85%RH and 82°C, in which some of the specimens were stressed with a stationary wedge during the conditioning phase prior to mechanical testing. The stressed specimens show a clear negative influence on the durability compared to the unstressed specimens. However, due to possible crack propagation during the conditioning phase, this method is not suitable for design purposes, since it does not always represent the real condition of the bonded joint in its service environment.

Multiple studies have shown that moisture has the most significant negative impact on an adhesive bonded joint, but that stress and temperature accelerate the process of degradation due to moisture [2], [3], [6], [16], [20], [21]. Research also shows that water uptake by the adhesive lowers the glass transition temperature (T_g), the strength and the stiffness of the adhesive [6], [20], [22]. There are studies that apply an elevated temperature to the specimen during the mechanical test, but an elevated relative humidity is not included during the test [23], [24]. Kinloch advices to continuously stress an adhesive specimen during the durability test, but not to precondition it unstressed and then test it. This is essential especially in case the adhesive system is meant for structural applications [6].

However, the aforementioned durability test approaches do not provide information when a specific degradation level for the bonded joint will be reached over time. The component time is not always considered solely but it is perhaps the most important element of durability, even if the environmental conditions are not considered as hostile, there could still be degradation of the mechanical properties of the bonded joint under influence of time. This could be related to creep of a material, where the stressed material plastically deforms over time [20], [25]–[27]. Temperature plays a role in creep behaviour but in case of adhesives it could already take place at relatively low values like, for instance, room temperature.

The durability of a bonded joint is even more critical if there is a crack, void, or defect present in the adhesive of the bonded joint. Over time the crack can growth even though the energy release rate is below the fracture toughness. Same as with creep, there is a time dependent mechanism that drives the crack to propagate. In this case it is referred to as creep crack growth and can be considered as durability of a bonded joint [28]. From here on if durability of a bonded joint is mentioned it refers to creep crack growth.

1.2.2. Creep crack growth

Following the Griffith's criterion, a crack should not grow if the applied energy release rate is below the fracture toughness. However, in reality, crack propagation can take place below the fracture toughness if creep crack growth is present in a bonded joint. At high deformation rates a polymer adhesive behaves like a (elastic) solid and at low deformation rates as a fluid (viscous), which is known as the viscoelastic behaviour of a material [29]. The crack can grow over time because of the viscoelastic deformation in the fracture process zone [28]. Thus, understanding the viscoelastic creep crack growth and how it affects the performance of the bonded joint over time is essential for the design of durable bonded joints and maintenance protocols. Creep in metals have been researched extensively in the last few decades. The mechanism of slip lines and sliding of grain boundaries that

are involved with creep in metals is rather well understood [30]–[33]. Creep and creep crack growth in polymers and specifically adhesively bonded joints has only been studied more extensively in the last two decades [25], [28], [34]–[39]. Therefore, models are not widely available yet. A model is used to make prediction of how a material will behave. A model can describe an expected behaviour from a material when certain loads and conditions are applied. However, the model needs to be validated with experimental results. Although research on creep and creep crack growth recently has been done more extensively, there is still a lack of experimental test methods to properly characterize creep crack growth in polymers, which will be addressed in the next section.

1.2.3. Creep crack growth test methods

Standardized mode I test for bonded joints

A crack can grow in an adhesively bonded joint due to a load that acts in different modes, these modes are I, II and III, or a combination of them, known as mixed mode. For a bonded joint mode I (opening in perpendicular direction) is in general the weakest mode. Therefore, in this work only mode I will be considered. A quasi-static mode I test could be performed to determine the fracture toughness (critical energy release rate) of the bonded joint. One can measure mode I fracture toughness of a bonded joint by cleaving or peeling the bonded joint. The most common standardised test method is the Double Cantilever Beam test (DCB) described in ASTM D5528-01 [40] and ISO-25217 [41] standards (Figure 1-2). The later DCB test standard describes three data reduction methods: the Simple Beam Theory (SBT), the Corrected Beam Theory (CBT) and Experimental Compliance Method (ECM). For all three data reduction methods, the measurement of the crack length is required, which is preferably avoided since it is difficult to measure where exactly the crack tip is located and makes it a rather subjective measurement. Alternatively, to avoid crack measurement, the J-integral method can be used that makes use of the relative rotation of the adherends [19], [42]. Inclinometers can be used to measure the relative rotation of each individual adherend.

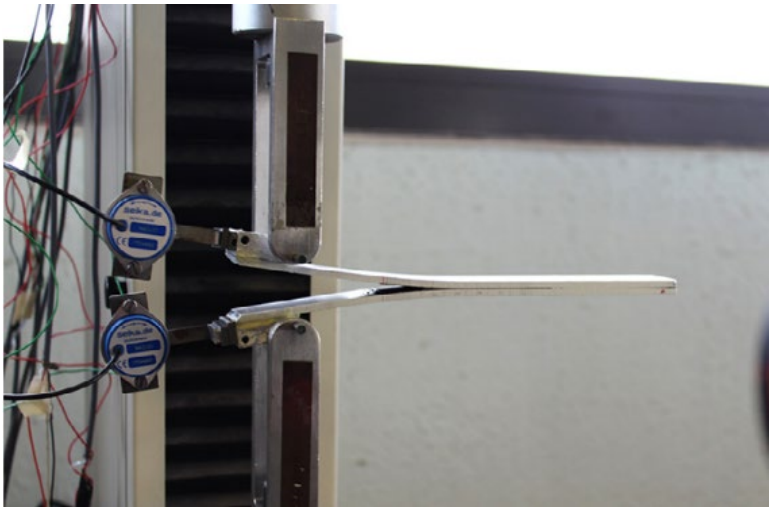

Figure 1-2. DCB test on a bonded joint with two inclinometers attached to the loading block of each adherend [43].

Wedge driven test

A bonded joint can also be cleaved by using a wedge [44], [45]. The same type of specimen as the DCB test is used, whereas in this case a wedge is driven in between the two adherends (beams). Variations on the wedge test have been designed like, the wedge driven test (WDT) [43], [46] (Figure 1-3). A wedge test seems to be a good alternative to the DCB test to determine the fracture toughness of an adhesive bonded joint. Crack measurement can be done in a more objective way compared to the DCB test by measuring wedge displacement or even eliminate it. The hypothesis is that in a wedge driven test on average the crack extension equals the wedge displacement during the crack propagation phase [46]. As a result, the crack measurement can be done in a more objective way by directly measuring the wedge displacement. This is an advantage compared to the DCB test where visual crack measurement is used. If there is no friction between the wedge and adherends, then crack measurement could be completely eliminated [47]. Considering a quasi-static condition, to determine the fracture toughness of the bonded joint using a wedge, the energy dissipated by the friction between the wedge and the adherends needs to be taken into account [48]. However, it is demonstrated that the friction coefficient between the wedge and the adherends is difficult to determine, also because the friction coefficient does not remain constant during the test [43]. It has

been tried to eliminate the friction completely or reducing it to a minimum by using rollers [47], [49]. But it is unclear if the friction can indeed be completely neglected in the data reduction.

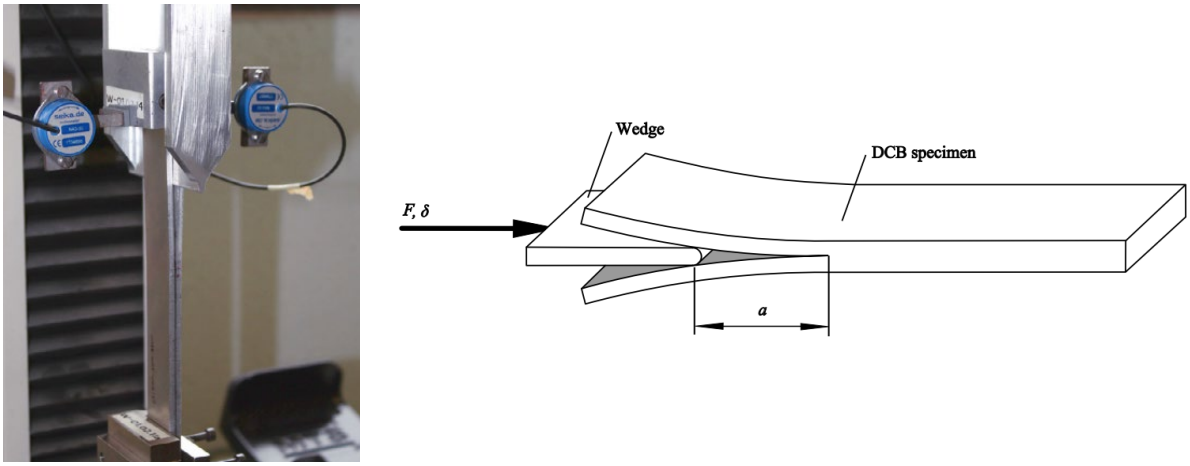

Figure 1-3. Left: wedge driven test (WDT) [43]*. Right: schematic view of WDT* [46]*.*

Bonded joint durability wedge test

A well-known wedge test for durability testing of bonded joints is the ´Boeing wedge test´ (Figure 1-4). ASTM D-3762 [50] was the standard test method for this specific wedge test. In 2019 the test standard was withdrawn since it was not updated in the last eight years. The idea of this test is to enter a wedge into a DCB-like bonded joint, which initiates a crack. The wedge is kept in its position and over time the crack will start to propagate, mainly influenced by environmental conditions. After a certain time, the bond quality is checked in a qualitative manner. Multiple researchers have tried to use this method to determine fracture toughness and/or crack growth rate in bonded joints [6], [20], [51], [52]. However, this test method was never designed to be used for a quantitative measurement, but solely to determine qualitatively if an adhesive bonded properly to an adherend. Measuring the crack extension over time with this method is difficult and therefore only conservative results could be obtained.

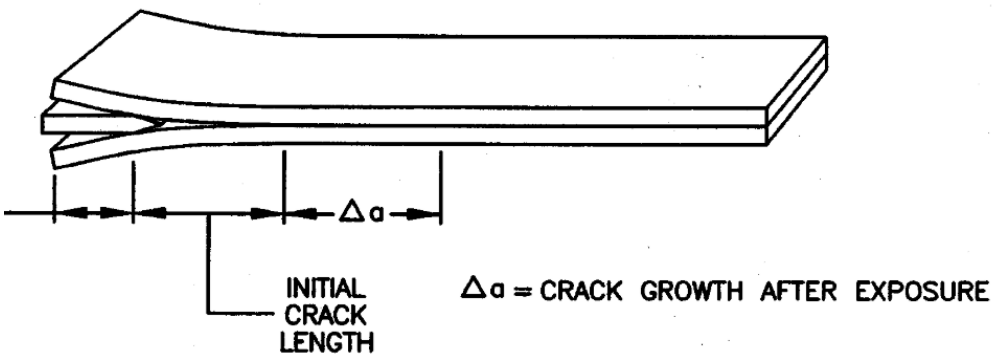

Figure 1-4: Wedge test ASTM D-3762 [50].

Constant energy release rate

Plausinis et al. [52] relate the energy release rate to the creep crack growth that was measured using the "Boeing wedge test". The relationship is based on a path independent J-integral method that makes it independent of the crack length to determine the energy release rate at the crack tip. A drawback of using a stationary wedge like the "Boeing wedge test" is that the energy release rate decreases when the crack propagates. Since energy release rate is directly related to the creep crack growth the measured crack growth rate also decreases constantly. Different authors have tried to design a test setup that keeps the energy release rate constant at the crack tip. Some have made use of a cable system with hanging weights (Plausinis et al. [53] and Dillard et al. [54]) and others have used springs (Lefebvre et al. [55] and Nakamura et al. [56]) to apply a constant energy release rate. All these tests are load controlled and use DCB-like specimens. A disadvantage of a DCB-like specimen is that the distance between the load point and the crack tip will increase during crack propagation. The energy release rate decreases at the crack tip and the load needs to be corrected constantly to rectify for this decrease in energy release rate. A more complex computer-controlled system could be used that constantly calculates the energy release rate and corrects the load accordingly [38], but this kind of sophisticated equipment is expensive and not widely available. Instead of an opening load also a bending moment could be applied to specimen. The bending moment is constant along the whole specimen regardless of the crack length. Sørensen et al. [57] and Lindgaard et al. [58] use a wire system

in combination with lever arms to introduce a bending moment to the specimen. Another possibility is to use a different type of specimen like for instance, the Tapered Double Cantilever Beam (TDCB) specimen [41]. Due to the geometry of the TDCB the compliance rate with respect to the crack length remains constant. As a result, the energy release rate remains constant when applying a constant load [59]. In literature multiple researches can be found where a TDCB specimen is used for mode I tests on adhesively bonded joints [60]–[66]. A disadvantage of the TDCB is that a specific geometry must be determined beforehand and that it needs to be manufactured using a milling machine. Based on the literature a wedge seems to be a good candidate if the wedge does not remain stationary during the test. A moving wedge follows the crack tip and as a result the energy release rate at the crack tip remains constant.

1.2.4. Creep crack growth numerical models

Models that describe material behaviour under certain conditions can assist engineers with durable design of complex adhesively bonded joints. Nowadays designs are analysed with numerical tools like the finite element method (FEM). Material models can be implemented in FEM and therefore be used to predict behaviour of complex structures. Numerical models have been developed for creep analysis in adhesives that can be used for the analysis of bonded joints [67]–[70]. Nevertheless, what is missing are creep crack growth criteria that can be implemented in numerical models to provide a simplified prediction of creep crack growth in a bonded joint. As was described before, fatigue is researched extensively and therefore numerical models for fatigue simulation in bonded joints exist [13], [14], [71]–[75]. In fatigue the well-known Paris law [76] (a power law) describes the log-linear relationship between energy release rate (or stress intensity factor) and crack growth rate. For creep crack growth multiple researchers have plotted on a log-log scale the energy release rate or the stress intensity factor against crack growth rate obtaining a log-linear trendline [28], [52], [77]. For creep crack growth the crack growth rate is expressed in time (da/dt) instead of the number of cycles (da/dN) as in fatigue. The log-linear trendline in creep crack growth can also be described by a power law. In this

way creep crack growth has an analogy with fatigue. What is missing is a similar implementation of creep crack growth model in FEM software as is done for fatigue [71], [78]–[80]. The FEM software of Abaqus [81] has commercially available modules like direct cyclic (DC) and virtual crack closure technique (VCCT) that are used by multiple researchers to numerically model fatigue [78], [82]–[87]. VCCT is based on a predefined pair of connected nodes that release when a certain criteria is met and works well for predefined crack path. Since bonded joints have a clear bondline it can be predicted that the crack will grow inside the bondline, i.e., a predefined crack path. As far as the author knows similar commercially available modules to model numerically creep crack growth are not available yet.

1.3. Motivation

Having more reliable information about the expected creep crack growth, a bonded joint can be designed in such a way that creep crack growth is allowed to take place during its service lifetime. The bonded joint could be designed, for example, with a design criterion that that the crack should never reach its critical crack length before the end of its service lifetime. Therefore, it needs to be known what the creep crack growth rate is in that specific bonded joint. In reality bonded joints are used in more complex structures than is usually tested in the laboratory. Numerical tools can be utilised to analyse these complex structures with bonded joints for creep crack growth. This means there is need for creep crack models to be implemented in commercially available FEM software. However, there are no simple methods available to determine accurately the creep crack growth in adhesively bonded joints. It has been tried with simple methods like the Boeing wedge test, but the stationary wedge results in constantly changing energy release rate at the crack tip during crack propagation. Qualitative obtained results cannot lead to the development of predictive models. Other methods have been tried to improve the results by applying a constant energy release rate, like springs [55], [56], weight-wire [53], [54] and computer-controlled systems [38] but make the test method rather complex. A moving wedge appears to be a good alternative to apply a constant energy release rate to a bonded joint in mode I. Creep crack growth models can be derived from the experimental test results by applying a

constant energy release rate to a bonded joint and measure the crack growth over time. Similar approach as with fatigue testing and modelling can be used to implement the obtained crack growth model into numerical tools. The numerical models for creep crack growth are essential to make reliable prediction for the durability of complex structures involving bonded joints, which are currently lacking in industry. Therefore, determining the durability of a structural bonded joint for the design of a structure remains often uncertain. Designing bonded joint solely based on mechanical properties obtained from quasi-static experimental tests will likely overestimate the long-term capacity of the bonded joint.

1.4. Objectives

The main objective of this research is to develop a method to measure creep crack growth in an adhesively bonded joint by applying a constant energy release rate in mode I. An experimental method is developed to obtain creep crack growth curves from an adhesively bonded joint. From the creep crack growth curves a model is derived that describes the relationship between the energy release rate and the creep crack growth rate. The model is applied to a commercially available numerical tool and used a demonstrator.

The following steps need to be taken to fulfil the main objective:

- Design of a mode I test setup that can apply a constant energy release rate.
- Development of a test methodology to obtain the energy release rate and validate it against a standardised test method.
- Development of a test method to obtain creep crack growth curves of an adhesively bonded joint.
- Validation of the method by performing experimental tests with a different method and specimen geometry.
- Demonstrate that a creep crack growth model can be implemented in an existing commercially available numerical model to simulate creep crack growth in a bonded joint.

The previous steps contribute to a methodology to obtain a creep crack growth model from experimental results that can be implemented in numerical tools.

1.5. Thesis layout

This thesis is a compendium of articles where each one of them contribute to achieve the main objective and the tasks as described in section 1.4. The articles can be found in the body or the Thesis as chapters 2 to 4. As it is stated by the criteria for formatting doctoral theses document of Doctoral School, if the articles are published openly they have to appear in the thesis in the same format as in

the journal where they are published. This is the case for the articles presented in chapters 2 and 3. The article in chapter 4 has been submitted but not peer-reviewed yet at the moment of submission of this Thesis, and therefore appears in the submitted pre-print version. Each chapter containing an article has a title page with the journal information followed by a short overview of the article and how it fits in the thesis as a whole.

Chapter 2 covers the development of a mode I low friction roller wedge driven test setup.

Chapter 3 presents the work towards a methodology of a creep crack growth test that utilises a constant energy release rate applied to an adhesively bonded joint in mode I. The goal of the method is to obtain creep crack growth curves of a bonded joint.

Chapter 4 describes the analysis of creep crack growth model based on a Paris´ law-like approach. The proposed creep crack growth model is validated against another test method with different specimen geometry. It is demonstrated that proposed model can be used in existing commercially available FEM software.

The articles are followed by a general discussion and conclusions, which are chapter 5 and 6, respectively. The last chapter also contains recommendations for possible future work.

2. Analysis of mode I fracture toughness of adhesively bonded joints by a low friction roller wedge driven quasi-static test

E. Meulman[a*], J. Renart[a,c*], L. Carreras[a], J. Zurbitu[b]

[a]AMADE, Polytechnic School, University of Girona, Campus Montilivi, s/n, 17071, Girona, Spain

[b]Ikerlan Technology Research Centre, Basque Research and Technology Alliance (BRTA), Arrasate-Mondragón, Spain

[c]Serra Húnter Fellow, Generalitat de Catalunya, Spain

This paper has been published with open gold access in the international journal of Engineering Fracture Mechanics, vol. 271, no. May, p. 108619, 2022

Doi: 10.1016/j.engfracmech.2022.108619, ISSN: 0013-7944, Impact Factor: 4.898, ranked 19/138 in the category of Mechanics (1st quartile)

Overview

With the aim of developing a methodology for creep crack growth a test setup needs to be developed to apply a constant energy release rate to the crack tip. In this chapter a low friction roller wedge test setup is presented named the Roller Wedge Driven (RWD) test and is compared to a standardised method to determine the mode I fracture toughness of bonded joint, the DCB test method. The work presented in this chapter is limited to quasi-static tests to validate the use of a roller wedge. It must be mentioned that the energy release rate in this work relates to quasi-static conditions in which other energy dissipative mechanisms are not considered. For relative high rates the energy release rate results could be questionable for the adhesive used in this test campaign.

It is demonstrated that the roller wedge is suitable tool to fracture a bonded joint in mode I. The idea is that the roller wedge reduces friction between the wedge and the specimen adherends to a minimum. As a result, the friction force could be completely neglected in the data reduction method to determine the energy release rate. This assumption is based on literature and validated by experimental tests on DCB-like bonded joints. An advantage of using a moving wedge is that on average the distance between the wedge and the crack tip remains constant during crack propagation. Thus, the energy release rate is constant at the crack tip and the wedge displacement can be used to measure the crack length increase over time. Two requirements to be able to make creep crack growth plots.

The results have shown that when using a roller wedge (RWD) the friction forces are significantly lower compared to a sliding wedge. However, comparing the RWD with the DCB results show that the overestimation of the energy release rate using the RWD data reduction method is likely caused by the friction in the roller wedge that is still present. It is also shown that the RWD data reduction method is less sensitive to a measurement error than the J-integral method. The simplicity of the method offers the possibility to create a test setup that can be used without a test machine.

Engineering Fracture Mechanics 271 (2022) 108619

Contents lists available at ScienceDirect

Engineering Fracture Mechanics

journal homepage: www.elsevier.com/locate/engfracmech

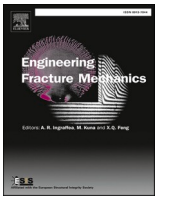

Analysis of mode I fracture toughness of adhesively bonded joints by a low friction roller wedge driven quasi-static test

E. Meulman [a,*], J. Renart [a], L. Carreras [a], J. Zurbitu [b]

[a] AMADE, Polytechnic School, University of Girona, Campus Montilivi, s/n, 17071 Girona, Spain
[b] Ikerlan Technology Research Centre, Basque Research and Technology Alliance (BRTA), Arrasate-Mondragón, Spain

ARTICLE INFO

Keywords:
Wedge driven test
Fracture energy
Mode I
Bonded joint

ABSTRACT

In structural bonded joint design, mode I fracture toughness is a key mechanical property. Using a sliding wedge driven test to measure the fracture toughness of an adhesive is a good alternative to the standardised DCB test. However, with a sliding wedge driven test, the friction between the wedge and the specimen is difficult to determine and has an influence on the fracture toughness data reduction. In this work, we present a relatively small and simple mode I fracture toughness test setup with a roller wedge, which can potentially be used without a test machine to make a quick and affordable approximation of the mode I fracture toughness. DCB test results of the specimens are used as a reference to compare the roller wedge driven test method against. Results show that the friction of the roller wedge is significantly lower than a sliding wedge, and thanks to the low friction of the rollers the required driving force of the wedge is likewise low. Therefore, a human hand can apply a high enough force to the wedge by rotating a threaded bar to push down the wedge. Controlling the displacement rate by rotating a threaded bar by hand is difficult, therefore this method appears to be only suitable for non-rate sensitive adhesives. By comparing the roller wedge force and J-integral data reduction method, it has been shown the roller wedge force data reduction method is less sensitive to measurement errors. The proposed Roller Wedge Driven test method could potentially be an alternative mode I fracture toughness test method for bonded joints.

1. Introduction

Structural adhesive bonds are increasingly used in industry as an alternative to mechanical joints [1]. One of the advantages of structural adhesive bonds is that the need for more traditional fasteners becomes obsolete, consequently making the structure lighter, smoother and distributing stresses over a larger area (i.e., stress concentrations are limited). Nevertheless, there are some disadvantages to using adhesives for structural bonding such as limited capacity for visual inspection, high quality surface preparation being required, controlling process parameters being important and adhesives are environmentally sensitive. Material characterisation of an adhesive is essential to design a structural bond for its service load cases.

When designing a bonded joint, one of the key adhesive mechanical properties is fracture toughness. A bonded joint is usually loaded with a mixed mode which is a combination of mode I and II [1]. Pure mode I and II fracture toughness test results show that, in

* Corresponding author.
E-mail addresses: edwin.meulman@udg.edu (E. Meulman), jordi.renart@udg.edu (J. Renart), laura.carreras@udg.edu (L. Carreras), jzurbitu@ikerlan.es (J. Zurbitu).

https://doi.org/10.1016/j.engfracmech.2022.108619
Received 15 February 2022; Received in revised form 19 May 2022; Accepted 10 June 2022
Available online 14 June 2022

Nomenclature

a	crack length
a_c	corrected crack length
a_e	crack length with exact contact point
B	width of specimen
C	compliance
d_{ini}	initial wedge displacement for fracture toughness calculation
d_{lim}	wedge displacement limit
E_x	longitudinal Younǵs modulus
E_f	back-calculated modulus of the substrate
Δ	correction by taking the intercept of $C^{1/3}$ against a
D_w	diameter of the wedge
E_y	transversal Younǵs modulus
F_{push}	force to push the wedge
$F_{Push\|s}$	force to push the wedge simplified data reduction method
G	energy release rate
G_c	critical energy release rate
G_e	energy release rate with exact contact point
G_{xy}	in-plane shear modulus
h	thickness of the adherend
J	energy release rate with J-integral method
N	correction to compensate for the stiffness of the DCB bonding blocks
P	opening force
t_a	bondline thickness
r_w	radius of the wedge
δ_y	opening displacement
θ	adherend tip rotation angle
θ_c	adherend tip rotation angle at critical energy release rate
θ_{ini}	adherend initial rotation angle
μ	friction coefficient
χ	crack length correction factor
CBBM	Compliance Based Beam Method
CBT	Corrected Beam Theory
COF	Coefficient of Friction
DCB	Double Cantilever Beam
LVDT	Linear Variable Displacement Transducer
RWD	Roller Wedge Driven
WDT	Wedge Driven Test
WDT+	Wedge Driven Test simplified data reduction method

general, fracture toughness in mode I is lower than in mode II [2]. To measure pure mode I fracture toughness, the bonded joint is cleaved or peeled. This can be done with different test methods, the most common of which are standardised test methods based on the double cantilever beam test (DCB) and are described in ASTM D5528-01 [3] and ISO-25217 [4]. The beams can be separated by load control, something which is rarely done, or by a constant opening displacement rate [5]. With a constant opening displacement rate of the beams, the crack growth rate (crack growth over time) will not be constant during the test. On the other hand, applying a constant load will very likely result in unstable crack propagation.

The data reduction method described in ISO-25217 [4] is based on corrected beam theory (CBT). For the CBT data reduction method, the measurement of crack length is required, which is preferably avoided since this could introduce significant errors as a result of the non-objective visual method that is generally used for crack length measurement [6]. Alternative data reduction methods that do not require crack length measurements are the compliance based beam method (CBBM) [7] and the J-integral method [8]. For the CBBM method, the flexural modulus of the specimen needs to be obtained. Therefore, testing specimens with different materials means the CBBM method is labour intensive. The J-integral method, however, only depends on rotation measurements of the adherend tip and the applied load.

Another method to cleave a bonded joint is by using a wedge. The same type of specimen as in the DCB test is used but in this case a wedge is introduced in between the two adherends (beams) until crack propagation starts. Then the wedge is retained in its position and over time the crack will continue to propagate. ASTM D-3762 [9,10–12], also known as the Boeing wedge test, used to be the standard wedge test method. However, in July 2019 the standard was withdrawn because it had not been updated for the last eight

years. The wedge test was never originally designed to be used for a quantitative measurement of mode I fracture toughness but instead was meant to be used as a qualitative test to determine if an adhesive properly bonds to an adherend. Authors like Cognard et al. [13] and Plausinis et al. [14] have tried to use the Boeing wedge test to obtain quantitative properties for bonded joints. Variations on the wedge test are designed like, for example, the wedge driven test (WDT) [6,15–17]. A significant advantage of the wedge driven test is that it can be assumed that the crack length during propagation is on average constant. In this case, the crack length is defined as the distance between the crack tip and the tip of the wedge. As a result, crack measurement is objective since during the crack propagation phase (only the case for stable crack propagation) the incremental displacement of the wedge, provided by the test setup crosshead, equals the crack length increase. This principle could also be used for creep or durability testing where a constant load is applied to the wedge, which then moves, under stables crack propagation, at the same rate as the crack tip. This means for a certain load a constant crack growth rate could be obtained over the complete crack length. Unlike the Boing wedge test, where the crack growth rate slows down when the crack is propagating, because the wedge is stationary.

To determine the fracture energy with a test, the total energy that goes into the system and how much of this energy is used for creating the crack surfaces (energy release rate, G) needs to be known. The critical energy release rate (G_c) is a material property and indicates the resistance to crack growth. In other words, if $G \geq G_c$ crack growth occurs in the material [18]. Considering a WDT, the wedge is in direct contact with the adherends and slides along them creating friction. The energy that is required to overcome the friction force is difficult to measure directly. Therefore, determining the fracture toughness based on the total amount of energy put into the system is not evident unless the friction force can be eliminated. Different authors have shown that, even when using low friction materials, the sliding friction forces cannot be neglected when determining fracture toughness [19,20]. Likewise, it is also not evident to determine the friction coefficient as a single value since the friction coefficient is not constant during the test [6]. Glessner et al. [21] proposed a WDT design that uses a roller wedge to separate the adherends and reduce friction force to a minimum. Potentially the rollers result in a low enough friction force that the friction force can be neglected. However, the authors did not present

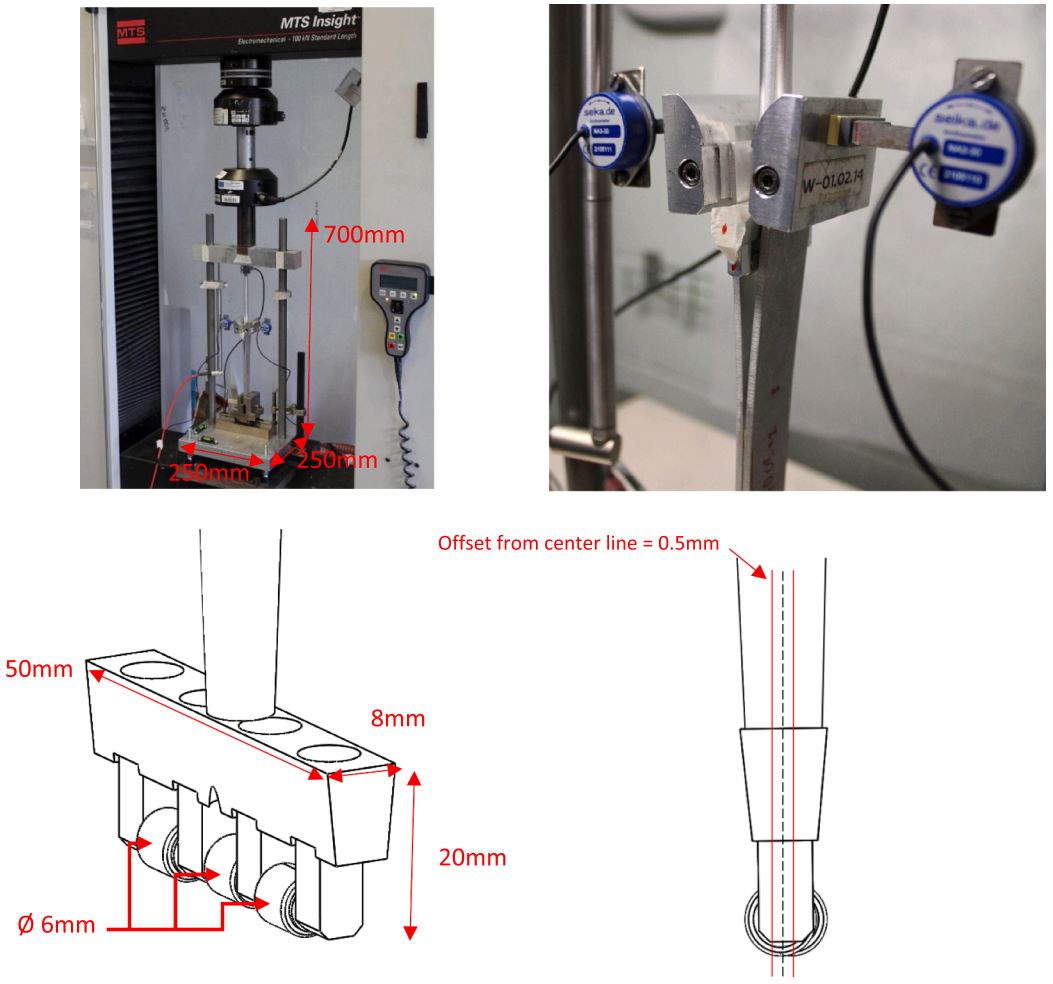

Fig. 1. Top left: RWD test setup. Top right: Roller wedge inserted in specimen. Bottom left: Sketch of roller wedge design with three rollers. Bottom right: Side view sketch of wedge where the middle roller and the two outer rollers have an offset of 0.5 mm (solid red line) from the wedge centre line (black dashed line).

the friction force of the roller wedge compared to a different method to show that the friction force can indeed be neglected when using a roller wedge. Adams et al. [22] designed the 'Smart Wedge' concept which also uses rollers to separate the adherends. The rollers are directly connected to a load cell, therefore the specimen opening load can be directly measured. With the 'Smart Wedge' concept, crack measurement is not required to be estimated during the test, however, flexural rigidity of the adherends does need to be measured to be able to calculate the crack length when post-processing the test results.

For the WDT, Renart et al. [20] developed a data reduction method to determine fracture toughness. The data reduction method requires the measured load to drive the wedge into the specimen and takes the friction coefficient into account. Manterola et al. [6] simplified the WDT data reduction method by making use of inclinometers to measure the rotation of the adherend tips and, as a result, obtain the fracture toughness of the bonded joint. This simplified method avoids a coefficient of friction (COF) estimation and the bondline thickness is taken into account. The proposed simplified data reduction method (WDT +) has shown to be less sensitive to displacement rate, bondline thickness, wedge thickness and type of adhesive.

All the Mode I fracture toughness test methods found in literature require a test machine to perform the experimental test. For quality control, the DCB is the accepted standardized test method in industry. For instance, for preliminary design purposes like material selection, it could be desired to test some different material combinations to obtain a fracture toughness approximation. The DCB test, which requires a test machine, can be time consuming and costly to perform. It would be beneficial to have a test method that can measure the mode I fracture toughness of a bonded joint in a faster and simpler way. In this work, we present the Roller Wedge Driven (RWD) test setup design which, when compared to the other methods described in this introduction, is a simpler test method. The RWD test setup is based on a concept design from Glessner et al. [21] and a patent of the Ikerlan Technology Research Centre and AMADE [23]. The latter proposes a roller wedge with a data reduction method that is based on adherend rotation measurement with inclinometers. Measuring directly the wedge driving force to obtain fracture toughness properties is likely a better option. This is also what Glessner et al. did by assuming that the friction of the roller wedge is zero. However, no comparison was made with other methods to confirm the friction can indeed be assumed zero. The authors of this work believe this deserves further investigation.

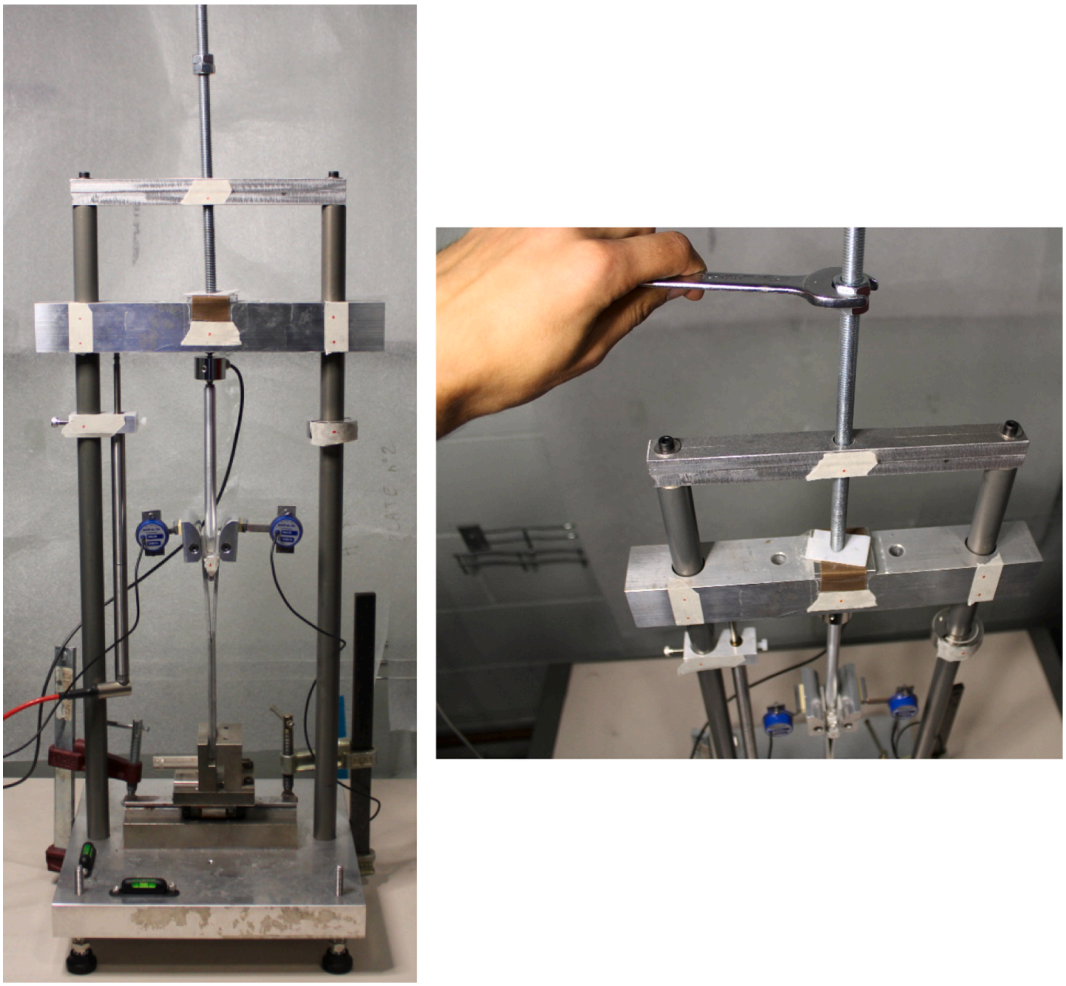

Fig. 2. RWD manual test setup configuration with a threaded bar that pushes the loading beam of the wedge down when rotated with a spanner.

In theory, one could apply the manual load by just pressing the wedge into the specimen by hand, however this will probably result in unstable crack growth since applying the force by pushing by hand is difficult to control. A manual mechanism is required to apply a more control displacement to the wedge. As a result making it a quick and easy-to-perform test that can assess many specimens in a relatively short timeframe.

In section 2, the authors present the RWD test method and setup, as well as the experimental testing campaign carried out in two different laboratories. The comparison between the DCB and RWD test results are presented in section 3 and the results obtained are discussed in section 4. Finally, section 5 describes the conclusions of this work.

2. Methodology

2.1. The roller wedge driven test (RWD)

The RWD test setup (Fig. 1, top left) has a wedge that consists of three rollers (Fig. 1, bottom left). A clamp and a linear carriage system hold the specimen in a vertical position in line with the roller wedge. A bearing connects the roller wedge with the horizontal loading beam. The bearing makes it possible that the roller wedge can rotate around its longitudinal axis making sure all rollers make contact with the adherends and preventing potential mode III loading of the specimen. An aluminium block is mechanically attached to each end of the adherend. These aluminium blocks (Fig. 1, top right) open the ends of the adherends when the roller wedge is pushed against the aluminium blocks. This makes it possible to smoothly enter the round rollers of the wedge in between the narrow gap between the adherends [20].

An HBM WA-T-50 linear variable displacement transducer (LVDT) with a precision of 0.2% measures the displacement of the roller wedge. The LVDT attaches to one of the vertical guiding columns and is in contact with the horizontal support beam of the roller wedge. The support rod of the roller wedge contains a load cell (HBM U9C-500) with a precision of 0.2% to be able to measure the applied force that drives the roller wedge into the specimen. An inclinometer (NA3-30 from SEIKA Mikrosystemtechnik GmbH) with a precision of 0.005° is attached to each of the aluminium blocks at the opening end of the adherends to be able to measure the rotation angle of the adherend tips (Fig. 1 top right). As explained in section 1, the inclinometers are only required for the J-integral data reduction methods and therefore used as a reference measurement. We use an MTS Insight 100 kN for the RWD quasi-static mode I fracture tests. The RWD quasi-static tests are performed with displacement control. All displacement data in this research are measured with the LVDT. Additionally, it is possible to run the test manually (by hand) by moving the RWD test setup loading beam with a threaded bar and a support allocated on top of the two guiding columns (Fig. 2).

The calculation of the energy release rate applied to the specimen is based on the WDT data reduction method [20] and reads:

$$G = \frac{3}{4}\frac{E_x h^3 \delta_y^2}{a_c^4} \tag{1}$$

where E_x is the longitudinal Youngs modulus of the adherend, h is the thickness of the adherend, a_c is the corrected crack length and δ_y is the opening displacement at the contact point between the roller and the adherend. It is assumed that the roller wedge rollers are small enough in diameter that the simplified contact point principle can be applied [20] and additionally taking into account the bondline thickness (t_a) and the diameter of the wedge (D_w) [6]:

$$\delta_y = \frac{D_w - t_a}{2} \tag{2}$$

The corrected crack length (a_c) in the data reduction method (1) takes into account the flexibility of the adherends and corrects the crack length (a) with the following equation:

$$a_c = a + \chi h \tag{3}$$

Parameter χ is the crack length correction factor [24]:

$$\chi = \sqrt{\frac{E_x}{11G_{xy}}\left[3 - 2\left(\frac{1.18\frac{\sqrt{E_x E_y}}{G_{xy}}}{1.18\frac{\sqrt{E_x E_y}}{G_{xy}} + 1}\right)^2\right]} \tag{4}$$

where E_x and E_y are the Youngs modulus in the longitudinal and transversal direction, respectively and G_{xy} is the in-plane shear modulus. The crack length correction factor is added to crack length a after multiplication by h, which is the thickness of the adherend. The crack length correction factor compensates for the rotation of the adherends near the crack tip, since the elastic beam theory does not take this rotation into account and therefore underestimates the crack length.

Since the simplified contact point between the rollers and the adherends is assumed, the simplified data reduction method can also be used [20]:

$$F_{Push|s} = \frac{E_x B h^3 r_w \left(\frac{3r_w}{2a} + \mu\right)}{2a^3\left(1 - \frac{3r_w}{2a}\mu\right)} \tag{5}$$

In which $F_{Push|s}$ (the applied force) is measured with the load cell, B is the width of the specimen, h is the thickness of the adherend and r_w is the wedge tip radius (i.e., the roller radius). The friction coefficient μ is assumed to be negligible and therefore taken as zero [21]. After performing the test, $F_{Push|s}$ is known from the test results. This means only one unknown variable remains: a. Numerically solving a in equation (5) and substituting that value in equation (3) will provide parameter a_c. The value of a_c can be used to determine G with equation (1). By combining equations (1) to (5), the RWD force equation is obtained:

$$G = \frac{3}{4}\frac{E_x h^3 \delta_y^2}{\left(\sqrt[4]{\frac{3}{4}\frac{E_x B h^3 r_w{}^2}{F_{Push|s}}} + \chi h\right)^4} \tag{6}$$

The principle of the J-integral method used for the DCB test can also be used for the RWD test if inclinometers are used and is based on [6]:

$$J = 2\frac{P}{B}\tan\theta \tag{7}$$

where B is the specimen width, P the adherend opening force and θ is the adherend tip rotation angle. In the DCB test the adherend opening force P can directly be measured with the load cell, whereas with a wedge test a conversion needs to be performed to obtain the adherend opening force P from the measured driving force of the wedge [6]:

$$P = \frac{E_x B h^3 \delta_y}{4a^3} \tag{8}$$

In case of the simplified contact point between the roller and the adherend, δ_y can be determined with equation (2). The crack length a can be estimated based on the opening displacement and the adherend tip rotation angle [6]:

$$a = \frac{3}{2}\frac{\delta_y}{\tan\theta} \tag{9}$$

Equations (7) to (9) can be combined into a single equation, RWD J-integral:

$$J = \frac{4}{27}\frac{E_x h^3 \tan^4\theta}{\delta_y^2} \tag{10}$$

The J-integral method as described is a useful method to be able to compare obtained energy release rates and fracture toughness from the different test methods used for this experimental campaign.

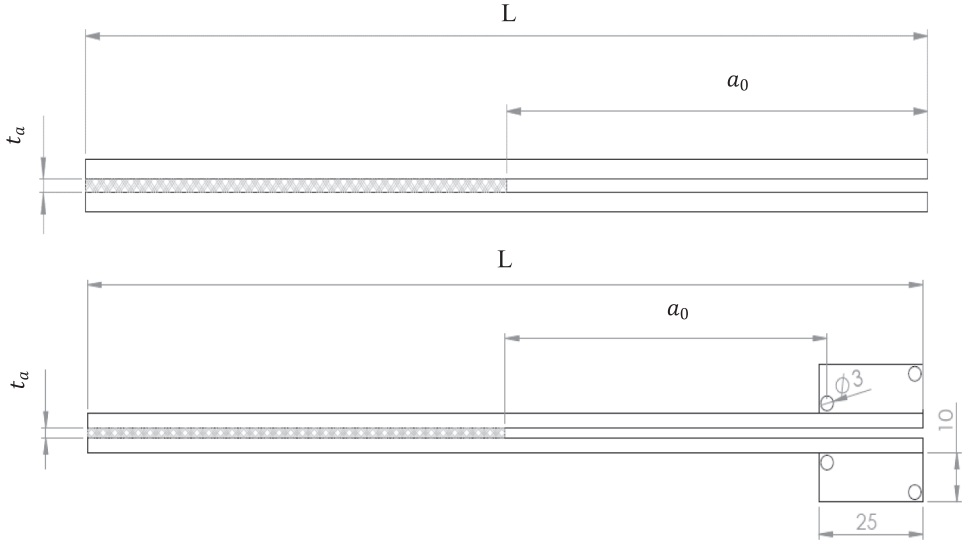

Fig. 3. Specimen geometry, top: for RWD test, bottom: for DCB test including two blocks with holes to attach the specimen to the test machine. Only the two holes in the block closest to the adherends are used to make the block function as a hinge. The second hole is only there so the blocks can be re-used for another DCB test.

2.2. DCB tests

The DCB tests were performed according to the DCB test standard [4]. Both the CBT and DCB J-integral based data reduction methods were applied to the results to obtain the mode I fracture toughness of the specimens. For the CBT method, the crack length needs to be measured. We measured the crack length visually with a camera (Canon 550D and macro lens EF100). By marking the side of the specimen, it is possible to determine what the crack length is at any moment during the test. The DCB J-integral method makes use of the rotation of the adherends and the applied opening load during the test. The inclinometers measured the rotation angle of the adherends and are the same inclinometers as used for the roller wedge driven test. The equation for the DCB J-integral is [6,25]:

$$J = \frac{P}{B}\theta_{rel} \tag{11}$$

The load that is measured to open the DCB specimen is P, the width of the specimen is B and θ_{rel} is the relative rotation between the adherends.

2.3. Experimental testing campaign

We manufactured the specimens in the AMADE research group laboratory. Two 200 mm long, 25 mm wide and 3 mm thick aluminium Al 7075-T6 adherends were bonded with a rigid structural adhesive. The bondline thickness t_a was between 0.4 and 0.6 mm (Fig. 3). The rigid adhesive is a methacrylate-based Araldite 2021–1. Araldite 2021–1 has a glass transition temperature of 80 °C. The aluminium adherend has a Young's modulus of 71 GPa, shear modulus of 27GPa and a yield strength of 550 MPa [6,26].

We pre-treated the adherends by sanding them with sandpaper P80, degreasing them with acetone and, just before bonding, cleaning them with high grade alcohol. The adhesive was cured in an oven set at 60 °C for 16 h. Teflon spacers ensured a constant bondline thickness of the specimen during its manufacture. The Teflon spacers were removed once the curing process had been completed. The initial crack length (a_0) was 100 mm for the RWD specimens and 37 mm for the DCB specimens. The DCB standard [4] states that the DCB specimens should be painted white and marked on one side to be able to visually measure the crack length during a test. Metal blocks with holes bonded to the DCB specimen made it possible to attach the specimens to the testing machine.

We performed all the RWD tests in this research in the ISO17025 and NADCAP certified AMADE research group testing laboratory at the University of Girona, testing at an ambient temperature ($23^{\circ}\pm2^{\circ}C$, 50 ±5 % RH). A total of five specimens were tested with the DCB test method: three specimens at the AMADE laboratory (DCB_01 to DCB_03) and two at the IKERLAN Technology Research Centre (DCB_04 & DCB_05). The test machine applied an opening displacement rate of 2 mm/min to the DCB specimens. Four specimens were tested with the RWD test setup (RWD_01 to RWD_04) at a wedge displacement rate of 5 mm/min. Additionally three specimens (RWD-M_01 to RWD-M_03) were tested with the RWD test setup without using the test machine, but by manually applying a load to the wedge (as described in section 2.1). Table 1 shows an overview of the tested specimens.

3. Results

This section describes the results from the three types of mode I fracture tests. First, we present the DCB test results, followed by the results from the RWD test method using the RWD force data reduction method to determine the fracture toughness. Then, we describe the results from the RWD manually-loaded test method using the same RWD force data reduction method. This section also contains the results from the RWD J-integral data reduction method applied to both test methods. Finally, an overview of all the test methods and different data reduction methods is visually depicted using a bar plot.

3.1. DCB test

The force–displacement curves of the DCB specimens are plotted in Fig. 4. The initial stiffness of all five specimens is very similar. The peak force is for all specimens at a similar opening displacement.

The rotation angles measured at the adherend tips are used to determine the energy release rate with the DCB J-integral method [25] (Fig. 5). The first 5 to 10 mm of the opening displacement after the peak force shows some deviation between the different specimens in terms of energy release rate. Later during the test, the energy release rate of most specimens converges to range between 2.5 and 3.5 N/mm (considering the range between the peak force and 30 mm of opening displacement).

The CBT method is based on a visual discontinuous measurement of the crack length. All the data points related to the crack length

Table 1
Overview of tested specimens.

Specimen	Test method	Disp. rate (mm/min)	Specimen thickness (mm)	t_a(mm)	No. of specimens
DCB_0x	DCB	2	6.47 ± 0.04	0.47 ± 0.04	5
RWD_0x	RWD	5	6.46 ± 0.04	0.46 ± 0.04	4
RWD-M_0x	RWD Manual	38.2*	6.48 ± 0.09	0.48 ± 0.09	3

* Could only be determined after the test and is the average measured displacement rate.

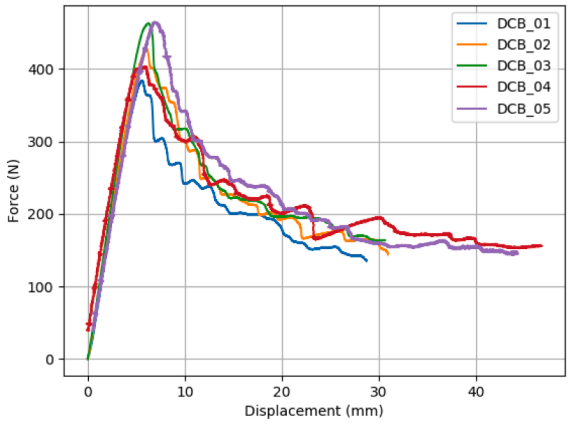

Fig. 4. Force-displacement curves of DCB specimens.

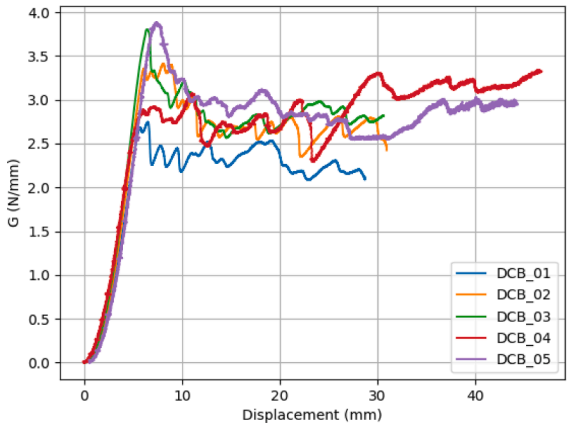

Fig. 5. Energy release rate vs. opening displacement of DCB specimens determined with the DCB J-integral method.

measurement are expressed in energy release rate and plotted against the opening displacement in Fig. 6. The same behaviour as the DCB J-integral method can be observed, where the energy release rate converges to a range between 2.5 and 3.5 N/mm.

In Fig. 7, both the results of the DCB J-integral and CBT method are plotted as comparison. The specimens on the left in Fig. 7 are those that were tested at the AMADE laboratory and those on the right were tested at the Ikerlan Technology Research Centre. Both methods show a good correlation as the difference between the two data reduction methods is less than 2% for the average energy release rate for all tested DCB specimens.

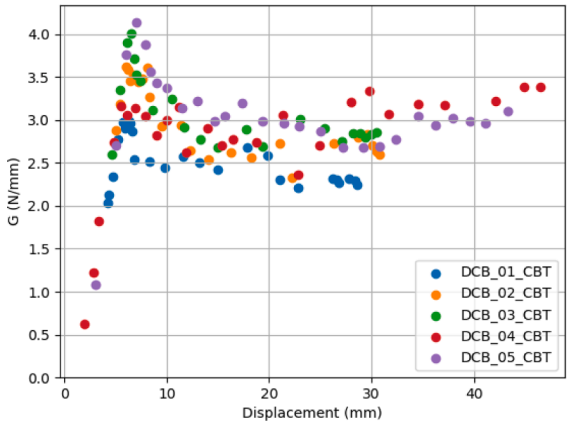

Fig. 6. Energy release rate vs. opening displacement of DCB specimens determined with the CBT method.

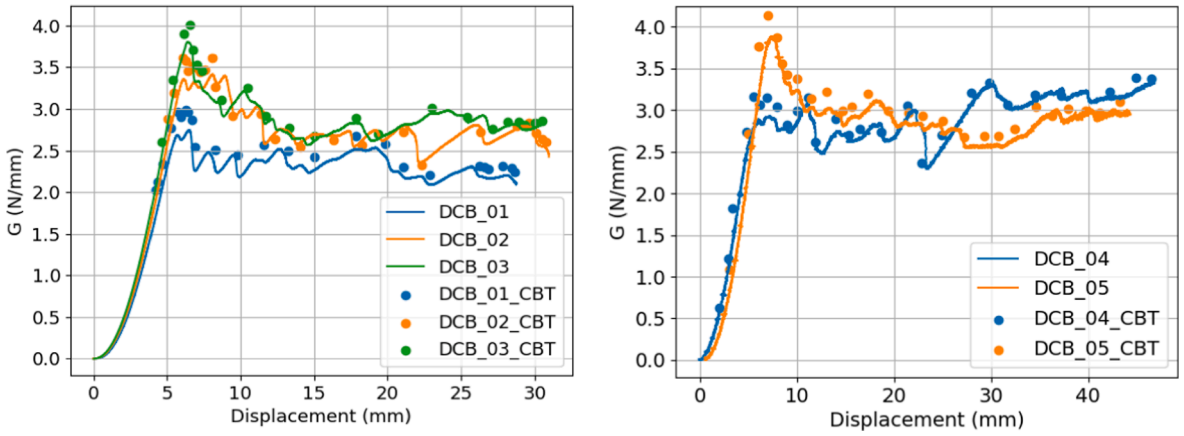

Fig. 7. Comparison of DCB J-integral and CBT method. Specimens on the left were tested at the AMADE laboratory and those on the right at the Ikerlan Technology Research Centre.

For all specimens we observed a cohesive failure of the adhesive like, for example, specimen DCB_03 shown in Fig. 8. To the right of the red line is the fracture surface created during the DCB test. The adhesive is a glassy polymer that forms voids during the fracture process as can be seen as small black dots in the DCB crack propagation section. To the left of the red line, the fracture surface was formed by opening the specimen using lab tools to be able to inspect the fracture surface of the specimen (this is not part of the test). It is observed that the fracture surface changes, this could indicate that this type of polymer is strain rate sensitive, however, the failure mode remains as cohesive failure.

Table 2 shows the average values obtained from the DCB tests. The average is taken from the peak force until the test was stopped. The average energy release rate of this range, where stable crack propagation take place, is considered as the fracture toughness of the specimen. There is some spread in the average values of the energy release rates for the different specimens. The average of all specimens is 2.719 N/mm with a standard deviation of 0.228 N/mm, and 2.772 N/mm with a standard deviation of 0.184 N/mm for the DCB J-integral and CBT method, respectively. The averages of both methods correlate well (difference less than 2%) and fall within standard deviation. The DCB test and the CBT data reduction method are standardised and widely accepted, therefore these results were used as a benchmark for the other test results presented in the following sections.

Table 2 shows a column indicated with E_f which is the back-calculated modulus of the substrate [27] and is used to check the stiffness of the substrate against the expected modulus of 71000 N/mm^2. The equation for E_f is [27]:

$$E_f = \frac{8(a+|\Delta|)^3}{(C/N)Bh^3} \tag{12}$$

Where a is the crack length, C is the compliance,B specimen width, h adherend thickness, Δ a correction by taking the intercept of $C^{1/3}$ against a and N a correction to compensate for the stiffness of the DCB bonding blocks. In Table 2 the standard deviations in the column are the standard deviations found for the result of one specimen (i.e. the average value from the propagation points). The

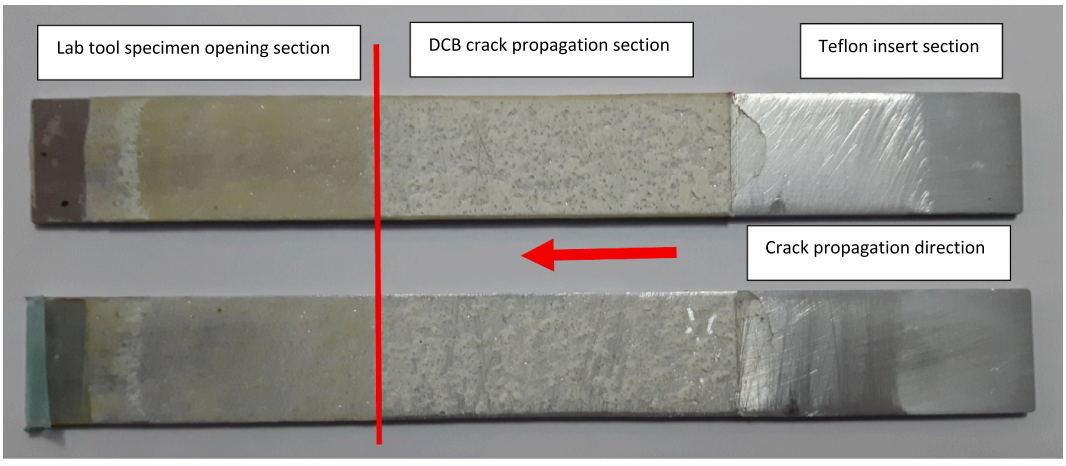

Fig. 8. Cohesive fracture surface of specimen DCB_03, to the right of the red line the adhesive fractured during the DCB test, to the left the specimen fractured during the process of splitting the adherends with lab tools to be able to inspect the fracture surface (later not part of the test).

Table 2
Overview of average DCB test results. The standard deviations in the column are the standard deviations found for the result of one specimen. The standard deviation in the last row is the standard deviation found when taking the average value for all specimens tested.

Specimen	G_c- J-int (N/mm)		G_c– CBT (N/mm)		E_f(N/mm^2)	
	Avg.	Std. Dev.	Avg.	Std. Dev.	Avg.	Std. Dev.
DCB_01	2.299	0.127	2.461	0.133	61120*	1397
DCB_02	2.676	0.125	2.662	0.189	77,685	2123
DCB_03	2.811	0.130	2.915	0.177	69,586	574
DCB_04	2.951	0.256	2.888	0.252	72,323	1943
DCB_05	2.856	0.154	2.933	0.181	73,113	1234
Average:	2.719		2.772		70,765	
Std. Dev.	0.228		0.184		5482	

* The back-calculated modulus deviates more than 10% from the expected modulus (71000 N/mm^2) and therefore the fracture toughness results of this specimen should be considered suspect [27].

standard deviation in the last row is the standard deviation found when taking the average value for all specimens tested.

3.2. Roller wedge driven test

The force–displacement curves of the RWD specimens are plotted in Fig. 9 (left y-axis). The initial stiffness of the specimens is very similar for the four specimens tested with the RWD test setup. This is followed by a peak force where, once the force drops, moves into a more stable region. Specimen RWD_01 shows a high rise in force - around 40 mm of wedge displacement (dotted line), indicating an increase in resistance that is likely caused by an external influence. After testing, none of the adherends showed any permanent deformation. Likely, the resistance changed due to local adherend surface change. In Fig. 8 a thin layer of adhesive is visible on the non-bonded adherend surface where there is the transition from bonded to non-bonded area. There was a Teflon spacer placed to during manufacturing to create the adhesively bonded and non-bonded area. Adhesive flowed underneath the Teflon spacer during the specimen manufacturing process when the adherends were pressed together. This part of the specimen is neglected for the fracture toughness calculation and in the following plots.

The RWD force data reduction method (equation (6)) is applied to determine the energy release rate of the RWD specimens that are plotted in Fig. 9 (right y-axis). Since the RWD force data reduction method only uses the measured force from the test results as the input value, the plot is similar to the force–displacement plot and, therefore, both can be plotted using two y-axes (Fig. 9). To determine the average fracture toughness of the specimens, the same cut-off criteria as for the DCB J-integral method is used, i.e., after the crack has initiated. Fig. 10 shows an example of the measured rotation angles where a dashed line named d_{ini} indicates the initial wedge displacement where it is assumed that the crack propagation phase already has initiated. The dashed line of d_{lim} cuts out the spikes in the results caused by the roller wedge being in contact with the adhesive. The section between d_{ini} and d_{lim} can be plotted as a resistance curve (R-curve), as shown in Fig. 11. The average energy release rate of the R-curve is considered as the fracture toughness of the specimen. About 25 mm is the maximum crack extension that can be measured with these type of specimen before the roller wedge meets the adhesive, which then influences the measured results by increasing the resistance to the wedge. It seems that, besides the fluctuations in the R-curve of the different specimens, all converge to an energy release rate of about 3 N/mm.

It must be noted that the average rotation angle as is, for example, plotted in Fig. 10, is not directly used in the RWD J-integral reduction method. After manufacturing the specimens it was noticed that, besides using Teflon spacers to ensure a constant bondline thickness, the adhesive shrinks slightly during the curing the process. This results in the adherends not being completely parallel and showing a minimal V like shape. This initial rotation, θ_{ini}, of the adherends is calculated based on specimen dimensions and is added as

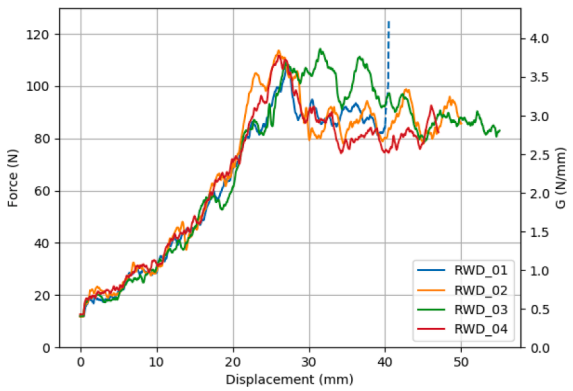

Fig. 9. Force-displacement and G-displacement curves of RWD specimens.

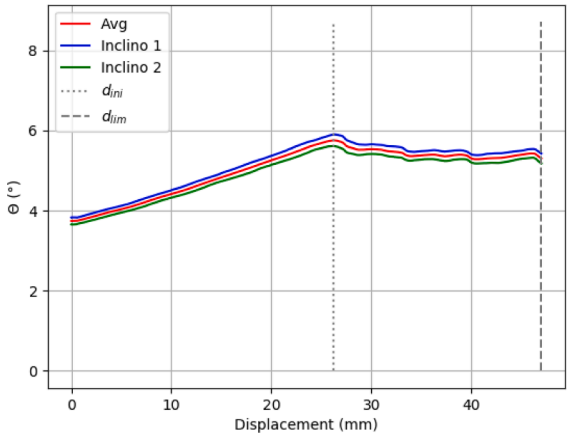

Fig. 10. Specimen RWD_04 as an example of how the d_{ini} and d_{lim} cut-offs determine the range over which the average energy release rate is calculated and is considered as the fracture toughness of the specimen.

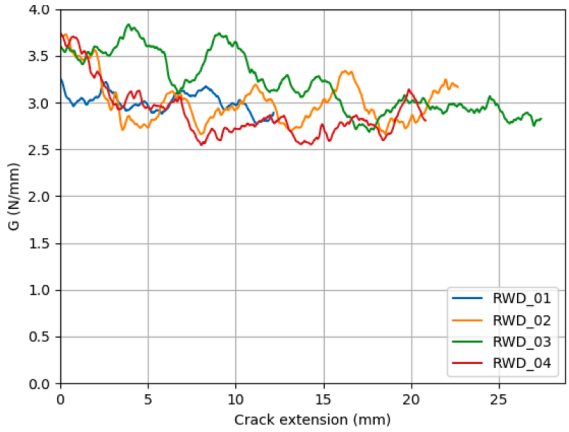

Fig. 11. Resistance curves (R-curves) of RWD specimens.

a correction factor to the average measured rotation angle. At the bonded section of the specimen, 30 mm and 90 mm from the short side of the specimen, a thickness measurement is taken using a micrometre. Over this distance the difference in thickness is used to calculate the initial angle (θ_{ini}) of the adherends relative to each other. The average value for θ_{ini} found for all RWD specimens is 0.042°.

In Fig. 12, the results obtained with the RWD J-integral data reduction method are plotted. The same initial peak is observed after

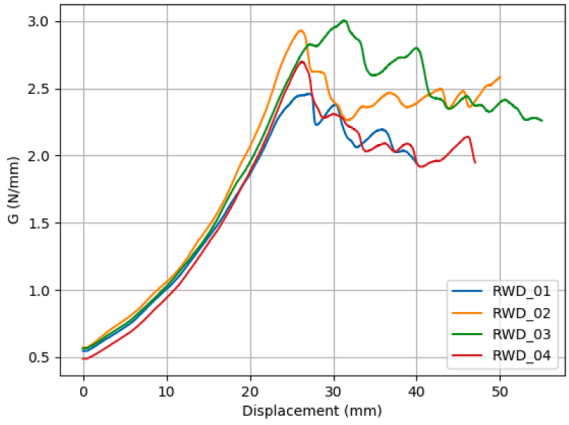

Fig. 12. Energy release rate vs. roller wedge displacement of RWD specimens determined with the RWD J-integral data reduction method.

which the energy release rate drops to a more stable value. The fluctuations with the inclinometers are less severe compared to using the measured force to determine the energy release rate. Using the RWD J-integral data reduction method, the energy release rate converges for specimens RWD_02 and RWD_03 to 2.4 N/mm, while specimens RWD_01 and RWD_04 are lower and converge to 2.0 N/mm.

For all the specimens, the cohesive failure of the adhesive is observed as being similar to specimen RWD_01 shown in Fig. 13. To the right of the red line is the fracture surface created with the roller wedge, while to the left is the fracture surface caused by opening the specimen completely with use of lab tools to be able to inspect the fracture surface of the specimen. This is the same behaviour of the failure surface as observed in the DCB tests.

Table 3 shows an overview of the average results obtained from the specimens tested with the RWD test method, where F_{push} and θ_c are the average values measured between d_{ini} and d_{lim} and are the test results' output values used in the RWD force and RWD J-integral data reduction methods to determine fracture toughness.

3.3. Manual loaded RWD test

The force and energy release rate against the roller wedge displacement curves of the two specimens tested with the RWD test setup loaded by manually driving the roller wedge into the specimen are shown in Fig. 14. The initial stiffness of all three specimens are very similar. After the peak force, the measured force of both specimens converges to 90 N, and the energy release rates to 3 N/mm. The same type of plots, as with the RWD test, are plotted in Fig. 15, the energy release rate against crack extension is plotted (R-curve), and in Fig. 16 the energy release rate calculated with the RWD J-integral method.

Table 4 shows the average values from the crack propagation phase. It can be observed that the average calculated fracture toughness using the RWD force data reduction method is significantly higher compared to the average fracture toughness obtained with the RWD J-integral method.

After the test, the displacement data from the LVDT was used to determine the actual displacement rate applied for the RWD manual test. Fig. 17 shows the slope of the displacement–time plot which equals the displacement rate. For RWD-M_01, this is 41.4 mm/min (0.69 mm/s), for RWD-M_02 and RWD-M_03 this is 36.6 mm/min (0.61 mm/s). A test machine can control a displacement rate very precisely, it is more difficult to do the manual test at a constant and pre-determined displacement rate using a spanner to rotate a threaded bar by hand. As can be seen in Fig. 17, the displacement rate over the whole test appears to be constant, but there are small fluctuations visible in the plotted lines.

3.4. Summary of results for ERR of DCB, RWD and RWD manual load

An overview of the average fracture toughness values for the different test methods and data reduction methods is shown in Fig. 18. With a similar standard deviation, the CBT and DCB J-integral methods correlate well for the DCB test. For the RWD test, the RWD force and RWD J-integral data reduction methods do not correlate as well with the benchmark fracture toughness from the DCB test: the RWD force data reduction method is 11% higher and the RWD J-integral method 15% lower compared to the DCB results. For the RWD manual test, the difference increases to 20% for the RWD force data reduction method while the difference remains similar at 14% lower compared to the DCB result for the RWD J-integral method. Looking at the results for both RWD force methods (test machine and manual), there is a 8% increase in measured fracture toughness measured when the RWD manual test is compared to the RWD machine

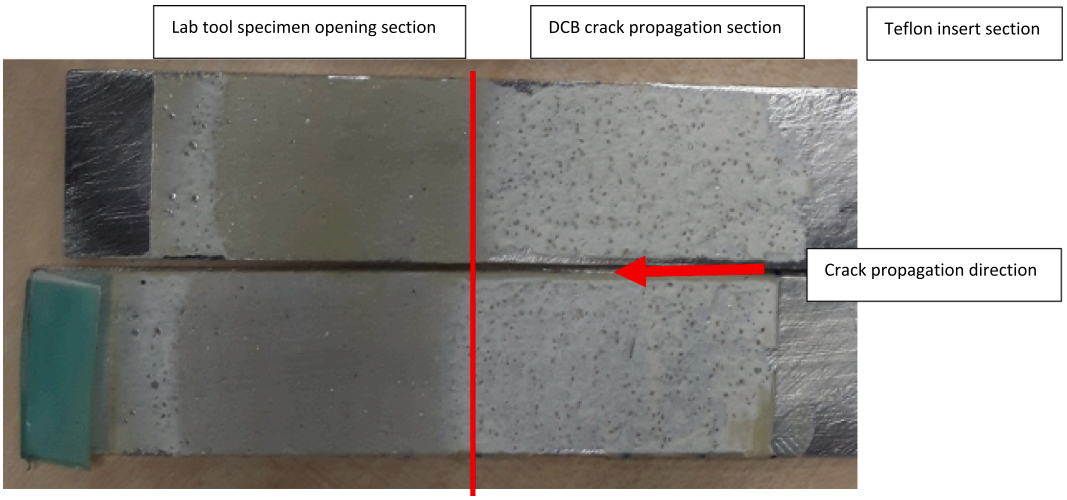

Fig. 13. Cohesive fracture surface of specimen RWD_01. To the right of the red line the adhesive is fractured with the roller wedge, while to the left of the red line the specimen was fractured post-test by splitting the adherends completely with lab tools to be able to inspect the fracture surface (later not part of the test).

Table 3
Overview of average RWD test results. The standard deviations in the column are the standard deviations found for the result of one specimen. The standard deviation in the last row is the standard deviation found when taking the average value for all specimens tested.

Specimen	F_{push}(N)		θ_c(°)		G_c– RWD force (N/mm)		G_c– RWD J-int (N/mm)	
	Avg.	Std. Dev.	Avg.	Std. Dev.	Avg.	Std. Dev.	Avg.	Std. Dev.
RWD_01	88.81	3.76	5.50	0.07	3.020	0.122	2.161	0.114
RWD_02	86.66	5.15	5.64	0.04	2.945	0.167	2.413	0.070
RWD_03	94.56	9.60	5.59	0.13	3.201	0.310	2.574	0.229
RWD_04	85.06	8.58	5.43	0.11	2.896	0.278	2.138	0.177
Average:	88.77		5.54		3.016		2.322	
Std. Dev.	3.60		0.08		0.120		0.180	

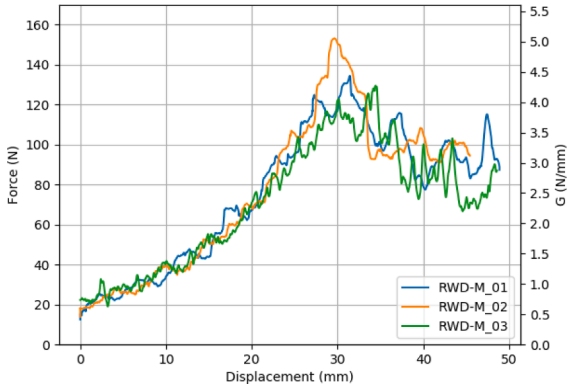

Fig. 14. Force and energy release rate vs. wedge displacement curves of manually loaded RWD specimens.

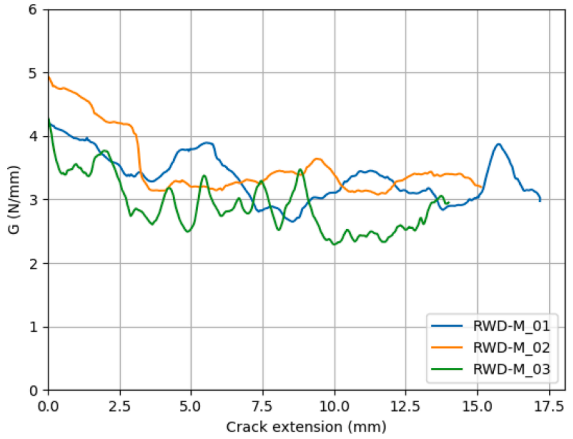

Fig. 15. Resistance curves (R-curves) of RWD manually loaded specimens.

test.

4. Discussion

In this section, observations from the test results and the RWD methods are discussed. Some parameters concerning sensitivity on the fracture toughness data reduction method are discussed. Finally, the RWD manually loaded test is discussed and compared to the RWD machine loaded test.

4.1. Simplified vs exact contact point for the roller wedge

As mentioned in section 2, the diameter of the roller wedge rollers are assumed to be small enough that the error introduced by using the simplified contact point and RWD force data reduction method does not result in a significant error in the calculation of the

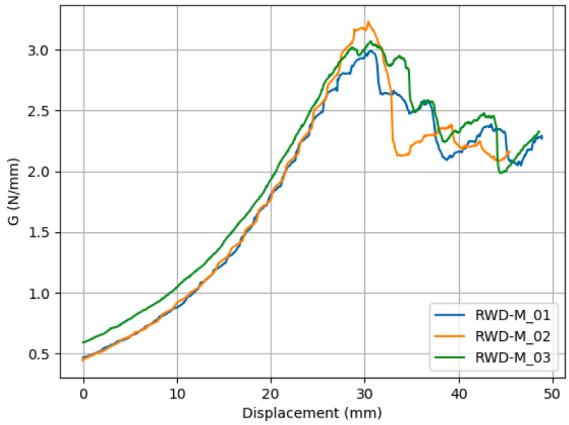

Fig. 16. Energy release rate vs. roller wedge displacement of RWD manually loaded specimens determined with the RWD J-integral method.

Table 4
Overview of average RWD manually loaded specimen test results. The standard deviations in the column are the standard deviations found for the result of one specimen. The standard deviation in the last row is the standard deviation found when taking the average value for all specimens tested.

Specimen	F_{push}(N)		θ_c(°)		G_c– RWD force (N/mm)		G_c– RWD J-int (N/mm)	
	Avg.	Std. Dev.	Avg.	Std. Dev.	Avg.	Std. Dev.	Avg.	Std. Dev.
RWD-M_01	98.36	11.6	5.59	0.11	3.328	0.374	2.324	0.186
RWD-M_02	105.58	16.02	5.57	0.18	3.550	0.511	2.360	0.323
RWD-M_03	84.78	11.35	5.41	0.1	2.878	0.367	2.313	0.161
Average:	96.24		5.523		3.252		2.332	
Std. Dev.	8.623		0.081		0.280		0.020	

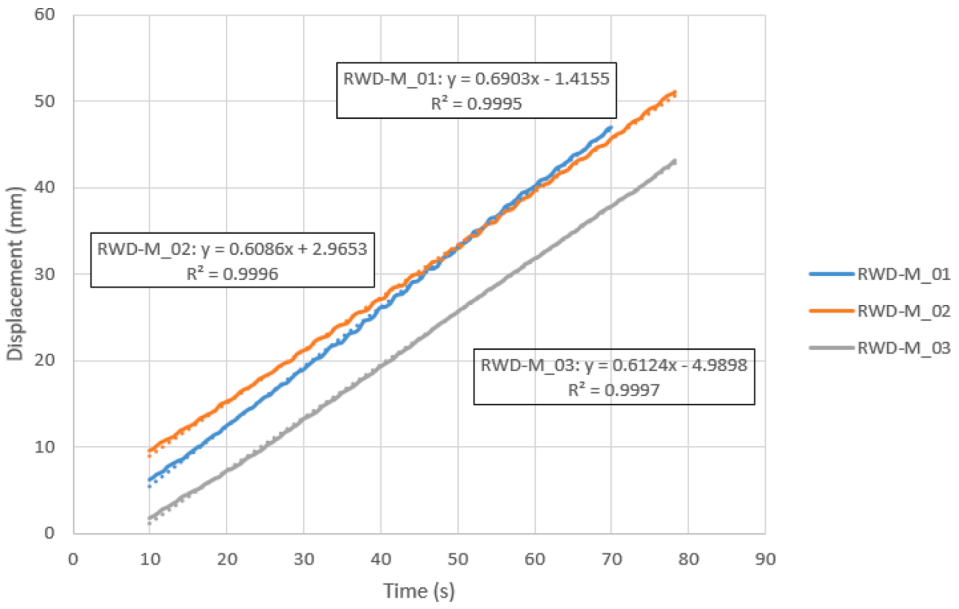

Fig. 17. Displacement-time plot of RWD manual test with the slope indicated, which equals the displacement rate.

energy release rate. The graph to the left in Fig. 19 shows there is no visible difference for the determination of the energy release rate using the exact (G_e) or simplified contact point (G) [6,20], the blue and orange lines are practically on top of each other. This is also visible in the graph to the right in Fig. 19, where the numerically solved crack length for the simplified and exact contact point are shown, a and a_e respectively. During the crack propagation phase the difference is less than 1% and, therefore, the simplified method is used for the RWD test setup. There is a more significant difference between the crack length a and the corrected crack length a_c

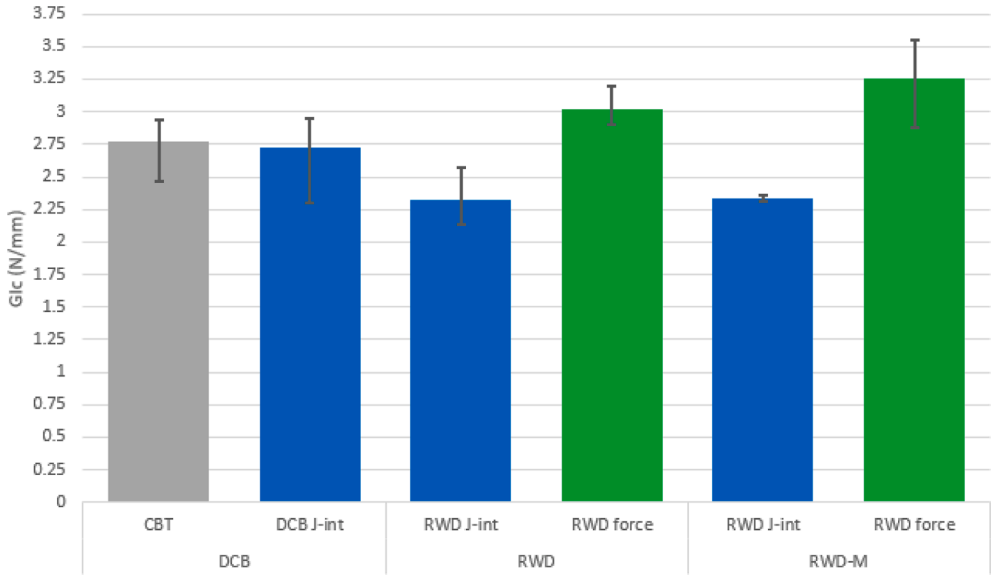

Fig. 18. Overview of average fracture toughness (and minimum and maximum values) results for the DCB, RWD and RWD Manual tests when using different data reduction methods (CBT, RWD J-int and RWD force).

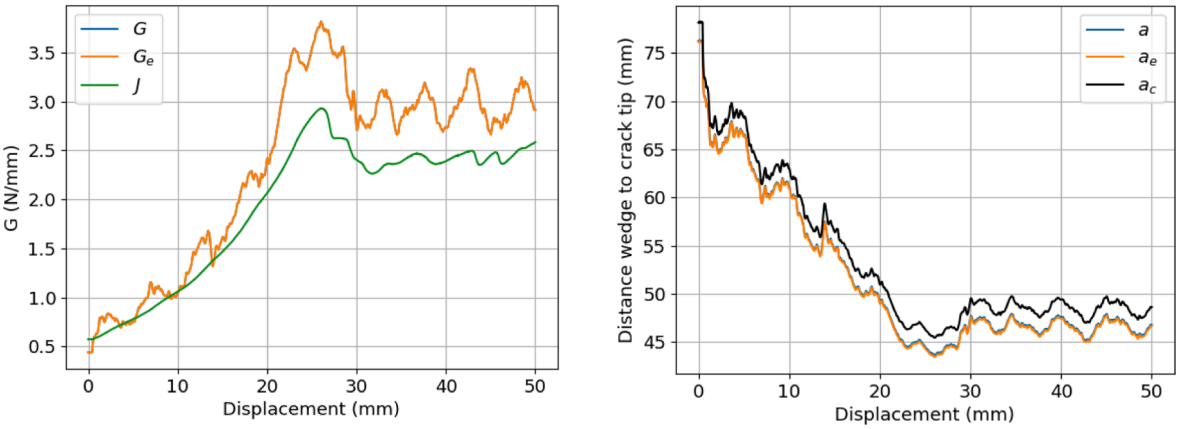

Fig. 19. Left: Specimen RWD_02 showing the difference between using the simplified and exact contact point for the RWD force data reduction method. Right: specimen RWD_01 plot of the numerically solved crack length with the simplified contact point a, for the exact contact point a_e and the corrected crack length..a_c

(equation (3)), therefore, the correction of the crack length cannot be neglected.

4.2. Overestimation of the calculated ERR when the RWD data reduction method is used

During the crack propagation phase there is a significant difference in the energy release rate determined with the RWD force reduction method and the RWD J-integral (Fig. 19 left). The roller wedge rollers have a low rolling resistance and it is assumed that this is much lower compared to, for instance, a sliding wedge which has a typical friction coefficient of about 0.3 (metal on metal) [20]. With the roller wedge, the energy dissipated by the test setup is considered to be low enough to be neglected and therefore the friction coefficient μ in the data reduction method is taken as zero [21] (as described in section 2.1). However, the energy addressed to the fracture toughness is higher compared to the J-integral, and thus energy has to be dissipated somewhere else in the system. The assumption of zero friction for a roller wedge, as proposed by Glessner et al. [21] seems to overestimate the calculated fracture toughness. One of the most likely locations for energy loss are the roller wedge rollers. It is not easy to determine the energy loss caused by rolling resistance. There could be different factors that influence such resistance, for instance, the type of load, wheel diameter, roller material/hardness, adherend material/finish and/or adherend surface conditions [28]. During the post-processing of the test results with the RWD force data reduction method, a value for the friction coefficient μ of 0.02 was found. Implementing this value makes the results of the energy release rate determined with the RWD force data reduction method correlate better with the RWD J-

integral method, as can be seen in Fig. 20. A friction coefficient of 0.02 is a small value compared to the friction coefficient of a sliding wedge, although it is clear from the results that the energy loss due to the rolling resistance of the rollers cannot be neglected in the RWD force data reduction method.

4.3. Sensitivity of the measured rotation angle and force

The RWD J-integral data reduction method presented in section 2.1 (equation (10)) has only the adherend rotation angle θ as the required measured value from the test. The average measured angle of the RWD specimens is 5.6°with a standard deviation of 0.11. The RWD force data reduction only has the measured force F_{Push} as an input value which is required from the test results. The average measured F_{Push} of the RWD specimens is 89 N with a standard deviation of 3.4. For the RWD J-integral and RWD force data reduction method the spread measured for θ or F_{Push} is amplified differently when the fracture toughness for a specimen is calculated, due to the behaviour of the data reduction methods, which is linear for the RWD force and exponential for the RWD J-int. The average measured force (89 N) and angle (5.6°) are normalized to 1. The same is done for the fracture toughness obtained with both data reduction methods using the average measured force and angle. This is depicted in Fig. 21, where both data reduction methods are plotted with the normalized average measured test input value (θ and F_{Push}) against the normalized calculated energy release rate. By using equation (6) presented in section 2.1, Fig. 21 is plotted over a range from zero to two times the normalized average force measured for the RWD specimens. Equation (10) from section 2.1 is also plotted in Fig. 21 over a range from zero to two times the normalized average θ measured for the RWD specimens. With Fig. 21 it is intended to show the difference of both data reduction methods in a qualitative way. The standard deviation is used to show the effect of an error or variation in the measurement on the calculation of the fracture toughness. A range of four times the standard deviation (4*SD) from the average can be applied to check the effect on the calculated fracture toughness [29]. Expressing the 4*SD as a fraction of the average for θ and F_{Push}, this becomes 0.08 and 0.15, respectively, which are shown in Fig. 21 as dotted lines for the θ and dashed lines for F_{Push}. It can be observed that the standard deviation for the θ is lower than the standard deviation of F_{Push} measured over all the RWD specimens, but that the spread obtained when calculating the fracture toughness higher for the RWD J-integral data reduction method compared to the RWD force data reduction. This means that, compared to the RWD J-integral data reduction method, the RWD force data reduction method is less affected by spread in the test measurement data and, therefore, is a more robust data reduction method. Another factor that increases the possible error in the RWD J-integral is the measurement of the θ_{ini} as described in section 3.2. The inclinometers are situated at the adherend tips of the non-adhesive side of the specimen, the initial angle of the adherend tips need to be determined for the RWD J-integral data reduction method. It is very difficult to measure the correct thickness of the specimen at the adherend tips when there is no adhesive present. Therefore, it is assumed the adherends are completely straight so the initial angle of θ can be calculated by measuring the specimen thickness at two points where there is adhesive located. Since the average found θ_{ini} is small, also a small estimation error on the straightness of adherends has a significant effect on the fracture toughness calculation. Potentially, this could also explain why there is a difference observed in the results of the RWD J-integral and DCB J-integral data reduction method, because the DCB J-integral does not require an initial θ correction.

4.4. Selecting the location of d_{ini}

Another factor that influences the calculated fracture toughness of a specimen is where the location of d_{ini} is selected. As described in section 3.2 and shown in Fig. 10, the location of d_{ini} is selected at the infliction point that can be observed in the rotation angle graphs of the inclinometers, which also correlates with the peak force in the force–displacement curve. However, this infliction point is not always very clear, especially when the location of d_{ini} is selected based on the force measurement as required in the RWD force data reduction method. For example, take specimen RWD_02 shown in Fig. 22, in the lefthand plot the d_{ini} is taken at the first infliction point but then the rotation angle increases slightly more, followed by a second infliction point. It can also be observed in the

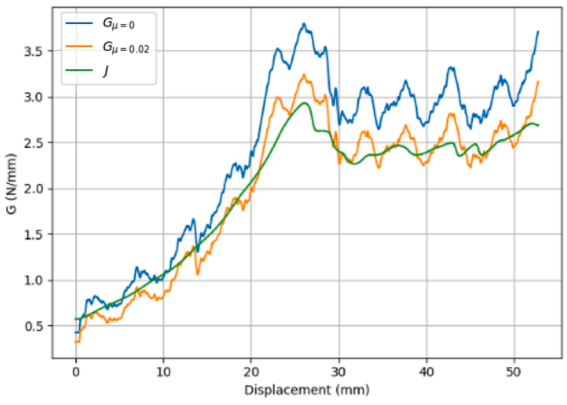

Fig. 20. Effect of friction parameter μ on the energy release rate G, results from specimen RWD_01 where the RWD J-integral functions as a reference value.

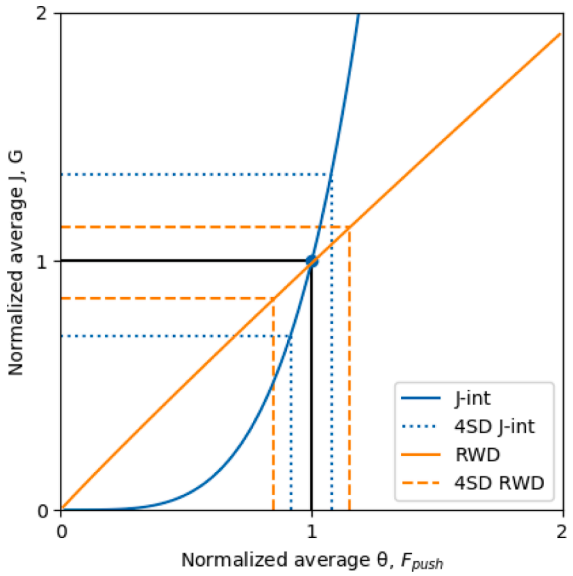

Fig. 21. Sensitivity of RWD J-integral data reduction method compared to RWD force data reduction method with the normalized average angle θ and force F_{Push} plotted against the normalized average calculated J and G.

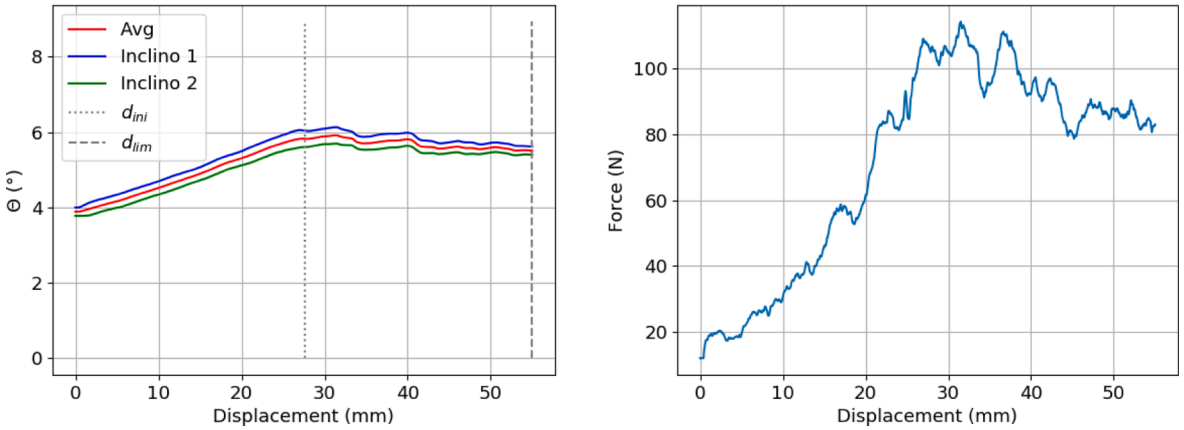

Fig. 22. Specimen RWD_03. Left: adherend rotation angle plot with d_{ini} and d_{lim} cut-off displacements indicated with dashed lines. Right: force–displacement plot showing multiple peaks at maximum force before the force declines.

force–displacement curve, Fig. 22 righthand plot, that there are three peaks at a similar force before the force declines to a more stable level later in the test. All the specimens tested show an initial high peak and this is very likely to be material-specific behaviour. However, for the force measurement most specimens show a clearer after-peak phase compared to the example specimen RWD_03.

The difference between the measured peak force and the average force measured later during the more stable phase of the test is more than 10% for most specimens. Therefore, including part of the peak will have an influence on the average calculated fracture toughness of that specific specimen. Consequently, a conservative approach could be taken where the d_{ini} line is selected far enough from the initial peak. However, this could result in a rather short measuring range for the fracture toughness calculation, and due to the fluctuations observed it is desirable to have a long crack propagation phase. Since d_{lim} is limited by the roller wedge encountering the adhesive of the bonded joint, the available measuring range with this specific wedge and specimen combination could be considered a limitation.

4.5. RWD test compared with the RWD manual test

The RWD test setup is a rather simple experimental test device that requires a DCB-like specimen, a wedge driving force and a load cell to measure the wedge driving force during the test. For the tested specimens, the force did not exceed 160 N as can be observed in Fig. 23. This is an amount of force that can be applied by a human hand. A spanner and a threaded bar are used to apply a certain displacement rate to the roller wedge. For all the specimens, once the peak force is reached, the force then tends to drop sharply. This

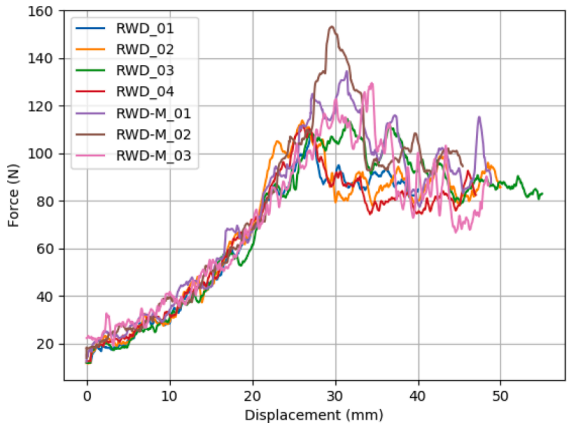

Fig. 23. Force-displacement curve comparison between the RWD test (RWD_01 to RWD_04) and RWD manual test (RWD-M_01 to RWD-M_03) specimens.

effect is more significant for the RWD manual test specimens compared to the RWD machine test specimens. Later, during the test, the measured force of both methods is much more similar, as can be seen in the plotted R-curve in Fig. 24. The overview plot of the different test methods in section 3.4 (Fig. 18) clearly shows a difference in the calculated fracture toughness for the RWD manual and RWD machine tests. The difference in calculated fracture toughness between the RWD manual and machine test method is probably caused by the rate sensitivity of the adhesive. The wedge displacement rate of the manual test is eight times higher compared to the machine test. Furthermore, the displacement rate of the manual test appears constant over the whole test, but locally it shows fluctuation, which likely influences the results when a rate dependent adhesive is tested. The higher peak force observed for the manual test, as can been seen in Fig. 23, and the change of fracture surface visible when the specimens are opened with a high rate using lab tools (Fig. 8 & Fig. 13) also indicate rate sensitivity. If a non-rate sensitive adhesive would be tested, it is possible that the RWD test could be performed without a test machine and skilled technicians, but this deserves further investigation by testing more and different materials with the RWD test method.

5. Conclusions

This work proposes a relatively small and simple mode I fracture toughness test setup that can potentially be used without a test machine to make quick and affordable approximation of the mode I fracture toughness and qualitatively check the bond quality of the bonded joint, for preliminary design purposes. Using a roller wedge instead of a sliding wedge significantly reduces the wedge resistance. Reducing the resistance of a wedge also reduces the force required to drive the wedge into a specimen. A human hand is capable of applying the low driving force to the roller wedge by turning a thread bar with a spanner. This could be done outside a test machine as long as the adhesive is not rate sensitive, since controlling the wedge displacement is difficult.

At first, the assumption was made that the resistance would be small enough that the friction coefficient can be neglected. However, test results between the RWD force data reduction method and the RWD J-integral method have shown that an amount of energy is dissipated by the system and that it cannot be neglected. It is likely that this energy is dissipated by the resistance of the rollers.

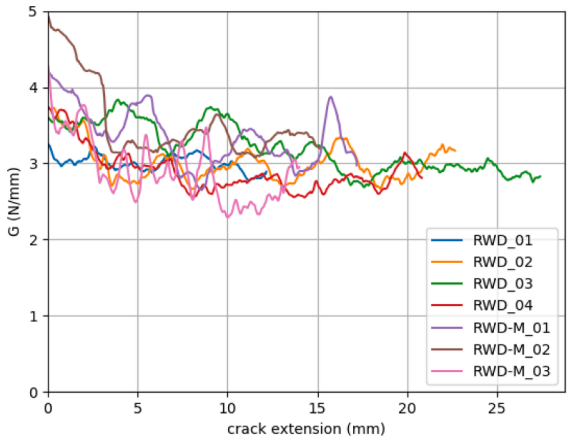

Fig. 24. R-curves of the RWD test (RWD_01 to RWD_04) and RWD manual test (RWD-M_01 to RWD-M_03) specimens.

The sensitivity of the measured rotation angle (θ) and force (F_{Push}) as input values for respectively the RWD J-integral and RWD force reduction methods are discussed. It is observed that a small spread in the measured rotation angle is amplified in the RWD J-integral method introducing a significant error in the fracture toughness calculation. On the other hand, it has been shown that in the RWD force data reduction method, spread in the measurement is not amplified for the calculation of the fracture toughness, making the RWD force data reduction method more robust than the RWD J-integral data reduction method.

The RWD test setup is relatively simple and small, in theory, if a non-rate sensitive specimen is tested, then the RWD manual test could be performed anywhere as long there is a data acquisition system available to log the force applied to the wedge during the test. However, the difference observed between the RWD machine and manual test is likely related to the rate sensitivity of the adhesive used for this research. For rate sensitive adhesives, a small electrical engine that turns the threaded bar, could be introduced to have a more constant wedge displacement, instead of the need of using a test machine. The RWD test method deserves further investigation by testing different materials and at different displacement rates.

CRediT authorship contribution statement

E. Meulman: Writing – review & editing, Writing – original draft, Visualization, Validation, Methodology, Investigation, Formal analysis, Data curation, Conceptualization. **J. Renart:** Writing – review & editing, Methodology, Investigation, Conceptualization. **L. Carreras:** Writing – review & editing, Methodology, Investigation, Conceptualization. **J. Zurbitu:** Writing – review & editing, Methodology, Investigation, Conceptualization.

Declaration of Competing Interest

The authors declare that they have no known competing financial interests or personal relationships that could have appeared to influence the work reported in this paper.

Acknowledgements

The authors would like to acknowledge the support of the Spanish Government, Ministerio de Economia y Competitividad, with funding from the Redbone project under contract RTI2018-099373-B-I00. The first author would also like to acknowledge the support received from the Universitat de Girona and Banco Santander through the fellowship grant IFUdG2021-AE, co-funded by the AMADE research group (GRCT0064). Open Access funding provided thanks to the CRUE-CSIC agreement with Elsevier. The work in this research has been made possible by patent 300352094, PCT/ES2020/070074 made available by IKERLAN, S.COOP. (IKER018) and the Universitat de Girona.

References

[1] L. F. M. da Silva, A. Öchsner, and R. D. Adams, Eds., *Handbook of Adhesion Technology*, 2nd ed. Springer International Publishing AG, 2011. doi: 10.1007/978-3-642-01169-6.
[2] Sørensen BF, Jørgensen K, Jacobsen TK, Østergaard RC. DCB-specimen loaded with uneven bending moments. Int J Fract 2006;141(1-2):163–76.
[3] "ASTM D5528 – 13: Standard test method for mode I interlaminar fracture toughness of unidirectional fiber-reinforced polymer matrix composites," vol. 03, no. Reapproved 2007. American Standard of Testing Methods, pp. 1–12, 2014. doi: 10.1520/D5528-13.2.
[4] "ISO 25217:2009 - Adhesives — Determination of the mode 1 adhesive fracture energy of structural adhesive joints using double cantilever beam and tapered double cantilever beam specimens." p. 24, 2009.
[5] da Silva LFM, Dillard DA, Blackman B, Adams RD, editors. Testing Adhesive Joints: Best Practices. KGaA: First. Wiley-VCH Verlag GmbH & Co; 2012.
[6] Manterola J, Renart J, Zurbitu J, Turon A, Urresti I. Mode I fracture characterization of rigid and flexible bonded joints using an advanced Wedge Driven Test. Mech Mater 2020;148(103534):13. https://doi.org/10.1016/j.mechmat.2020.103534.
[7] Fernández MV, de Moura MFSF, da Silva LFM, Marques AT. Composite bonded joints under mode I fatigue loading. Int J Adhes Adhes 2011;31(5):280–5. https://doi.org/10.1016/j.ijadhadh.2010.10.003.
[8] Sarrado C, Turon A, Costa J, Renart J. An experimental analysis of the fracture behavior of composite bonded joints in terms of cohesive laws. Compos Part A Appl Sci Manuf 2016;90:234–42. https://doi.org/10.1016/j.compositesa.2016.07.004.
[9] Kinloch AJ. Durability of structural adhesives. Netherlands: Springer; 1983.
[10] D. O. Adams, K. L. DeVries, and C. Child, "Durability of adhesively bonded joints for aircraft structures," 2012. http://depts.washington.edu/amtas/events/jams_12/papers/paper-adams_adhesive.pdf.
[11] Broughton W. In: Adhesives in Marine Engineering. Elsevier; 2012. p. 99–154.
[12] "ASTM D3762-03(2010) Standard Test Method for Adhesive-Bonded Surface Durability of Aluminum (Wedge Test) (Withdrawn 2019)." ASTM International, p. 5, 2010. [Online]. Available: https://www.astm.org/Standards/D3762.htm.
[13] Cognard J. The mechanics of the wedge test. J Adhes 1986;20(1):1–13. https://doi.org/10.1080/00218468608073236.
[14] Plausinis D, Spelt JK. Designing for time-dependent crack growth in adhesive joints. Int J Adhes Adhes 1995;15(3):143–54. https://doi.org/10.1016/0143-7496(95)91625-G.
[15] Dillard DA, Pohlit DJ, Jacob GC, Starbuck JM, Kapania RK. On the use of a driven wedge test to acquire dynamic fracture energies of bonded beam specimens. J Adhes 2011;87(4):395–423. https://doi.org/10.1080/00218464.2011.562125.
[16] Brown N, Adams D, Devries L. Test method development for environmental durability of bonded composite joints. The University of Utah; 2013. p. 30.
[17] S. LAZCANO UREÑA, G. SANTACRUZ RODRÍGUEZ, J. A. MAYUGO MAJO, J. COSTA BALANZAT, and J. RENART CANALIAS, "Procedimiento y dispositivo de determinación de la tenacidad a la fractura en un ensayo de introducción y avance forzado de una cuña a través de una unión adhesiva," 2460468, 2014.
[18] Kanninen MF, Popelar CH. Advanced Fracture Mechanics. OXFORD UNIVERSITY PRESS; 1985.
[19] R. Mansour, M. Kannan, G. N. Morscher, F. Abdi, C. Godines, and S. Dormohammadi, "The wedge-loaded double cantilever beam test: A friction based method for measuring interlaminar fracutre properties in ceramic matrix composites," in *Advances in High Temperature Ceramic Matrix Composites and Materials for Sustainable Development*, First edit., vol. CCLXIII, M. Singh, T. Ohji, S. Dong, D. Koch, K. Shimamura, B. Clauss, B. Heidenreich, and J. Akedo, Eds. 2017, pp. 273–282. doi: 10.1002/9781119407270.

[20] Renart J, Costa J, Santacruz G, Lazcano S, Gonzalez E. Measuring fracture energy of interfaces under mode I loading with the wedge driven test. Eng Fract Mech 2020;no. 239:15. https://doi.org/10.1016/j.engfracmech.2020.107210.
[21] Glessner AL, Takemori MT, Vallance MA, Gifford SK. Mode I interlaminar fracture toughness of ud cf composites using a novel wedge-driven delamination design. Compos Mater Fatigue Fract 1989;2:181–200. https://doi.org/10.1520/STP10416S.
[22] Adams D, McCartin H, Sievert Z. Development of Environmental Durability Test Methods for Composite Bonded Joints. *JAMS 2018 Technical Review* The Univeristy of Utah 2018:31.
[23] J. Manterola Najera, J. Zurbitu Gonzalez, M. J. Cabello Ulloa, I. Urresti Ugarteburu, J. Renart Canalias, and A. Turon Travesa, "Procedimiento y aparato para la determinación de la tasa de liberacion de energia de una probeta," 300352094, 2020.
[24] Williams JG. End corrections for orthotropic DCB specimens. Compos Sci Technol 1989;35(4):367–76. https://doi.org/10.1016/0266-3538(89)90058-4.
[25] Paris AJ, Paris PC. Instantaneous evaluation of J and C. Int J Fract 1988;38(1):19–21. https://doi.org/10.1007/BF00034281.
[26] Manterola J, Zurbitu J, Renart J, Turon A, Urresti I. Durability study of flexible bonded joints under stress. Polym Test 2020;88:9. https://doi.org/10.1016/j.polymertesting.2020.106570.
[27] Blackman BRK, Kinloch AJ, Paraschi M, Teo WS. Measuring the mode I adhesive fracture energy, GIc, of structural adhesive joints: The results of an international round-robin. Int J Adhes Adhes 2003;23(4):293–305. https://doi.org/10.1016/S0143-7496(03)00047-2.
[28] D. Lippert and J. Spektor, "Rolling Resistance and Industrial Wheels," *Hamilt. Caster*, no. 888, p. 8, 2013, [Online]. Available: http://www.mhi.org/media/members/14220/130101690137732025.pdf.
[29] Hamby DM. A Review of Techniques for Parameter Sensitivity. Environ Monit Assess 1994;32:135–54. https://doi.org/10.1007/BF00547132.

3. A methodology for the experimental characterization of energy release rate-controlled creep crack growth under mode I loading

E. Meulman[a*], J. Renart[a,c*], L. Carreras[a], J. Zurbitu[b]

[a]AMADE, Polytechnic School, University of Girona, Campus Montilivi, s/n, 17071, Girona, Spain

[b]Ikerlan Technology Research Centre, Basque Research and Technology Alliance (BRTA), Arrasate-Mondragón, Spain

[c]Serra Húnter Fellow, Generalitat de Catalunya, Spain

This paper has been published with open gold access in the international journal of Engineering Fracture Mechanics, vol. 283, no. April, 109222, 2023

Doi: 10.1016/j.engfracmech.2022.108619, ISSN: 0013-7944, Impact Factor: 4.898, ranked 19/138 in the category of Mechanics (1st quartile)

Overview

This chapter describes the proposed methodology for a creep crack growth test method. The RWD test setup presented in the previous chapter is used for this methodology since it is capable of applying a constant energy release rate to an adhesively bonded joint. Resulting in the RWD Creep (RWDC) test.

The goal of the creep crack growth method is to obtain creep crack growth curves, which is achieved by doing multiple tests at different constant energy release rates. To apply a constant energy release rate a weight is placed on top of the roller wedge. The weight will apply a constant load and therefore a constant energy release rate to the specimen during the creep crack growth test. Different specimens are tested with different weights. During the test the crack length increase is determined by measuring the wedge displacement with a visual method and by using an LVDT. After every test the creep crack growth rate can be determined by taking the average slope of crack length increase over time. Plotting the creep crack growth rate found for each specimen on a log-log scale against the energy release rate will provide a creep crack growth rate curve (da/dt versus G). In this work it was observed that the specimens show a transitory and steady-state creep crack growth phase. Therefore, it is advantageous to have a constant energy release rate, since with a changing energy release rate it would be not clear if crack propagation is taking place in the transitory phase or steady-state creep crack growth.

The results have shown that the creep crack growth of the tested adhesive system can be described by a power law. It was also demonstrated the importance of taking creep crack growth into consideration when designing bonded joints, since crack propagation was found at energy release rate levels significantly lower than the fracture toughness. Considering only the mechanical properties found in quasi-static testing will likely overestimate the durability of a bonded joint.

Engineering Fracture Mechanics 283 (2023) 109222

Contents lists available at ScienceDirect

Engineering Fracture Mechanics

journal homepage: www.elsevier.com/locate/engfracmech

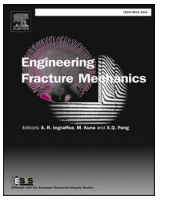

A methodology for the experimental characterization of energy release rate-controlled creep crack growth under mode I loading

E. Meulman [a,*], J. Renart [a,c,*], L. Carreras [a], J. Zurbitu [b]

[a] AMADE, Polytechnic School, University of Girona, Campus Montilivi, s/n, 17071, Girona, Spain
[b] Ikerlan Technology Research Centre, Basque Research and Technology Alliance (BRTA), Arrasate-Mondragón, Spain
[c] Serra Húnter Fellow, Generalitat de Catalunya, Spain

ARTICLE INFO

Keywords:
Bonded joint
Constant energy release rate
Creep crack growth
Fracture surface

ABSTRACT

Understanding the performance of a bonded joint over time is essential for the design of durable bonded joints and maintenance protocols. Viscoelastic creep crack growth and how it affects the mechanical behaviours of an adhesive is relevant information for a durable design. For this purpose, a method to obtain the average crack growth rate (da/dt) as a function of the energy release rate (G) was developed. The proposed roller wedge driven (RWD) creep crack growth methodology can provide creep crack growth rate curves for a constant applied energy release rate. The RWD test setup was designed by the authors to test mode I DCB-like specimens by using a roller wedge. An advantage of using a moving wedge is that, on average, the crack growth rate equals the displacement rate of the wedge. By changing G for different specimens, a G vs da/dt curve can be obtained for the methacrylate adhesive Araldite 2021–1. The power law regression line of the G vs da/dt curve provides a Pariś law-like equation. Data have shown that applying an energy release rate that is relatively low compared to the fracture toughness of Araldite 2021–1, found by quasi-static testing, will result in creep crack growth. Furthermore, a transition from cohesive to adhesive failure has been observed when the applied energy release rate is lowered. For durability design of bonded joints it must be considered that only using data from quasi-static testing will very likely overestimate the durability of the bonded joint.

1. Introduction

Structural adhesive bonds are an interesting alternative to mechanical joints from a design point of view [2]. Using a structural adhesive instead of mechanical fasteners to bond a joint makes the structure lighter, smoother and stress concentrations are reduced. However, using structural adhesives has some limitations, like difficult visual inspection, surface preparation prior bonding, influence of process parameters on the mechanical properties and environmental sensitivity [3]. Understanding the mechanical behaviour of a structural adhesive for different service load cases and environmental conditions is essential to design a durable adhesively bonded joint.

Creep behaviour of polymeric adhesives could be considered as a mechanism that negatively affects the durability of an adhesively bonded joint. Creep is a time and temperature dependent deformation of a stressed material. The level of applied stress and the

* Corresponding authors.
E-mail addresses: edwin.meulman@udg.edu, jordi.renart@udg.edu (J. Renart), laura.carreras@udg.edu (L. Carreras), jzurbitu@ikerlan.es (J. Zurbitu).

https://doi.org/10.1016/j.engfracmech.2023.109222
Received 23 December 2022; Received in revised form 17 March 2023; Accepted 21 March 2023
Available online 24 March 2023

Nomenclature

a_0	initial crack length
B	width of specimen
E_x	longitudinal Younǵs modulus
d	distance from the initial location of the bonded section
da/dt	crack growth rate
$F_{Push\|s}$	force to push the wedge simplified data reduction method
G	energy release rate
G_c	fracture toughness
h	thickness of the adherend
L	specimen length
r_w	radius of the wedge
t_a	bondline thickness
T_g	glass transition temperature
w	wedge displacement
δ_y	opening displacement
χ	crack length correction factor
DCB	Double Cantilever Beam
LVDT	Linear Variable Displacement Transducer
MMA	Methyl Methacrylate
RWD	Roller Wedge Driven

temperature related to the glass transition temperature of the adhesive influence the creep behaviour [4,5]. The analysis of the creep behaviour is relevant because it can occur with an applied stress that is below the yield strength of the material and, in case of polymers, creep can already occur at room temperature. Typically creep deformation passes through three stages. In the primary stage there is relative rapid creep deformation. In the secondary stage a linear increase in deformation relating to time can be observed. And in the tertiary phase the deformation increases exponentially which, could follow by sudden creep rupture [4,6].

The situation is different if a crack is already present in the adhesive of a bonded joint. For a constant level of load over time, creep behaviour at the crack tip could cause the crack to propagate, referred to as viscoelastic creep crack growth [7]. Polymer adhesives behave like a fluid (viscous) at low deformation rates and as an (elastic) solid at high deformation rates, therefore referring to viscoelastic behaviour of the material [8]. It is the viscoelastic deformation in the fracture process zone that provides the possibility for a crack to growth over time [7]. Thus, understanding the viscoelastic creep crack growth and how it affects the performance of the bonded joint over time is essential for the design of durable bonded joints and maintenance protocols.

For design purposes, it would be useful to have a creep crack growth curve for a certain adhesive system to predict creep crack growth behaviour, similar like the Pariś law-based expression [9]. Indeed, similar approaches have been developed to predict creep crack growth rate (da/dt) for a certain applied energy release rate [4,10,11]. For mode I it has been tried to obtain crack growth rates from the Boeing wedge test (ASTM D-3762) [12]. A wedge remains stationary in a DCB-like specimen and crack increment is measured over time [10,13]. However, with increasing crack length, the energy release rate decreases, resulting in a reduced crack growth rate. Also it has been tried to obtain crack growth rate from displacement controlled DCB and TDCB test where very slow displacement rates are applied, trying to keep the same load over time [14,15].

Considering creep crack growth, ideally the specimen should be loaded under a constant energy release rate, so crack growth rate predictions can be made based on the sustained applied load or stress state that is expected in a bonded joint during its service life. In this direction, there are standards for creep testing on polymers and bonded joints like, ASTM D1780 – 99, ASTM D2294 – 96 and ISO 15109:1998. In these standards a single lap joint is loaded in tension, so effectively testing the bonded joint in mode II. However, as far as the authors know, there is no standard for testing a bonded joint for creep crack growth in mode I. In this paper we propose a methodology for creep crack growth testing which, is based on the roller wedge driven (RWD) test methodology [1]. The idea of this method is that the roller wedge follows the crack tip during crack propagation. Following that when applying a constant load to the wedge, the energy release rate remains constant at the crack tip. It is assumed that on average the roller wedge displacement equals the crack length increase. Combining these two properties of the RWD result in a proposal for a new RWD creep crack growth methodology that can provide creep crack growth rate curves, useful for durability design purposes.

In section 2, we present the RWD creep crack growth test method, how the creep crack growth rate is determined and the experimental test campaign we carried out to prove the validity of the method. In section 3, we describe the RWD creep crack growth test results, which we discuss in section 4. In section 5 we conclude the work done for this manuscript.

2. Methodology

2.1. The roller wedge Driven (RWD) creep crack growth test

The RWD test setup (Fig. 1, left) was designed to test mode I DCB-like specimens by using a roller wedge. The roller wedge consists out of three rollers (Fig. 1, right) [1]. The specimen was clamped in vertical position. Bearings in the wedge support rod and a carriage system made sure unwanted loads on the specimen were avoided (mode II & III). The RWD test setup was also used for creep crack growth testing, where on top of the wedge a weight was placed (Fig. 1, left). When crack growth takes place, the wedge will follow that crack tip, while the applied load remains constant during the test.

The applied load to the wedge was measured with a load cell (HBM U9C-500) that has a precision of 0.2 %. The displacement of the wedge was measured with a HBM WA-T-50 linear variable displacement transducer (LVDT, 1 % precision) that was connected to the horizontal loading beam of the roller wedge. The displacement was also visually tracked by a camera (Logitech C920). The camera took pictures of two reference points every 120 min (see Fig. 1, left). The images were analysed with the ImageJ software to measure the displacement of the roller wedge. The software was used to measure pixels, which was done by user input, and transformed into distances. Two reference dots were used to calibrate the pixel measurement in the photos. In the rest of this manuscript the visual measurement method refers to the wedge displacement data obtained by the camera, and the LVDT measurement method refers to the data obtained by the LVDT. A second camera (Canon 550D and macro lens EF100) was used to take images from the adhesive to capture the propagation of the crack through the adhesive. For the quasi-static pre-cracking of the specimens, a picture was taken every-two seconds and for the creep crack growth test every 8 min. The RWD manual test method was used to pre-crack the specimen for about 10 to 15 mm of crack length before the creep crack growth test was initiated. For a more detailed description of the RWD manual test method, as well as the RWD test setup design, the reader is referred to the work of Meulman et al. [1].

In that same manuscript, the equation to determine the energy release rate (G) for the RWD test reads [1]:

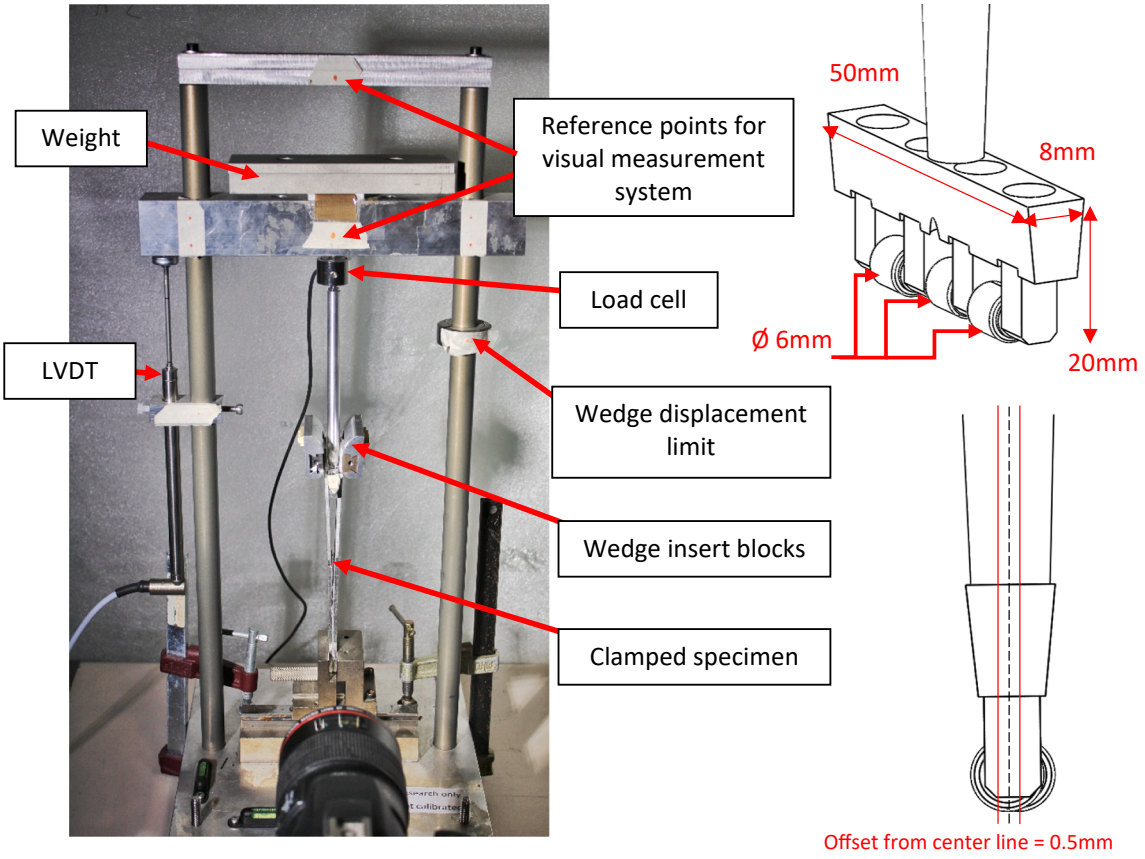

Fig. 1. Left: RWD creep crack growth test where the roller wedge was loaded with a weight. (The Logitech C920 camera for visual measurement is behind Canon 550D camera and not visible in the picture). Right: Sketch of the roller wedge design with three rollers and the offset of the rollers indicated [1].

$$G = \frac{3}{4}\frac{E_x h^3 \delta_y^2}{\left(\sqrt[4]{\frac{3}{4}\frac{E_x B h^3 {r_w}^2}{F_{Push|s}}} + \chi h\right)^4} \tag{1}$$

where E_x is the longitudinal Younǵs modulus of the adherend, h is the thickness of the adherend, δ_y is the opening displacement at the contact point between the roller and the adherend, B is the width of the specimen, r_w is the wedge tip radius (i.e., the roller radius), χ is the crack length correction factor [16], $F_{Push|s}$ is the applied force to the roller wedge measured with the load cell. It must be mentioned that the RWD force data reduction assumes zero friction in the system because of to the use of the roller wedge. The bondline thickness is indirectly considered in the equation, which is described in more detail in the RWD test methodology [1]. During the creep crack growth test the applied force provided by the weight remains constant, this results in a constant energy release rate during the test, since the other parameters of equation (1) are constants.

2.2. Crack growth rate

From the creep crack growth test, we want to obtain the average crack growth rate (da/dt) as a function of the energy release rate (G). An advantage of using a moving wedge is that, on average, the crack growth rate equals the displacement rate of the wedge, which will be discussed in more detail in section 4.1. When a given level of G is applied to a specimen so that it results in creep cracking of the adhesive, then the crack length can be measured over time and average da/dt can be determined. By changing G for different specimens a log–log linear regression G vs da/dt curve can be obtained, which governs the damage evolution over time in constant load tests.

2.3. Experimental testing campaign

To demonstrate the feasibility of the methodology, an experimental testing campaign was carried out with bonded joints between metallic adherends. Specimens were in-house manufactured by bonding aluminium Al 7075-T6 adherends with Araldite 2021–1. The same type of specimens were used in the RWD test design testing campaign [1]. Araldite 2021–1 is a methacrylate-based rigid structural adhesive with a glass transition temperature of 80 °C. The aluminium adherends were 200 mm long, 25 mm wide and 3 mm thick and had a Young's modulus of 71 GPa, shear modulus of 27GPa and a yield strength of 550 MPa [1,17]. The bondline thickness t_a was between 0.4 and 0.7 mm (Fig. 2, Table 1).

We used a sandblaster with brown fused aluminium oxide of 60 μm for surface treatment of the adherends. Afterwards, the adherends were cleaned with acetone and they were degreased with high grade alcohol just before applying the adhesive. Teflon spacers were used to achieve the desired bondline thickness. The Teflon spacer was placed in such a way that an initial crack length (a_0) of 100 mm was created. The adhesive was cured in an oven at 60 °C for 16 h. The specimens were manufactured and tested in the ISO17025 and NADCAP certified AMADE research group testing laboratory at the University of Girona. In the laboratory, there was an ambient temperature and relative humidity $(23 \pm 2)^{\circ} C$ and (50 ± 5) % RH, respectively. A variety of weight levels was applied to different specimens. The weights were selected based on the data obtained during the previous RWD experimental test campaign and are shown in Table 1.

3. Results

In this section, we present the results of the RWD creep crack growth test performed on adhesively bonded joints. First, the obtained crack growth versus time data is described. From this data, the average crack growth rate can be obtained, which is then plotted against the normalised applied energy release rate to be able to plot a log–log linear curve.

3.1. RWD creep crack growth test

The wedge displacement against time for specimen RWD-C_03 is shown in Fig. 3, which is representative for a specimen where the

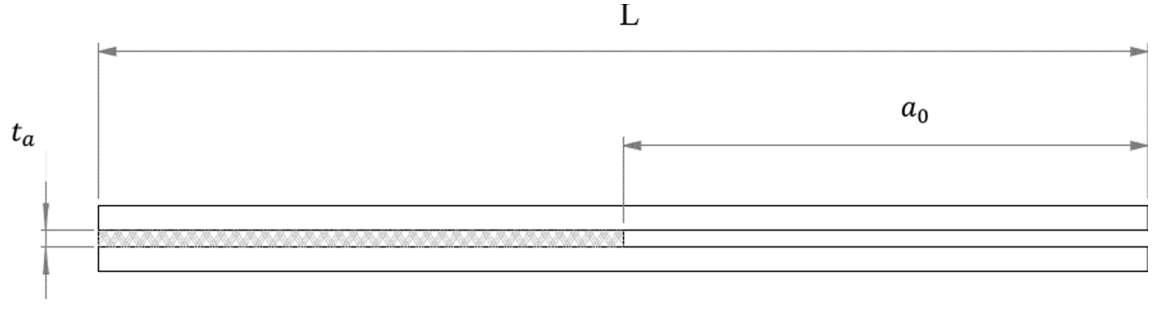

Fig. 2. DCB-like specimen geometry for the RWD creep crack growth test with L the specimen length, a_0 the initial crack length and t_a the bondline thickness [1].

Table 1
Overview table of tested specimens.

Specimen	Weight applied (N)	t_a (mm)	Measurement method
RWD-C_01	31	0.55 ± 0.02	Visual + LVDT
RWD-C_02	48	0.49 ± 0.03	Visual + LVDT
RWD-C_03	57	0.43 ± 0.04	Visual
RWD-C_04	70	0.51 ± 0.11	Visual + LVDT
RWD-C_05	80	0.51 ± 0.02	Visual
RWD-C_06	22	0.62 ± 0.06	Visual + LVDT
RWD-C_07	28	0.62 ± 0.06	Visual + LVDT
RWD-C_08	21	0.59 ± 0.06	Visual + LVDT
RWD-C_09	26	0.68 ± 0.03	Visual + LVDT

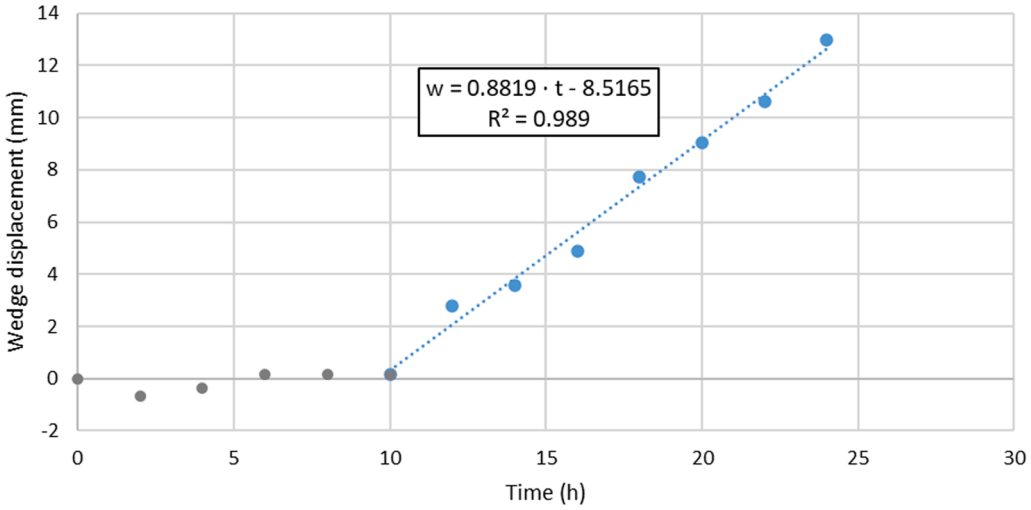

Fig. 3. Wedge displacement (w) in millimeters against time (t) in hours of specimen RWD-C_03 measured with the visual measurement method.

wedge displacement was only measured with the visual measurement method. It can be seen in Fig. 3 that there was first a transitory period where no displacement of the wedge was observed. After the transitory period, a linear trend line shows that, on average, the crack growths with a constant rate. The slope of the linear trend line can be considered as the average crack growth rate related to the

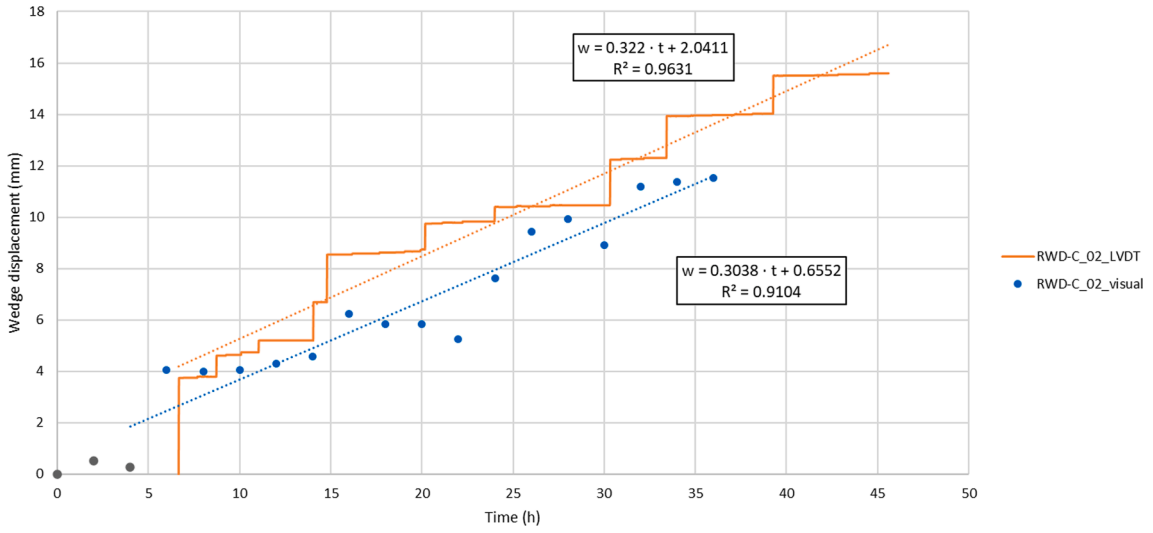

Fig. 4. Wedge displacement (w) in millimeters against time (t) in hours of specimen RWD-C_02 measured with the visual measurement method and the LVDT.

specific weight that was applied to the specimen (Table 1).

For specimen RWD-C_02 also the wedge displacement was measured with the LVDT (Fig. 4). The LVDT measurement is continuously, contrary to the visual measurement method. The LVDT measurement shows that the crack in this type of adhesive is not growing in a constant manner but rather in small jumps. If again a linear trendline is plotted it can be seen that the discontinue crack increments over a longer period follow on average a linear increase. In both the visual and LVDT measurement the transitory phase was not considered in determining the average crack growth rate, since no visible cracking took place during that phase. Comparing the wedge displacement data from the visual measurement method and the LVDT, it can be noticed that there is some off-set in the absolute wedge displacement measurement but that the slope obtained from both measurement methods are similar, resulting into close values of the average da/dt.

Table 2 shows an overview of the average crack growth rate obtained for each specimen and the corresponding energy release rate applied. The energy release rate is directly related to applied weight and is calculated with RWD data reduction method (equation (1). There is no visual measurement data available for specimen RWD-C_06 to RWD-C_09 because the displacements are too small to be able to measure it with the visual measurement method.

Plotting the average crack growth rate against the energy release rate for both measurement methods on a log–log scale produces Fig. 5. For the x-axis G is normalised with fracture toughness (G_c) that was found with the RWD test method in the previous test campaign and is 3.016 N/mm [1]. The specimens fit well on a power trend line which is presented as a straight line on a log–log scale. Close to $G/G_c = 0.3$ there is a sharp drop in the average crack growth rate and the power trend line is no longer being applicable for the specimens (RWD-C_06 to RWD-C_09) loaded below this threshold energy release rate. The specimens tested below this threshold had so low wedge displacement values that cracking of the adhesive could not be determined with certainty, therefore it is assumed that da/dt is equal to 0 mm/h. The standard error found for the power law coefficients are 0.319 and 0.465 for the LVDT method. For the visual method the standard error is 0.217 and 0.384.

3.2. Fracture surface and transition

After the tests were run, we opened the specimens and took pictures of the fractured surfaces. In each specimen, three different regions could be observed and are shown in Fig. 6. First, the pre-crack created with the RWD manual test method (region 1). A fracture surface with a cohesive failure was created. After the pre-cracking, the weight was placed on top of the wedge (Fig. 1, left) to initiate the RWD creep crack growth test (region 2). A transition was visible from cohesive to mostly adhesive failure. The specimen was completely opened with lab tools to inspect the fracture surfaces (region 3). Here a transition to cohesive failure was observed again, however this part was not intended to be part of the test and was solely to open the specimen for inspection. On both ends of the specimens, unbonded section (region 0), a Teflon spacer was located during manufacturing to control the bondline thickness. The spacer on the left side was removed before testing because that is the side of the specimen where the roller wedge was inserted. In region 0, the scratches on the aluminium adherends were caused by the lab tools during completely opening of the specimen, after the test was already finished.

In Fig. 7, fracture surfaces of specimens RWD-C_01 to 05 are presented where the specimens from left to right were tested with increasing load levels. Increasing load levels, and therefore increasing energy release rates as can be seen in Table 2. Fig. 5 shows that, when the energy release is increased also the average crack growth rate increases. It appears that, when the average crack growth rate increases, the fracture surface transitions from mostly adhesive to cohesive failure. It can be seen that specimens RWD-C_02 to 04 start to show an increasing cohesive part at the centre line of the specimen. Specimen RWD-C_05 shows for about 5 mm of crack propagation a clear cohesive failure and then transitions at the centre line to what seems to be more adhesive failure. However, specimen RWD-C_05 became unstable after about 5 mm of stable creep crack growth and the specimen failed completely until the wedge displacement limit. Therefore, this part of the fracture surface is not considered in the results.

4. Discussion

In this section, the results of the RWD creep crack growth tests are discussed. First, the crazing zone that was observed during

Table 2
Overview of specimen test data.

Specimen	G– RWD (N/mm)	da/dt_visual(mm/h)	St. Error (mm/h)	da/dt_LVDT(mm/h)	St. Error (mm/h)
RWD-C_01	1.09	0.05*	0.0073	0.09	0.0004
RWD-C_02	1.67	0.30	0.0246	0.32	0.0013
RWD-C_03	1.97	0.88	0.0379	–	–
RWD-C_04	2.38	1.07	0.1286	1.62	0.0396
RWD-C_05	2.71	3.04	0.1676	–	–
RWD-C_06	0.79	+	+	0.00017	–
RWD-C_07	1.01	+	+	0.00019	–
RWD-C_08	0.77	+	+	0.0001	–
RWD-C_09	0.93	+	+	0.0003	–

*Only data available of last part of the test, + displacement not measurable with visual measurement method.

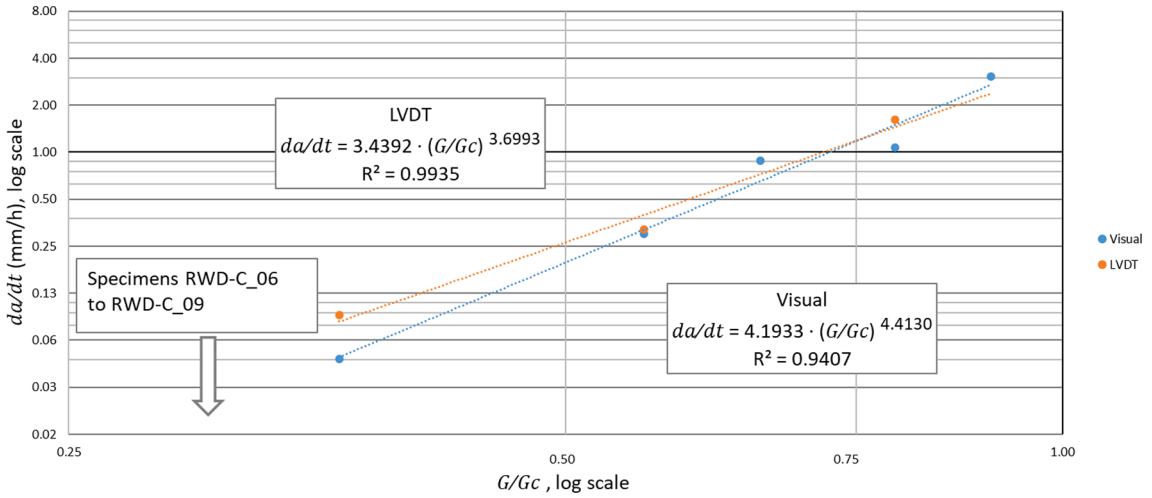

Fig. 5. Average crack growth rate (da/dt) against normalised energy release rate (G/G_c) on a log–log scale of the visual and LVDT measurement method. Specimens RWD-C_06 to RWD-C_09 are considered to have a da/dt of 0 mm/h and cannot be plotted on the log scale.

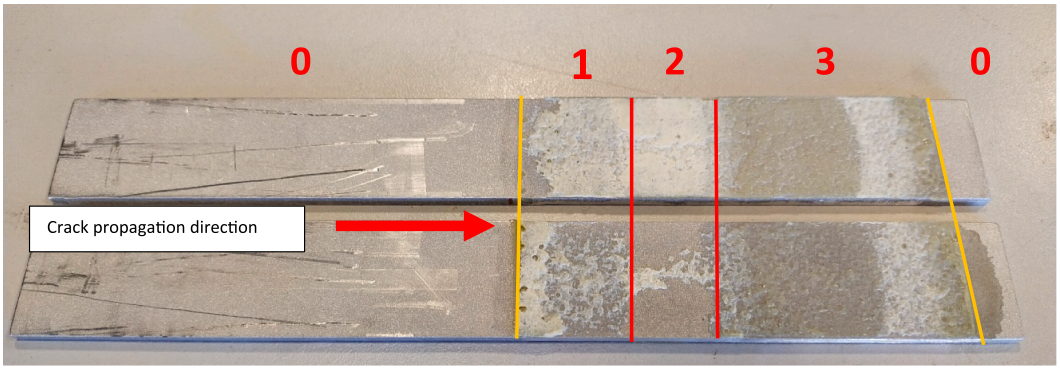

Fig. 6. Specimen RWD-C_03, 0: Teflon insert region, 1: Pre-crack region, 2: Creep crack propagation region, 3: Lab tool specimen opening region.

testing and the transitory phase before crack growth are discussed. Secondly, the rate sensitivity and fracture surfaces of the used adhesive system. Finally, the obtained average crack growth rates and the resulting log–log linear creep crack growth rate against normalised energy release rate curves.

4.1. Crazing zone

The two-component adhesive (Araldite 2021–1) that bonds the two aluminium adherends is a with rubber particles toughened methyl methacrylate (MMA)-based adhesive. When the adhesive was mixed during manufacturing it had a yellow colour, after curing and forming the bondline between the adherends it appeared to be greyish. It was noticed during testing that before a crack visual appeared the adhesive became whiter. When the crack tip became visible, the white area seemed to continue to increase with the same rate as the crack tip was going through the adhesive (Fig. 8).

By using the visual measurement (same method as the wedge displacement measurement described in section 2.1), the increase in the whitened area in the adhesive and the distance crack tip has moved through the adhesive was measured during the test and plotted in Fig. 9, which are the results of pre-cracking specimen RWD-C_05. In the first part of the pre-cracking the wedge was pressed into the specimen where the load on the adhesive was still too low to form a visual whiting zone. Then the adhesive started to turn white, and the area grew while there was no crack visible. After the crack became visible and grew, it followed a linear trendline. The white area in front of the crack grew with a similar linear trend. In literature, the same whiting of these type of materials have been reported and is very likely caused by micro voids forming in the adhesive in the zone in front of the crack tip [18]. As mentioned, Araldite 2021–1 is a rubber toughened adhesive, the rubber particles can enhance the forming of voids and result in a random multiplication of void initiation. The adhesive in between the voids starts to locally stretch and aligning the polymer chains forming so called fibrils [19–22]. The aligning of the chains and the forming of voids change the refractive index of the material, which changes the colour of the adhesive. This effect has been reported as stress whiting or craze forming [18,22]. Thus, the whiting zone observed for this specific type

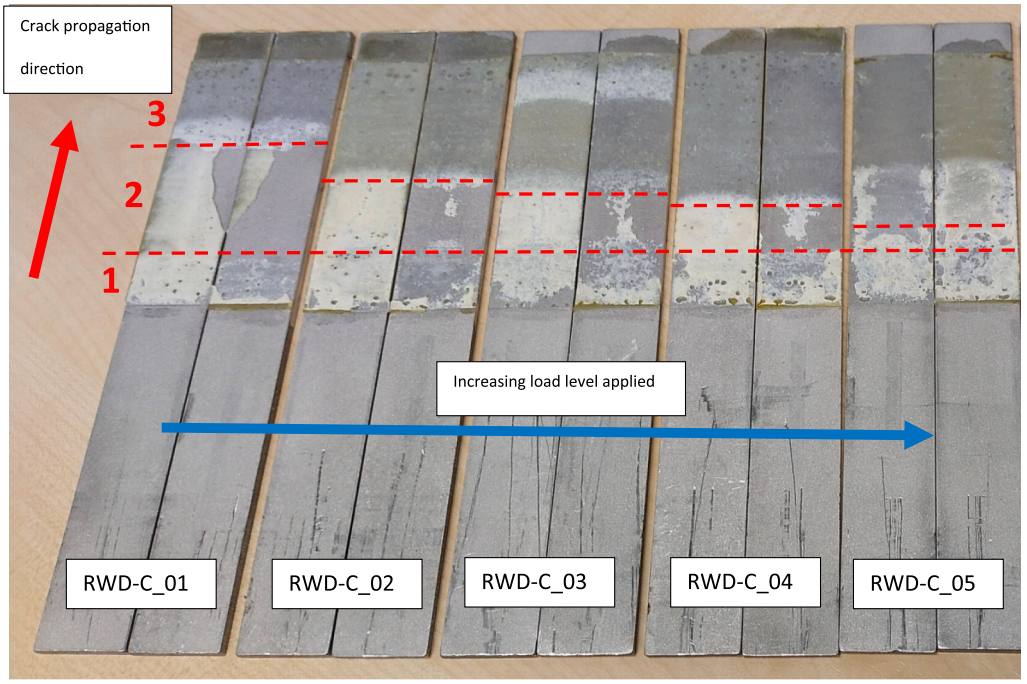

Fig. 7. Fracture surface of specimens RWD-C_01 to 05. With region 1 indicating the fracture surface created with the pre-crack, region 2 the RWD creep crack growth test and region 3 opening the specimen with lab tools to be able to inspect the fracture surface of the specimen. Scratches on the adherends are caused by the lab tools, after the tests were already finished.

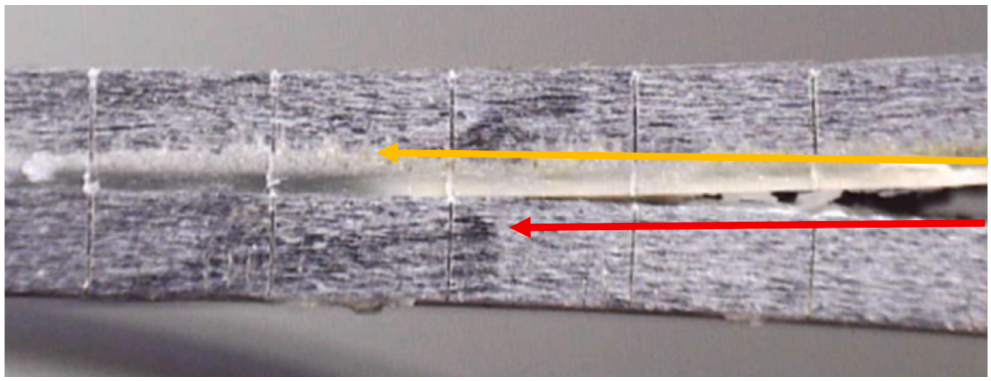

Fig. 8. Specimen RWD-C_05 with whitened adhesive ahead of the crack tip. The yellow arrow indicates the distance the whitened area had passed through the adhesive and the red arrow the crack tip.

of adhesive, could be considered as the crazing zone.

Fig. 10 shows the RWD creep crack growth test of specimen RWD-C_05, where both the crack tip and craze front were measured in the same way as in Fig. 9. Since the crazing zone was already formed in front of the crack tip during the pre-cracking phase there is not a clear difference between the crazing zone growth rate and average crack growth rate through the adhesive and thus a similar trendline for both is found. The average distance found between the craze front and the crack tip is 2.8 mm.

Specimen RWD-C_05 had a relatively high applied G compared to the fracture toughness. The crack tip and craze front progress immediately after the load was applied. This was not the case when a lower G was applied. For instance, the specimens that are shown in Fig. 3 and Fig. 4 first show a transitory phase before linear crack propagation occurred. Fig. 11 shows for specimens RWD-C_01 to RWD-C_05 the applied load against the transitory phase in hours. Although, a clear trendline cannot be found it seems that when G/G_c is increasing the transitory time is decreasing. More tests are required to find a plausible trendline describing the relationship between G and the transitory time before creep crack growth initiates. When the duration of the transitory phase is dependent on G, the question arises on how fast the energy release rate changes while it is still leading to the creep crack growth. In for example, the Boeing wedge test, one might be able to measure the instantaneous crack growth rate, but it is difficult to know if the measured crack growth rate

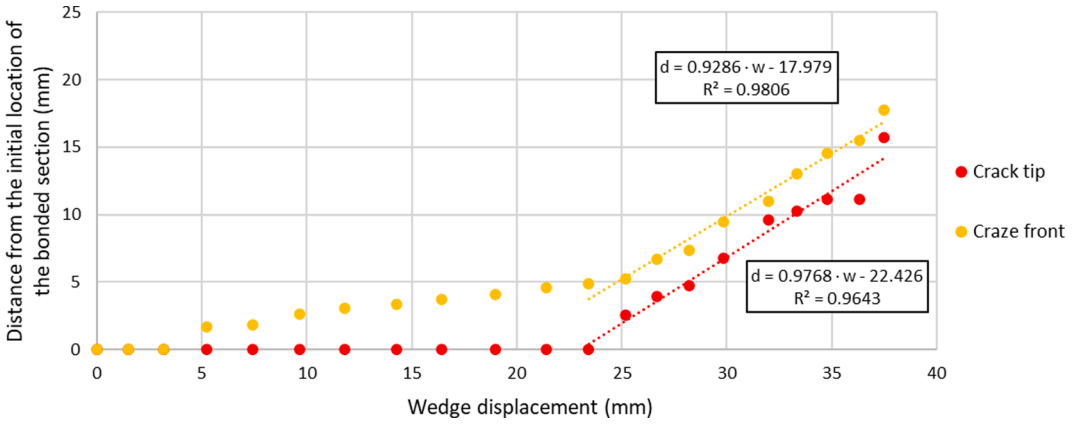

Fig. 9. Specimen RWD-C_05 pre-cracked visual measurement data of the craze front and the crack tip distance from the initial location of the bonded section (d).

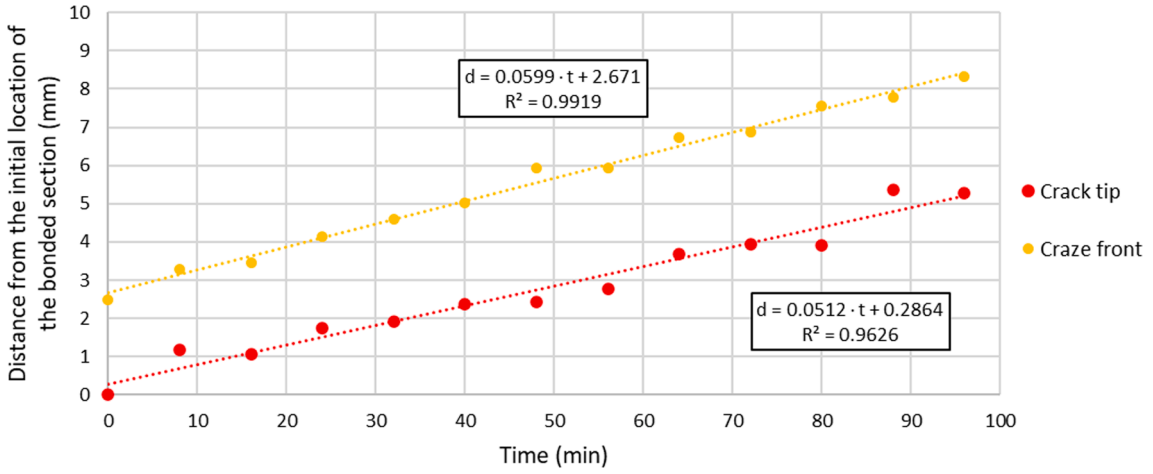

Fig. 10. Specimen RWD-C_05 creep crack growth phase with progressing craze front and crack tip in the adhesive, data normalized with the crack tip distance from the initial location of the bonded section (d).

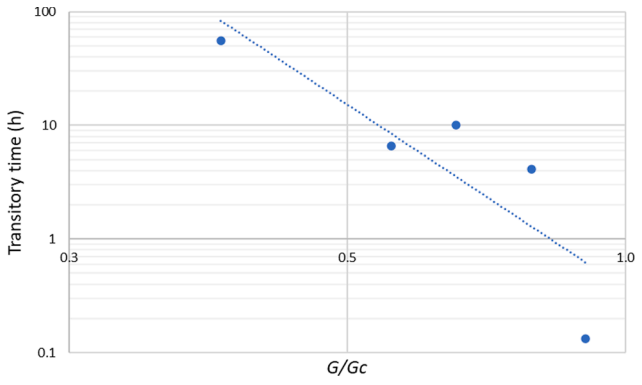

Fig. 11. Applied normalised energy release rate against the transitory time in hours found for specimens RWD-C_01 to RWD-C_05.

corresponds to the transitory or steady state propagation phase due to the decrease in energy release rate. Employing a constant energy release rate testing strategy is likely the most accurate approach when testing materials with expected relatively large FPZ, as in the case of adhesive joints, to prevent a too fast shedding rate that would lead to a different crack growth rate than observed in constant energy release tests.

When the pre-cracking is performed, the wedge is forced into the specimen with a certain rate. Therefore, also the forming of the craze zone and crack growth are forced to progress with a similar rate. It was demonstrated that, for this specific adhesive system, there is creep crack growth over time (Fig. 5). For the creep crack growth test, Fig. 4 shows that when considering the continuous measuring of the LVDT, the crack growths in a step like way for this specific adhesive. The step-like crack propagation indicates there are moments of crack arrest followed by sudden increase of the crack length. Slow crack growth in polymers could show this behaviour because part of the fibrillar zone at the crack tip ruptures, followed by a certain incubation time in which the fibrillar zone stabilizes before fibril rupture takes place again [22]. This effect could be considered as local and over a relatively short time compared to the total duration of the creep crack growth test. It was demonstrated that, over the whole creep crack growth test, a linear trendline can be found that describes the average crack growth rate for a specific specimen for a certain applied level of energy release rate. Since the fibrils are formed by the stress concentration at the crack tip, it could explain why at higher levels of applied energy release rate, and thus a higher stress at the crack tip, the fibrillar zone incubation time is shorter resulting in a shorter transitory time (Fig. 11) and higher obtained average crack growth rates. Another time dependent mechanism might be active in the graze zone which relates to the cohesive to adhesive fracture surface transition that was observed (Fig. 7). For all specimens the crack tip zone conditions were similar after the pre-crack was formed, like sharp crack tip, craze zone and cohesive failure. For lower applied G, besides the lower stress at the fibrils also the transition from cohesive to adhesive failure could result in the observed increase in the transitory time.

4.2. Rate sensitivity and effect on the fracture surface

The process of crazing in the fracture process is influenced by the strain rate during fracture of polymers. Polymeric materials are known for their strain rate sensitivity [23]. More specific the work Kozłowski et al. [24,25] shows for tensile tests of a MMA adhesive, that the test speed ranging from 1 to 100 mm/min, clearly influences the strength and stiffness of the adhesive which, confirms the viscoelasticity behaviour expected with this type of polymeric adhesive. Besides rate sensitivity it is also well known that temperature has a significant influence on the mechanical properties of a polymer. Low temperatures result in more brittle fracture behaviour of a polymer like MMA, and high temperatures relative to the glass transition temperature (T_g) result in more ductile fracture behaviour. Because of the viscoelastic nature of the polymer the change in fracture behaviour due to temperature can also be observed if the strain rate is changed. Where a high strain rate results in more brittle fracture behaviour and a low strain a more ductile fracture behaviour [26,27]. Arnott et al. [28] demonstrate with constant displacement mode I tests on adhesively bonded joints the influence of the displacement rate on the energy release rate and the fracture behaviour. In that work it is clearly visible that for higher rates the fracture surface shifts from primarily cohesive failure to complete adhesive failure. This is the same type of behaviour that was observed for the specimens tested with the creep crack growth test (Fig. 7). It must be noted that, the tests in the work of Arnott et al. were performed at an elevated temperature of 50 °C where in this work all the tests have been performed at $(23 \pm 2)^{\circ} C$. However, it was stated before that an increased temperature makes the fracture behaviour shift to a more ductile fracture behaviour. It can be assumed that if the tests were performed at a higher temperature likely more adhesive failure would have been observed if the same average crack growth rates would have been applied. Compared to quasi-static testing, creep crack growth tests below 50 % of G_c can be considered as relatively slow rate testing (Fig. 5), hence the pure adhesive fracture surface of specimen RWD-C_01 (Fig. 7). For bonded joint design purposes, characterizing the mechanical properties of a bonded joint only with quasi-static testing likely over-estimates the load bearing capabilities of the bonded joint. Especially when durability of the bonded joint is an important design criterion.

4.3. Average crack growth rate

What we are looking for in the RWD creep crack growth tests is obtaining the average crack growth rate. Since the RWD test method makes use of a roller wedge, it is assumed that the wedge follows the crack tip and therefore the distance between the roller wedge and the crack tip remain constant, on average, during the crack propagation phase. This assumption can be demonstrated in Fig. 9, where the crack length is plotted against the wedge displacement. During the crack propagation it follows a linear trend with a ratio close to one and has a good correlation between the crack length measurement and the wedge displacement. As shown in section 3.1, there is a difference between measuring the wedge displacement with an LVDT and using the visual measurement method. Since the latter is discrete the data points can show linear crack propagation (Fig. 3), while the continues measurement of the LVDT shows that this specific adhesive system accommodates a step-like crack propagation during a creep crack growth test (Fig. 4). The step-like crack propagation could be considered as a local and short time behaviour of the adhesive. For durability and creep crack growth predictions it is more interesting to know the behaviour of the adhesive system over a longer time period. In that case both measurement systems show a linear trendline with a similar slope which equals the average crack growth rate of that specific specimen. The test can be repeated with different specimens of the same type with every time applying a different load or in other words, a different energy release rate. The RWD force equation (1) was used to translate the applied force to energy release rate. It must be mentioned that this data reduction method overestimates the applied G slightly. This is because the friction of the roller is assumed to be zero, as mentioned in section 2.1. Fig. 5 shows there is more scatter in the results for the visual measurement method compared to the LVDT method, which is likely caused by the lower accuracy of the visual measurement method compared to the LVDT. However, the order of magnitude found for the coefficients of the power-law are similar.

5. Conclusions

This manuscript proposes a methodology for the experimental characterization of energy release rate-controlled creep crack growth under mode I loading. The proposed methodology makes use of the Roller Wedge Driven (RWD) test setup. The design of the RWD test setup makes it possible to obtain a creep crack growth rate curve by applying a constant load to the roller wedge. During the RWD creep crack growth test the energy release rate remains constant. Different average crack growth rates can be obtained when testing multiple specimens at different G (load) levels, resulting in a single log–log linear plot that shows energy release rate against average crack growth rate. The power law regression line provides a Pariś law-like equation. The specimens are required to be pre-cracked before performing the creep crack growth tests which, can be done inside the RWD test setup by forcing the wedge manually in the specimen with a threaded bar and a spanner, described in more detail in previous work [1]. Directly after pre-cracking a certain load can be applied to the roller wedge to initiate the RWD creep crack growth test.

Comparing the two measurement methods, visual and LVDT, it seems that using an LVDT provides more accurate results and gives better insight in the creep cracking behaviour of the adhesive, since it is a continues measurement. Thus, it was observed that this specific adhesive shows a step-like creep crack growth behaviour, but over a long time period the trendline was linear. Therefore, the average crack growth rates obtained from both measurement methods provided similar results, resulting in similar coefficients found for the power law regression.

Inspection of the fracture surfaces after testing showed a different response to the different average crack growth rates measured. It was observed that going from relatively high average crack growth rates to relatively low average crack growth rates it shifted the fracture surface from predominantly cohesive failure to adhesive failure.

For this specific adhesive system, data have shown that applying an energy release rate that is relatively low compared to the fracture toughness found by quasi-static testing, will likely result in creep crack growth. For durability design of bonded joints this behaviour must be taken into account and only using data from quasi-static testing will very likely overestimate the durability of the bonded joint. The power law coefficients found in the Pariś law-like equation could potentially be used for models in a similar way as the Paris law is used for modelling of fatigue. This could provide a valuable tool for engineers to make better predictions for creep crack growth in adhesively bonded joints. However, more tests and different tests are required to validate if the limited results in this work indeed follow a Pariś law-like equation.

Preprint submitted to International Journal of Engineering Fracture Mechanics December 23, 2022.

CRediT authorship contribution statement

E. Meulman: Conceptualization, Data curation, Writing – original draft, Writing – review & editing, Visualization, Investigation, Validation, Formal analysis, Methodology, Software. **J. Renart:** Conceptualization, Funding acquisition, Writing – review & editing, Visualization, Investigation, Validation, Formal analysis, Methodology, Supervision, Resources, Project administration. **L. Carreras:** Conceptualization, Writing – review & editing, Visualization, Investigation, Validation, Formal analysis, Methodology, Supervision. **J. Zurbitu:** Conceptualization, Writing – review & editing, Visualization, Investigation, Validation, Formal analysis, Methodology, Supervision.

Declaration of Competing Interest

The authors declare that they have no known competing financial interests or personal relationships that could have appeared to influence the work reported in this paper.

Data availability

Data will be made available on request.

Acknowledgements

The authors would like to acknowledge the support of the Spanish Government through the Ministerio de Ciencia, Innovacón y Universidades under the contract PID2021-127879OB-C21 and Grant RYC2021-032171-I funded by MCIN/AEI/ 10.13039/501100011033 and by “European Union NextGenerationEU/PRTR. The first author would also like to acknowledge the support received from the Universitat de Girona and Banco Santander through the fellowship grant IFUdG2021-AE, co-funded by the AMADE research group (GRCT0064). Open Access funding provided thanks to the CRUE-CSIC agreement with Elsevier. The work in this research has been made possible by patent 300352094, PCT/ES2020/070074 made available by IKERLAN, S.COOP. (IKER018) and the Universitat de Girona. Furthermore, the authors like to acknowledge the support from the AMADE research group testing laboratory.

References

[1] Meulman E, Renart J, Carreras L, Zurbitu J. Analysis of mode I fracture toughness of adhesively bonded joints by a low friction roller wedge driven quasi-static test. Eng Fract Mech 2022;vol. 271:108619. https://doi.org/10.1016/j.engfracmech.2022.108619.

[2] L. F. M. da Silva, A. Öchsner, and R. D. Adams, Handbook of Adhesion Technology, 2nd ed. Springer International Publishing AG, 2011. doi: 10.1007/978-3-642-01169-6.
[3] Ebnesajjad S. Adhesive Technology Handbook. 2nd ed. Wiliam Andrew; 2008.
[4] D. A. Ashcroft and D. Briskham, "Designing adhesive joints for fatigue and creep load conditions," Advances in Structural Adhesive Bonding, pp. 469–515, 2010, doi: 10.1533/9781845698058.4.469.
[5] W. Broughton, "Testing the mechanical, thermal and chemical properties of adhesives for marine environments," in Adhesives in Marine Engineering, First edit., Jan. R. Weitzenböck, Ed. Woodhead publishing, 2012, pp. 99–154. doi: 10.1533/9780857096159.2.99.
[6] Malinin NI. Creep of polymer materials in structural elements. J Appl Mech Tech Phys 1970;11:294–309. https://doi.org/10.1007/BF00908111.
[7] Bradley W, Cantwell WJ, Kausch HH. Viscoelastic creep crack growth: a review of fracture mechanical analyses. Mech Time-Dependent Mater 1997;1(3): 241–68. https://doi.org/10.1023/A:1009766516429.
[8] M. L. Cerrada, "Introduction to the Viscoelastic Response in Polymers," Thermal Analysis. Fundamentals and Applications to Material Characterization, pp. 167–182, 2005, [Online]. Available: https://ruc.udc.es/dspace/handle/2183/11487.
[9] Paris P, Erdogan F. A critical analysis of crack propagation laws. J Fluids Eng Trans ASME 1963;85(4):528–33. https://doi.org/10.1115/1.3656900.
[10] Plausinis D, Spelt JK. Designing for time-dependent crack growth in adhesive joints. Int J Adhes Adhes 1995;15(3):143–54. https://doi.org/10.1016/0143-7496(95)91625-G.
[11] A. AI-Ghamdi, Fatigue and Creep -of- Adhesively Bonded Joints. 2004. doi: 10.1017/cbo9781139175760.031.
[12] "ASTM D3762-03(2010) Standard Test Method for Adhesive-Bonded Surface Durability of Aluminum (Wedge Test) (Withdrawn 2019)." ASTM International, p. 5, 2010. [Online]. Available: https://www.astm.org/Standards/D3762.htm.
[13] D. O. Adams, K. L. DeVries, and C. Child, "Durability of adhesively bonded joints for aircraft structures," 2012. http://depts.washington.edu/amtas/events/jams_12/papers/paper-adams_adhesive.pdf.
[14] Korenberg CF, Kinloch AJ, Watts JF. Crack growth of struct adhesive joints in humid environ 2004;80(3):pp. https://doi.org/10.1080/00218460490279233.
[15] Aurore N, Julien J. Double cantilever beam tests on a viscoelastic adhesive: effects of the loading rate. Procedia Struct Integrity 2016;2:269–76. https://doi.org/10.1016/j.prostr.2016.06.035.
[16] Williams JG. End corrections for orthotropic DCB specimens. Compos Sci Technol 1989;35(4):367–76. https://doi.org/10.1016/0266-3538(89)90058-4.
[17] Manterola J, Zurbitu J, Renart J, Turon A, Urresti I. Durability study of flexible bonded joints under stress. Polym Test 2020;vol. 88:106570. https://doi.org/10.1016/j.polymertesting.2020.106570 [Online].Available:.
[18] Lampman S. Characterization and failure analysis of plastics. ASM International; 2003.
[19] E. J. Kramer and L. L. Berger, "Fundamental processes of craze growth and fracture," in Crazing in Polymers Vol. 2, Berlin, Heidelberg: Springer Berlin Heidelberg, 1990, pp. 1–68. doi: 10.1007/BFb0018018.
[20] Tijssens MGA, van der Giessen E, Sluys LJ. Simulation of mode I crack growth in polymers by crazing. Int J Solids Struct Nov. 2000;37(48–50):7307–27. https://doi.org/10.1016/S0020-7683(00)00200-6.
[21] M. Konstantakopoulou, A. Deligianni, and G. Kotsikos, "Failure of dissimilar material bonded joints," Physical Sciences Reviews, vol. 1, no. 3. De Gruyter, 2019. doi: 10.1515/psr-2015-0013.
[22] Michler GH, Baltá-Calleja FJ. Mechanical properties of polymers based on nanostructure and morphology 2005. https://doi.org/10.1201/9781420027136.
[23] Johnson FA, Radon JC. Strain rate-crack speed relation in steady state fracture processes. Int J Fract Mar. 1974;10(1):125–7. https://doi.org/10.1007/BF00955090.
[24] Kozlowski M, Bula A, Hulimka J. Determination of mechanical properties of methyl methacrylate adhesive (MMA). Architecture, Civil Eng Environ Jan. 2018;11 (3):87–96. https://doi.org/10.21307/acee-2018-041.
[25] Bula A, Kozłowski M, Hulimka J, Chmielnicki B. Analysis of methyl methacrylate adhesive (MMA)relaxation with non-linear stress–strain dependence. Int J Adhes Adhes Oct. 2019;94:40–6. https://doi.org/10.1016/j.ijadhadh.2019.05.011.
[26] Richeton J, Ahzi S, Vecchio KS, Jiang FC, Adharapurapu RR. Influence of temperature and strain rate on the mechanical behavior of three amorphous polymers: characterization and modeling of the compressive yield stress. Int J Solids Struct Apr. 2006;43(7–8):2318–35. https://doi.org/10.1016/j.ijsolstr.2005.06.040.
[27] Cessna LC, Sternstein SS. Viscoelasticity and plasticity considerations in the fracture of glasslike high polymers. Fracture of Metals, Polymers, and Glasses 1967: 45–79. https://doi.org/10.1007/978-1-4684-3153-7_4.
[28] Arnott DR, Kindermann MR. Durability testing of epoxy adhesive bonds. J Adhes 1995;48(1–4):101–19. https://doi.org/10.1080/00218469508028157.

4. Analysis of creep crack growth in bonded joints based on a Paris' law-like approach

E. Meulman[a*], J. Renart[a,c*], L. Carreras[a], J. Zurbitu[b]

[a]AMADE, Polytechnic School, University of Girona, Campus Montilivi, s/n, 17071, Girona, Spain

[b]Ikerlan Technology Research Centre, Basque Research and Technology Alliance (BRTA), Arrasate-Mondragón, Spain

[c]Serra Húnter Fellow, Generalitat de Catalunya, Spain

This paper has been submitted to the international journal of Engineering Fracture Mechanics, 2023

ISSN: 0013-7944, Impact Factor: 4.898, ranked 19/138 in the category of Mechanics (1st quartile)

Overview

Engineers need tools to make reliable prediction of how a crack will propagate in an adhesive of a bonded joint during a long period of time. Models can provide such a tool and can be implemented in numerical software to make analysis of more complex structures.

In this chapter a creep crack growth model based on a Paris´ law-like approach is proposed and validated. For the validation a TDCB specimen is used, that is loaded with a weight. When applying a constant load to a TDCB specimen the energy release rate at the crack tip remains constant and therefore also the crack growth rate. Thus, the TDCB constant load test is a good candidate to validate the RWD creep crack growth method, since no transient effects due to changing loading conditions are present. Since the creep crack growth model describes a Paris´ law-like expression there is an analogy with fatigue testing. It is demonstrated that the creep crack growth model can be implemented into an existing commercially available fatigue model. In Abaqus the Direct Cyclic (DC) module is available that, together with the Virtual Crack Closure Technique (VCCT), can simulate a discrete crack propagating in a bonded joint.

The results have shown that there is a good correlation between the RWD and TDCB creep crack growth results. The RWD results have been implemented in a TDCB FEM model showing that implemented creep crack growth model describes indeed the relationship between the energy release rate at the crack tip and the expected creep crack growth and it does so regardless of the specimen geometry.

Analysis of creep crack growth in bonded joints based on a Paris' law-like approach

E. Meulman[a*], J. Renart[a,c*], L. Carreras[a], J. Zurbitu[b]

[a]AMADE, Polytechnic School, University of Girona, Campus Montilivi, s/n, 17071, Girona, Spain

[b]Ikerlan Technology Research Centre, Basque Research and Technology Alliance (BRTA), Arrasate-Mondragón, Spain

[c]Serra Húnter Fellow, Generalitat de Catalunya, Spain

Abstract

The durability of bonded joints is key for the safety of structures over long periods of time. Creep crack growth is one of the factors that could affect the durability of a bonded joint. However, numerical tools and test methods relating to creep crack growth in bonded joints are not widely available yet. In this work a Creep Crack Growth Model (CCGM) is proposed for adhesively bonded joints. The idea is that the crack growth rate (da/dt) is controlled by the energy release rate (G) and can be described by the proposed model. The CCGM is validated against the developed tapered double cantilever beam (TDCB) constant load test and it is demonstrated that the proposed model can be implemented into an existing commercially available finite element method (FEM) code. The FEM results show that creep crack growth in bonded joints can be simulated by any existing fatigue model based on a Paris´ law-like approach. The FEM results also show that the CCGM can predict the experimental results when a different specimen geometry is used. The authors are aware that the used existing commercially available finite element model in this work is not designed for creep crack growth modelling but are convinced that the model can be easily modified to simulate it in a more realistic manner.

Keywords: Creep crack growth, Bonded joint, FEM, CCGM, TDCB, RWDC

*Corresponding author.

Email addresses: edwin.meulman@udg.edu (E. Meulman*), jordi.renart@udg.edu (J. Renart*), laura.carreras@udg.edu (L. Carreras), jzurbitu@ikerlan.es (J. Zurbitu)

Preprint submitted to International Journal of Engineering Fracture Mechanics May 23, 2023

Nomenclature

a	Crack length
B	Width of specimen
c	Empirical parameter for the creep crack growth model
C	Compliance
da/dt	Crack growth rate
dC/da	Compliance rate related to the crack length
G	Energy release rate
G_c	Fracture toughness
h	Thickness of the adherend
m	Specimen geometry factor
P	Applied load
s	Empirical parameter for the creep crack growth model describing the slope
t_a	Bondline thickness
BK	Benzeggagh and Kenane fracture criterion
CBT	Corrected Beam Theory
CCGM	Creep Crack Growth Model
CZM	Cohesive Zone Model
DC	Direct Cyclic
DCB	Double Cantilever Beam
ECM	Experimental Compliance Method
FEM	Finite Element Method
LVDT	Linear Variable Displacement Transducer
RWD	Roller Wedge Driven
RWDC	RWD creep crack growth
TDCB	Tapered Double Cantilever Beam
VCCT	Virtual Crack Closure Technique

1. Introduction

The durability of bonded joints is essential for ensuring the safe and reliable operation of structures over long periods of time. One of the factors which can reduce the strength and longevity of the joint is creep crack growth. Creep crack growth in bonded joints is influenced by the type of material, the geometry of the joint, and the environmental conditions. Selecting the appropriate adhesive can help to improve the durability of the joint [1]–[5]. The question is, how to determine if an adhesive has the desired resistance to creep for that specific bonded joint geometry and environmental conditions. Test methods relating to creep crack growth in bonded joints are not widely available yet. Some researchers have tried to use existing methods like, for example, the Boeing wedge test [6] (standard withdrawn in 2019) that was originally designed for qualitative testing but using it to obtain quantitative data [7], [8]. In this test the wedge remains stationary inside the specimen, resulting in a change of the stress state at the crack tip when the crack propagates. In previous work it has been shown that for instance the adhesive Araldite 2021-1 shows for the creep crack growth a transitory phase before steady-state crack propagation is reached [9]. The question arises how fast the energy release rate changes when a stationary wedge is used, while it is still leading to the steady state creep crack growth. Because, a stationary wedge test would likely lead to a too fast shedding rate preventing the stabilization of the fracture process zone, and thus leading to a different crack growth rate than the one observed in a constant energy release test. Different test setup configurations have been developed to test with a constant energy release rate at the crack tip. Plausinis et al. [10] and Dillard et al. [11] make use of a cable system with weights and Lefebvre et al. [12] and Nakamura et al. [13] use springs trying to keep the energy release rate constant. All these examples make use of double cantilever beam (DCB) specimens, and the test is load controlled by using weights or springs. Although, when a DCB specimen is loaded under load control, the distance between the load point and the crack tip increases during crack propagation. This makes it very difficult to keep the energy release rate constant at the crack tip. Schrader et al. [14] has tried to solve that by using a computer controlled system that constantly calculates the energy release rate at the crack tip with the J-integral method

and corrects the load applied by the test machine. This requires sophisticated test equipment which is not widely available. Meulman et al. [9], [15] have tried to simplify the test setup configuration by making use of a moving roller wedge that is loaded with a small weight, so there is no need of a test machine or large complex test setup. The advantage of a moving wedge is that on average the distance between the wedge and crack tip remains constant during the crack propagation phase [9], [16], [17]. Another option could be to change the type of specimen and use for instance a tapered double cantilever beam (TDCB) specimen instead of a more commonly used DCB specimen [18]. The main advantage of the TDCB is that the compliance rate with respect to the crack length remains constant due to the tapered section of the adherends [19]. This means that during crack propagation the load remains constant and therefore also the the energy release rate if a constant load is applied [18]. TDCB specimens used for mode I tests on adhesively bonded joints can be found in literature [20]–[26]. However, as far as the authors know, it has not been used for creep crack growth testing by applying a constant load to the TDCB specimen. For creep testing of bulk material the simplest test method is to apply a constant load to the material by use of weights [27], [28]. Similar approach could be applied to a TDCB specimen. A certain known weight can be hung at the bottom adherend, using the same connecting pin system as would be used for a quasi-static TDCB test in a tensile test machine. Over time the crack will propagate under influence of the energy release rate at the crack tip provided by the constant load. Measuring the crack propagation over time will provide the data required to determine creep crack growth curves. These curves could be used for a finite element method (FEM) for durability design purposes. As far as the authors know, a commercial available FEM module to simulate creep crack growth in a bonded joint is not available yet. A similar approach is used for simulating fatigue with FEM [29]–[32]. Experimental tests provide fatigue crack growth curves that are directly implemented in already widely available commercially FEM fatigue models like, for instance, the Direct Cyclic (DC) module in the FEM software of Abaqus [33]. Examples of models that make use of the DC module for fatigue simulation in Abaqus are Pirondi et al., Dávila et al. and Teimouri et al. [34]–[36]. The DC module requires the input of a Paris´ law-like expression to simulate

the crack growth rate belonging to a certain energy release rate that is present at the crack tip. The required input parameters are obtained from experimental results where the crack growth rate per cycle (da/dN) is plotted against the energy release rate on a log-log scale. Most common approaches to implement the crack growth rate into FEM are the cohesive zone model (CZM) [30], [37], [38] or Virtual Crack Closure Technique (VCCT) [29], [39]–[41]. CZM is a more advanced technique that can simulate more complex crack patterns but requires more material data input which, is not always easy to obtain from experimental tests. The VCCT is a simpler technique that releases predefined pairs of nodes when a certain energy criterion is met. The energy criterion in VCCT is determined with the Benzeggagh and Kenane (BK) [42] criterion that converts mode I, II and III into a single equivalent fracture toughness. When the energy release rate at the crack tip nodes reaches the equivalent fracture toughness, it releases the nodes, resulting in crack propagation with a crack length increase equal to the element size. Since the VCCT is related to a single row of paired nodes, it means that the VCCT can only be used for discrete crack simulation. In case of TDCB and DCB bonded joints, the adhesive layer is where the crack will propagate. Therefore, the VCCT technique is a good option to simulate crack propagation in TDCB and DCB bonded joints. The authors demonstrate that using the VCCT in combination with the DC module could be used to simulate creep crack growth of bonded joints.

2. Methodology

In this section, first the authors propose a Creep Crack Growth Model (CCGM). Secondly, the roller wedge driven creep crack growth (RWDC) method, that was proposed in previous work [9], is briefly described. This is followed by an explanation of how the CCGM is implemented in an existing commercially available numerical model. Ultimately, the validation process is described relating to the experimental tests where TDCB specimens are loaded with a constant load.

2.1 Creep Crack Growth Model

The CCGM is based on the hypothesis that the crack growth rate (da/dt) is controlled by the energy release rate (G). In the proposed model a Paris´ law-like power law describes this relationship:

$$da/dt = c \cdot \left(\frac{G}{G_c}\right)^s \tag{1}$$

where da/dt is the crack growth rate, G the energy release rate, c and s are empirical material parameters. If the fracture toughness (Gc) of the specimens to be tested can be obtained from quasi-static testing, then the energy release rate can be normalized with the fracture toughness. The idea is that, if CCGM is plotted on a log-log scale, it forms a log-linear trendline, similar as can be found in experimental fatigue results. Experimental tests must be performed at different levels of G to find the material parameters c and s so that the model describes the creep crack growth curve for that specific adhesive system.

2.2 RWD creep crack growth test method

The RWDC test method makes use of a roller wedge [9] to determine the parameters c and s. The roller wedge is inserted in a DCB-like specimen which is clamped in vertical position (Figure 1). On top of the roller wedge a weight is placed so that during the creep crack growth test a constant load is

applied to the crack tip, regardless of the crack length. During crack propagation the roller wedge will follow the crack tip, so that on average the displacement of the wedge equals the crack length increase. With a Linear Variable Displacement Transducer (LVDT) the displacement of the roller wedge is measured over time. The RWD data reduction method [9] is used to convert the constant load, that is applied to the roller wedge, to energy release rate. Combining both elaborated test results in a log-log plot will give a log-linear trendline that can be described with the CCGM (equation 1).

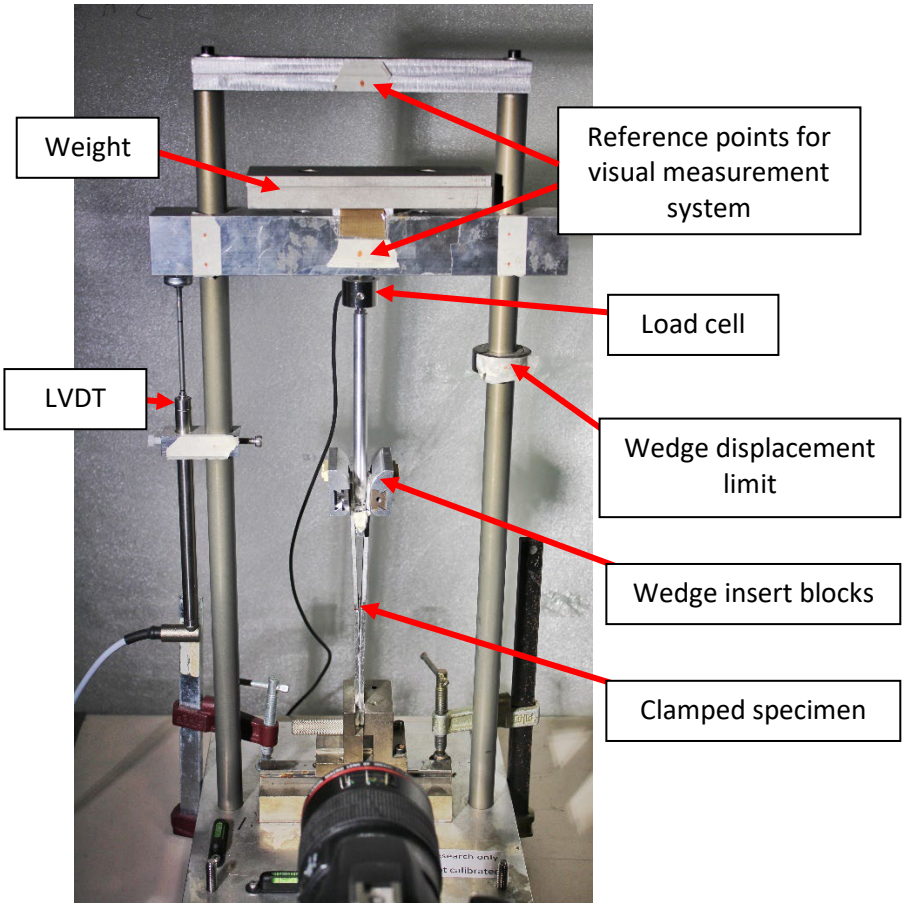

Figure 1. Test setup of the RWDC test method. The specimen is vertically clamped and loaded with a weight on top of the wedge [9].

Figure 2 gives an example of an obtained creep crack growth curve with the RWDC test method. The results are from DCB-like aluminium specimens bonded with Araldite 2021-1, that were tested in previous work [9] and are used to validate the CCGM with the TDCB constant load tests. Also, the results are used to demonstrate that the CCGM can be implemented in an existing commercially available numerical model.

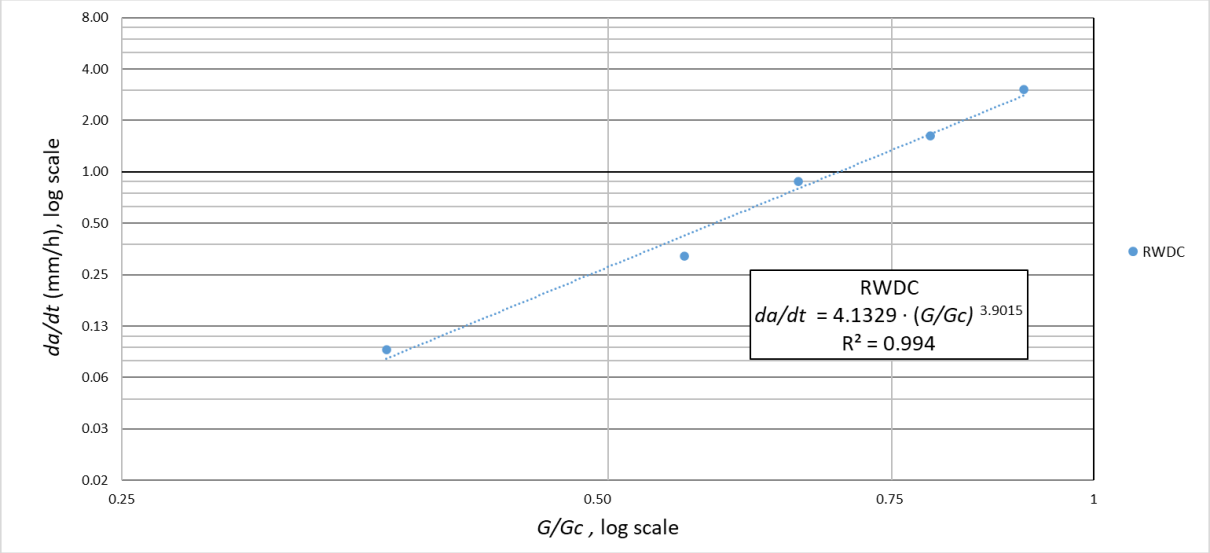

Figure 2. Example of creep crack growth curve obtained with the RWDC test method in previous work [9].

2.3 Creep crack growth numerical model

As stated before, a commercial available FEM module to simulate creep crack growth in a bonded joint is not available yet. Therefore, a 2D finite element model of a TDCB specimen is created in Abaqus/CAE (6.14-2) [33] to demonstrate that an existing fatigue model that is based on a Paris´ law-like expression can be used to simulate creep crack growth based on the proposed model and experimental results of the RWDC test method. The TDCB adherends are modelled with 4-node bilinear plane strain elements with incompatible modes (CPE4I) (for more details about the element the reader is referred to the Abaqus Analysis User's Manual [33]). In Abaqus a discrete crack can be defined using the VCCT model. VCCT is applied to a row of nodes connecting the two adherends which then represents the adhesive. The mode I fracture toughness of the adhesive is entered in the BK fracture criterion model, that releases the VCCT nodes when the critical energy release rate is reached at the crack tip, propagating the crack to the next pair of nodes. The DC model is used to simulate crack propagation over a certain time period. The DC module is developed for direct calculation of a structure's cyclic response under various repetitive loading cycles and is useful for low-cycle fatigue analysis. Taking a frequency of 1Hz automatically results in $da/dN = da/dt$ (dt in seconds), in that way, da/dt obtained

from the creep crack growth test results can be directly implemented in the Paris´ law-like equation of the DC module. In this specific model the material parameters from the RWDC results (Figure 2, 4.1329 and 3.9015) are entered in the DC module. Figure 3 shows the cycle that the DC module in Abaqus needs, to simulate the creep crack growth in a bonded joint. The amplitude of 1 relates to the constant load (nodal point load in y-direction) applied to one of the adherends, at this loading point the adherend is only constraint in x-direction. The other adherend is constraint in both x and y-direction at a single node directly opposite to the loading point, so that the specimen can open freely. The VCCT is not affected by the closing part halfway the cycle. We are interested in the energy release rate at the crack tip at the start and end of each cycle which will drive the crack propagation following the entered CCGM parameters in the Paris´ law-like equation of the DC module. Results can be plotted by only considering the last increment of the cycle to obtain similar results as found in the experimental tests. Running the FEM model for different constant loads will result in different energy release rates at the crack tip and as a result different creep crack growth rates.

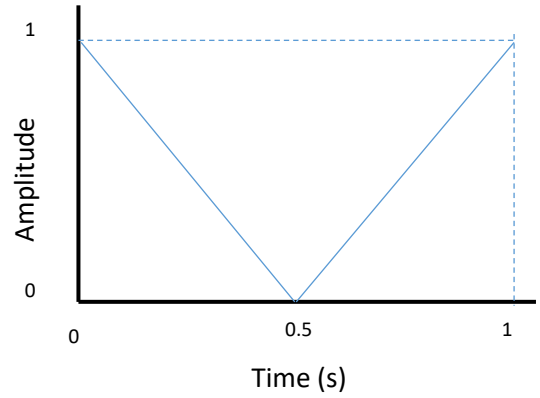

Figure 3. Required input cycle in the DC module of Abaqus to simulate creep crack growth in a bonded joint.

2.4 Validation of the creep crack growth model

The TDCB quasi-static test is described in the ISO standard 25217:2009 [18]. The more commonly used DCB test for bonded joints is also described in the same ISO standard since these test principles are

very similar, mainly the geometry is different. For the TDCB the experimental compliance method (ECM) reads:

$$G_{Ic} = \frac{P^2}{2B}\frac{dC}{da} \tag{2}$$

with P being the applied load, B the width of the specimen, C the compliance (specimen opening displacement divided by the load) and a the crack length. The standard mentions that the ECM and the corrected beam theory (CBT) are the most accurate data reduction methods [18]. Based on results from a round robin test campaign, it shows that for TDCB specimens there is a good agreement between the ECM (equation 2) and the CBT method [20]. Thus, for sake of simplicity the authors decided to use the ECM instead of the CBT method. In a TDCB test the value for dC/da is constant and follows directly from the slope obtained by plotting the experimental results of the compliance against the crack length. The crack length was measured by using a traveling camera and marks on the side of the specimen. The specimen was loaded by an MTS insight 5kN tensile test machine with a constant displacement rate of 2mm/min.

For the TDCB specimen the parameter B and dC/da are both constant, therefore if the load is constant also the energy release rate remains constant during the test, as can be seen in equation 2. Applying a constant load to TDCB specimen results in a constant crack growth rate, which then can be plotted on a log-log scale with da/dt vs G. When different specimens are tested with different constant loads it is expected that a similar creep crack growth curve can be produced as with the RWDC method (Figure 2). A test frame is designed to be able to test two TDCB constant load tests in parallel (Figure 4). The specimens are first pre-cracked for about 15mm in the MTS insight 5kN tensile test machine. The same loading blocks and pins are used to connect the specimens to the test frame as used for the quasi-static test. At the bottom a weight is applied to the specimen that allows the specimen to freely open when the crack propagates. Two canon cameras with a macro lens are used to take photos at 12 hours interval to capture the crack propagation over time.

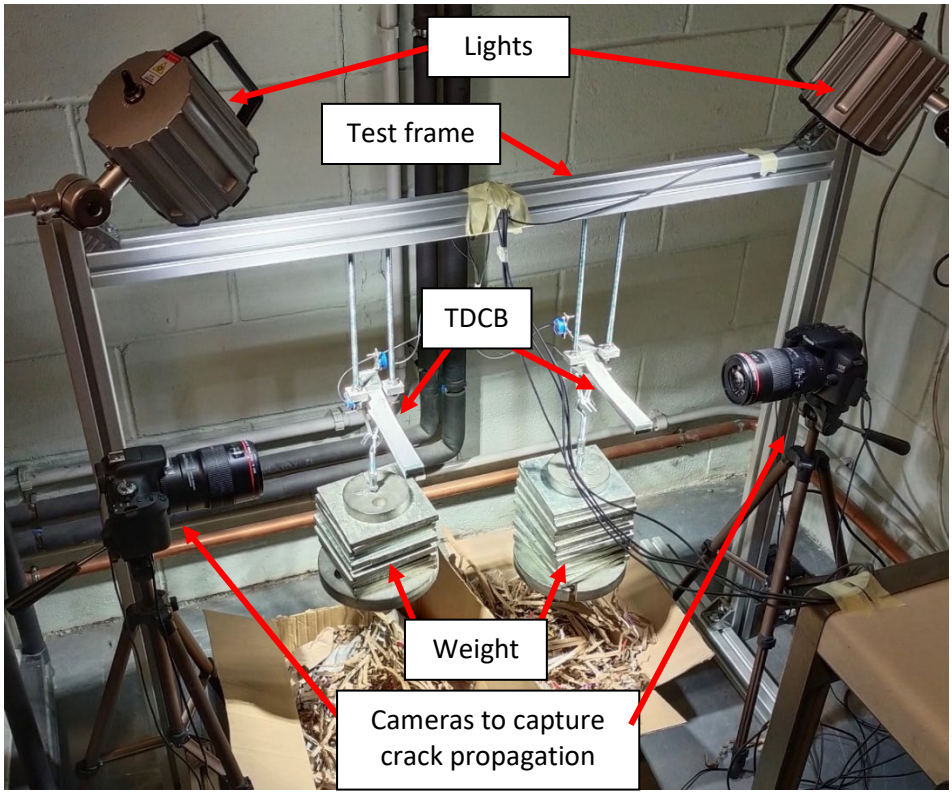

Figure 4. TDCB constant load test frame and canon cameras to capture the crack propagation over time. The two cardboard boxes below the weights are just there to provide a soft landing for the weights when the specimens fail.

The specimens are painted white and marks are applied in the same way as was done for the quasi-static TDCB test. Software, called ImageJ, is used to manually measure the crack length in the photos. The marks are used to calibrate the visual measurement. Figure 5 shows an example of a painted and marked TDCB specimen, where the blue arrow indicates the calibration of the pixel measurement in the photo. The red arrow indicates how the crack length is determined measured from the tip of the pre-crack.

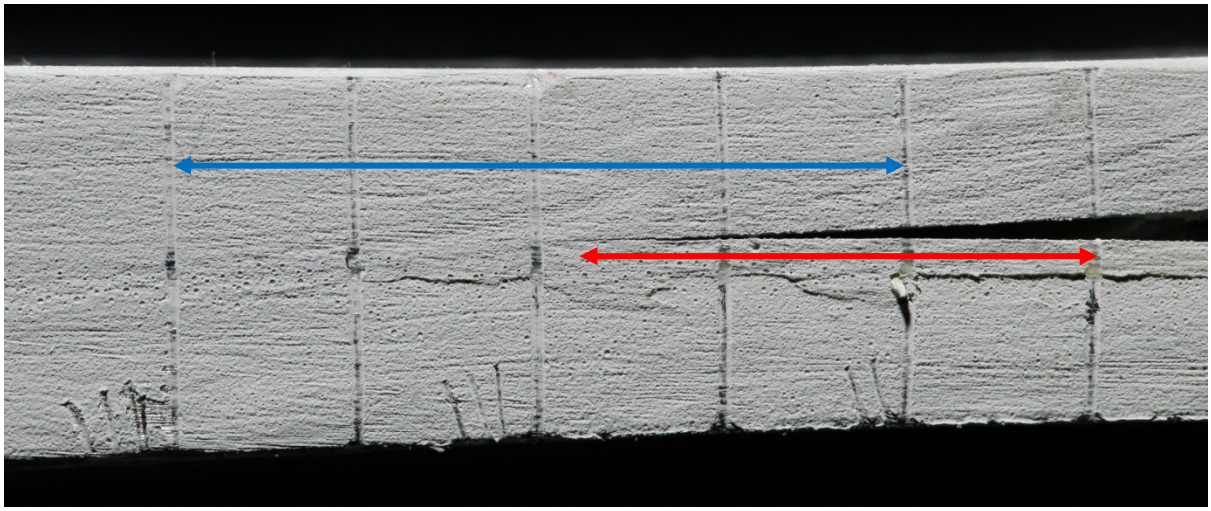

Figure 5. Example of TDCB specimen with the blue arrow indicating the measurement distance for the calibration of the pixels in the photos and the red arrow the crack length measurement from the tip of the pre-crack.

To have a constant compliance rate, the thickness of the adherends has to increase with an increasing crack length. Therefore, the thickness of the adherend is a function of the crack length. The equation describing this relationship reads:

$$m = \frac{3a^2}{h^3} + \frac{1}{h} \tag{3}$$

where h is the adherend thickness and a the crack length. The adherend thickness (h) has to be chosen in such a way that the specimen geometry factor m remains constant while a is increasing [18]. Figure 6 shows the TDCB specimen geometry design for this experimental test campaign.

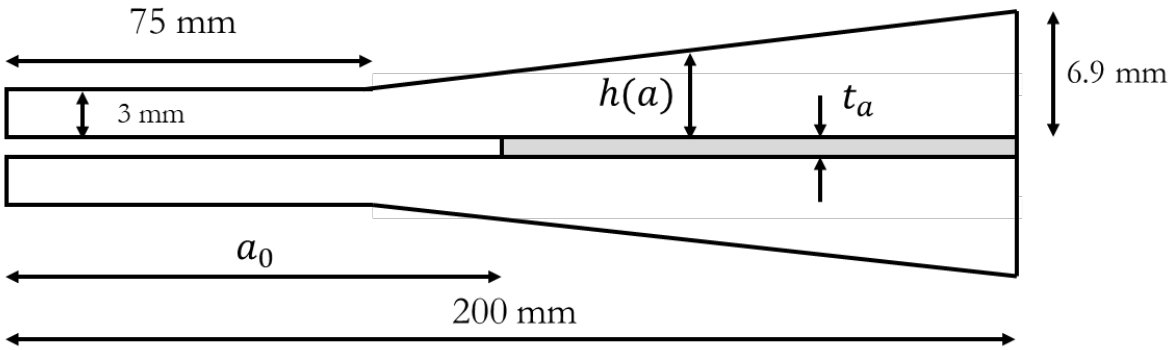

Figure 6. TDCB specimen geometry with m =278 mm^{-1}.

Besides the tapered section, everything else is the same as the DCB-like specimens used for the RWDC tests in previous work [9]. The adherends are made out of aluminium Al 7075-T6 with a width of 25mm and a Young's modulus of 71 GPa, shear modulus of 27GPa and a yield strength of 550 MPa. The adhesive is Araldite 2021-1 which is a methacrylate-based rigid structural adhesive with a glass transition temperature of 80°C. The specimens were tested and manufactured at the AMADE research group testing laboratory at the University of Girona (ISO17025 and NADCAP certified). The temperature and relative humidity in the laboratory are $(23 \pm 2)\ °C$ and (50 ± 5) %RH, respectively. Before bonding, the adherends received a surface treatment with a sandblaster using brown fused aluminium oxide of 60 microns. After sandblasting, the adherends were cleaned using acetone and just before applying the adhesive the adherends were decreased with high grade alcohol. Teflon spacers were used to create the bondline thickness. To enhance the curing process the specimens were placed in a 60°C oven for 16 hours. Table 1 shows an overview of the specimens tested with the number of specimens per type of test method.

Table 1. Tested specimens overview.

Specimen	**Test method**	**Disp. rate (mm/min)**	t_a **(mm)**	**No. of specimens**
TDCB_0x	TDCB quasi-static	2	0.89 ± 0.05	3
TDCB_CL_0x	TDCB constant load	-	0.79 ± 0.09	4

3. Results

Results of the TDCB quasi-static test, constant load test and FEM model are presented in this section. First the fracture toughness is obtained from three TDCB specimens that are quasi-static tested. With the TDCB constant load test the creep crack growth rates are obtained for different applied loads and plotted on a log-log scale to obtain the creep crack growth curves. In the final part of this section FEM results are presented and compared with the RWDC method and the TDCB constant load test.

3.1 TDCB quasi-static test

The results of the quasi-static tests are shown in Figure 7 where the energy release rate is plotted against the crack length. The energy release rate for every individual specimen stays relatively constant during crack propagation. However, there is some spread observed between the three specimens. TDCB_03 shows a sharp drop after the initial phase but recovers to a more constant energy release rate at a longer crack length. TDCB_01 lacks data for the initial phase because no clear crack propagation can be observed in the photos, so the crack length cannot be determined. Considering the data after the initial phase (100mm of crack propagation), then the values are ranging from 2 to 3 N/mm.

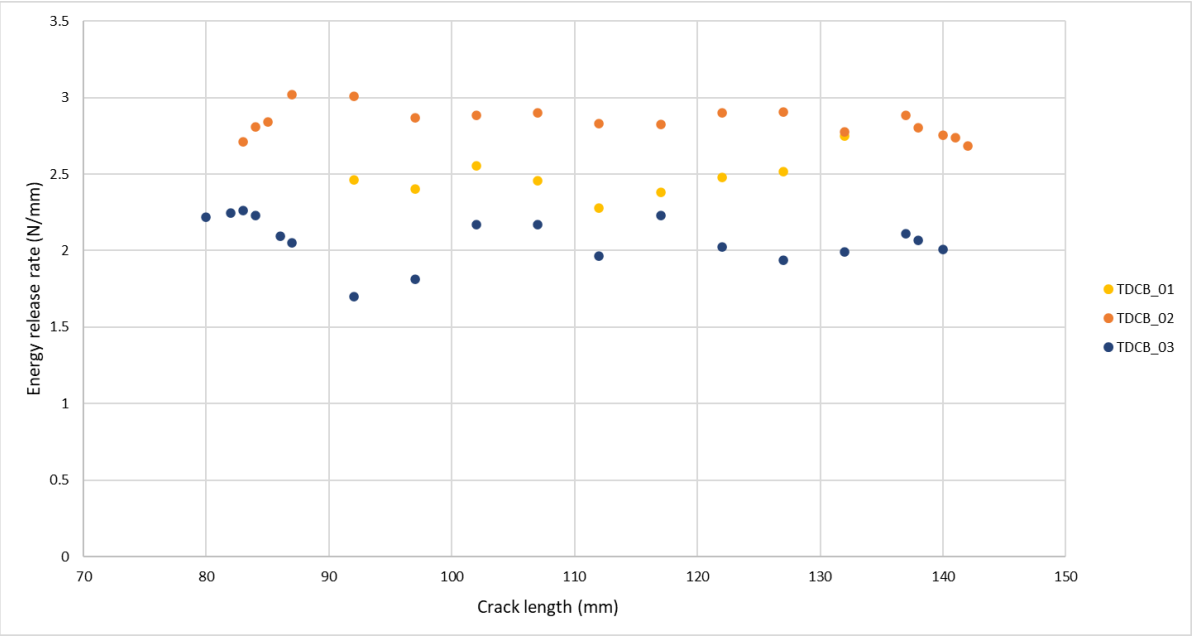

Figure 7. Energy release rate vs crack length of the three quasi-static TDCB tests. Energy release rate determined with the ECM data reduction method.

The specimens are opened completely after the quasi-static tests to be able to inspect the fracture surfaces. All three specimens show cohesive failure. Specimen TDCB_01 is shown in Figure 8 as an example of the cohesive fracture surface observed. This type of fracture surface was also found in previous work for DCB and RWD test with the same adhesive [15].

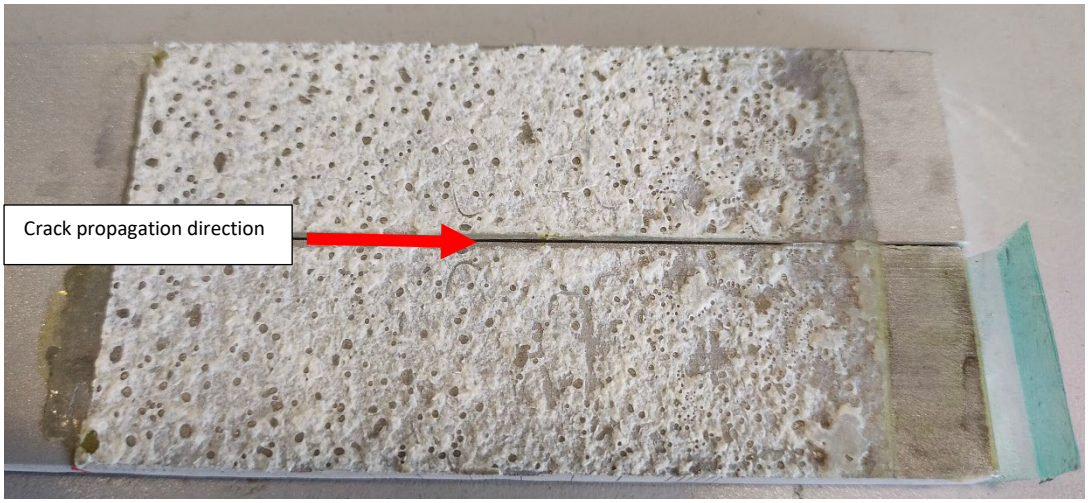

Figure 8. The cohesive fracture surface of specimen TDCB_01

Table 2 shows data of the three specimens with, B the width of the specimen, dC/da which is the slope found when the compliance is plotted against the crack length, and the fracture toughness determined with the ECM data reduction method (equation 2) [18].

Table 2. Overview of the three TDCB specimens that are tested quasi-static.

Specimen	G_c - ECM (N/mm)		dC/da (N^{-1})	B (mm)
	Avg.	Std. Dev.		
TDCB_01	2.488	0.136	0.0013	24.95±0.04
TDCB_02	2.823	0.071	0.0014	24.93±0.02
TDCB_03	2.067	0.094	0.0013	24.84±0.04
Average: (Batch)	2.459			
Std. Dev. (Batch)	0.309			

3.2 TDCB constant load test

Based on results of the quasi-static TDCB tests and the RWDC results, different loads are selected to be applied to the specimens for the TDCB constant load tests. The load applied to each specimen is presented in Table 3. The constant energy release rate applied to the specimen can be calculated by using the ECM data reduction method (equation 2). Applying a subcritical load to the specimen results in an energy release rate below the fracture toughness which in theory should result in no crack propagation when general fracture mechanics are considered.

Table 3. Overview of the four TDCB specimens that are tested with a constant applied load.

Specimen	Load (N)	G - ECM (N/mm)	da/dt (mm/h)	B (mm)
TDCB_CL_01	203	1.07	0.312	24.90±0.08
TDCB_CL_02	222	1.29	0.493	24.84±0.04
TDCB_CL_03	242	1.49	1.343	24.91±0.04
TDCB_CL_04	274	1.96	1.714	24.93±0.10

Crack propagation has been observed over a longer period of time, which was expected because of the properties of this particular adhesive, as indicated by previous research [9]. This can be shown in Figure 9 where the crack length is plotted against the time. The initial part shows already crack growth but at a relatively low rate compared to the second part. This initial part is considered as the onset slope. The second part of the curve starts after about 75 hours, and it is the propagation slope. For this specific test the propagation slope ends at around 180 hours, because the crack approaches almost the end of the specimen and results in sudden complete rupture of the specimen. It was demonstrated in previous work that this particular adhesive system shows a transitory phase before the crack propagation phase [9]. In the proposed creep cack growth rate model, only the propagation phase is considered.

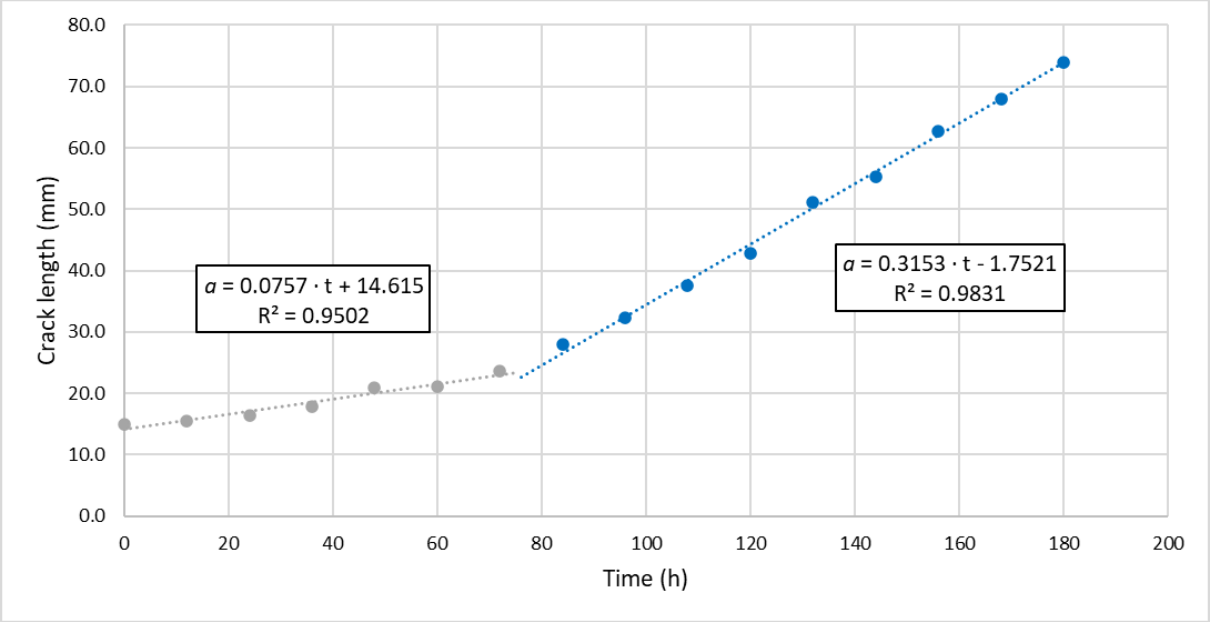

Figure 9. Crack length (a) measured in the photos taken during the test of TDCB_CL_02 and plotted against time (t) in hours. The slope of the blue trendline is considered to be the propagation slope and provides the average creep crack growth rate.

For the other specimens' similar curves were observed with different slopes related to the applied constant load. The plot in Figure 10 can be produced by normalizing the applied energy release rate (Table 3) with the fracture toughness found for each specimen. The RWDC results in Figure 10 are from Figure 2 and described in section 2.2. There is some offset between both curves. Although, they are different types of specimens and loaded in a different manner, the coefficient that describes the slope of the power law is similar.

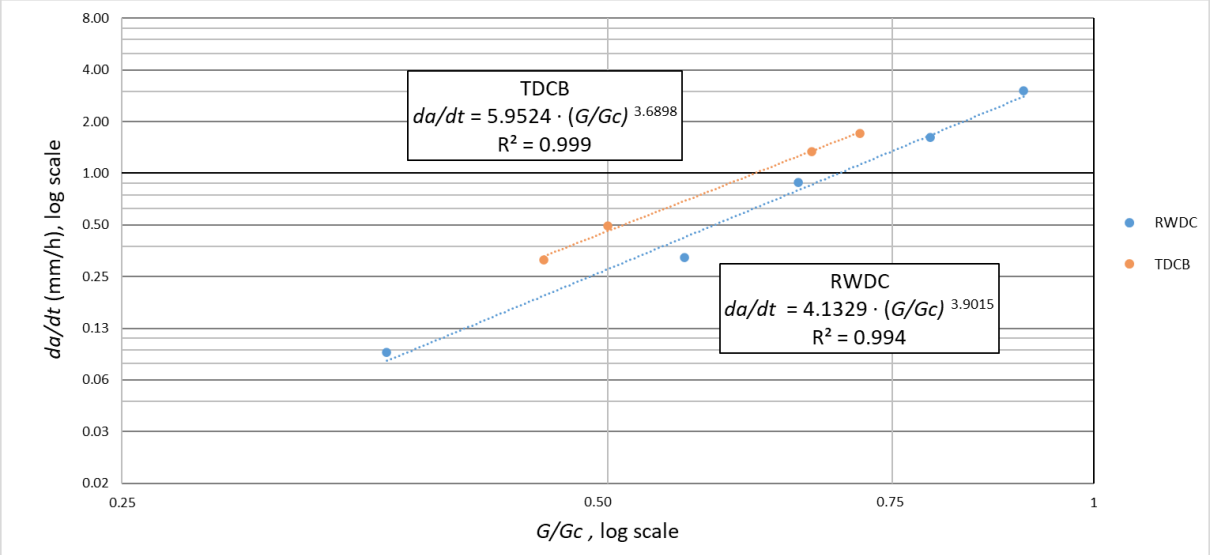

Figure 10. Crack growth rate (da/dt) against normalised energy release rate (G/G_c) on a log-log scale with the data of the RWDC tests and the results found for the constant load TDCB tests [9].

The fracture surfaces of the four tested specimens are shown in Figure 11. The pre-crack shows primarily cohesive failure as was observed for the specimens tested quasi-static. Then a transition to adhesive failure is visible. When the specimens fail, the last part of the adhesive, it fractures in an unstable manner which, relates to a much higher crack growth rate and therefore a transition to cohesive failure is observed again. This last part is not considered in the results as presented in Figure 9. It can also be noticed that, if a higher constant load is applied to the specimen the proportion of adhesive failure reduces and more parts of cohesive failure are visible. In both the TDCB constant load and the RWDC test there was no clear creep deformation observed prior creep crack growth. Therefore, creep deformation is not considered in this work and only creep crack growth is considered.

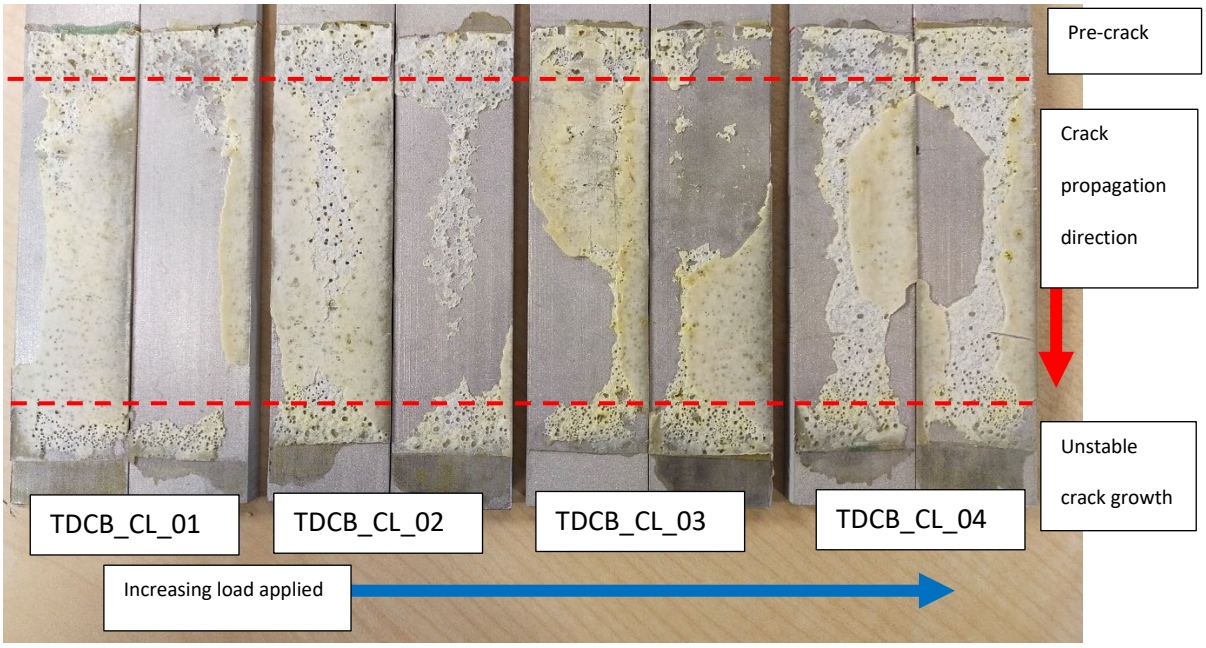

Figure 11. Fracture surface of the TDCB constant load specimens with from left to right increasing load applied.

3.3 TDCB numerical model with RWDC data

Four simulations were run with similar loads (Table 4) that were applied in the TDCB constant load tests (Table 3). The obtained energy release rate (G) at the initial step is from the crack tip node. The resulting crack growth rate is presented in the numerical model as number of cycles, which in this case equals to seconds, for one element length to propagate in the VCCT layer, as described in section 2.3. Converting the crack propagation from seconds per element to da/dt results in the crack growth rates presented in Table 4.

Table 4. Overview of the data from the four TDCB FEM simulations.

Specimen	Load (N)	G (N/mm)	da/dt (mm/s)
TDCB_FEM_01	200	1.09	$1.40 \cdot 10^{-5}$
TDCB_FEM_02	220	1.31	$2.85 \cdot 10^{-5}$
TDCB_FEM_03	240	1.55	$5.80 \cdot 10^{-5}$
TDCB_FEM_04	270	1.99	$1.54 \cdot 10^{-4}$

The TDCB FEM results can then be plotted (Figure 12) together with the RWDC and TDCB creep crack growth data by converting the crack growth rate to mm/h and normalizing G with G_c that was found in the RWD quasi-static tests [15]. The TDCB FEM model follows the RWDC experimental data, as expected, since the CCGM parameters are inserted in the Paris´ law-like equation in the DC module, which are taken from the RWDC test results.

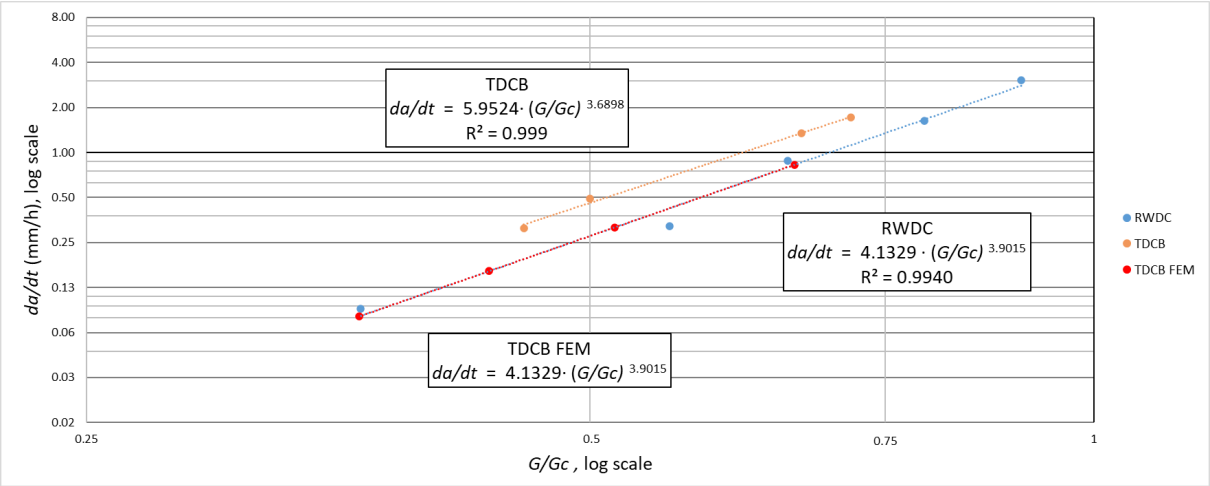

Figure 12. Creep crack growth rate against normalised energy release rate on a log-log scale with the data of the RWDC tests, constant load TDCB tests and the TDCB FEM model.

4. Discussion

Two main results of this work are discussed in this section. Firstly, the TDCB constant load test results compared to the proposed CCGM. Secondly, how the CCGM could be used in existing numerical models and how those results correlate with the experimental work.

4.1 TDCB versus CCGM

There is quite some spread in the TDCB quasi-static test results between the three tested TDCB specimens (Figure 7). It is likely related to variation in the adhesive properties since this variation in the fracture toughness was also found for this adhesive system when DCB tests were performed in previous work [15]. Different from DCB and RWD tests is that there is no high initial peak as was observed for this adhesive. For the TDCB tests, once the fracture toughness is reached it remains quite stable during the rest of the crack propagation phase. The sharp drop for specimen TDCB_03 in the initial crack propagation phase could have been caused by some local defects in the adhesive (Figure 7). However, it quickly recovers close to an energy release rate found at the initial propagation values. For the RWDC test method the applied energy release rate is normalized with the average fracture toughness found with the quasi-static RWD test setup [15]. With this method the initial propagation values cannot be used to determine the fracture toughness properly. Further away from the initial crack tip the energy release rate stabilizes and goes to a value that could be considered as the fracture toughness. The same principle has been tried for the TDCB constant load test results. Although, it was discovered that there is also spread in the results between the quasi-static TDCB tests and the individual specimens for the TDCB constant load test. Looking to the different load levels applied and the creep crack growth rates observed for the different specimens (Table 3), a linear trendline on a log-log scale is expected as was found for this adhesive in the RWDC test method. As mentioned before, the found fracture toughness of an individual TDCB specimen is quite close to the initial propagation energy release rate values with an average difference of 4.1%. Therefore, the energy release rate found at the pre-cracking phase of each individual specimen could be used to normalize

the applied energy release rate in the TDCB constant load test. Which, then produces the graph as shown in Figure 10, where it can be observed that the slope of the creep crack growth curve is similar for both the RWDC and TDCB. Although, the other coefficient is slightly off and could be caused by the overestimation of the RWDC test method. From previous work it is known that the RWD test method very likely overestimates the fracture toughness due to the friction in the roller wedge [15]. The presented RWDC curve assumes that the friction in the roller wedge can be neglected since it is so low and therefore taken as zero. It is not known what the exact friction coefficient for the roller wedge is since it is not evident to determine the friction coefficient properly. It was demonstrated that the magnitude for friction coefficient of the roller wedge is likely around 0.02 [15]. In Figure 13 the RWDC curve is corrected assuming the friction coefficient is 0.02. The slope of the RWDC gets even closer to the slope found with the TDCB but the offset between both curves only gets slightly closer.

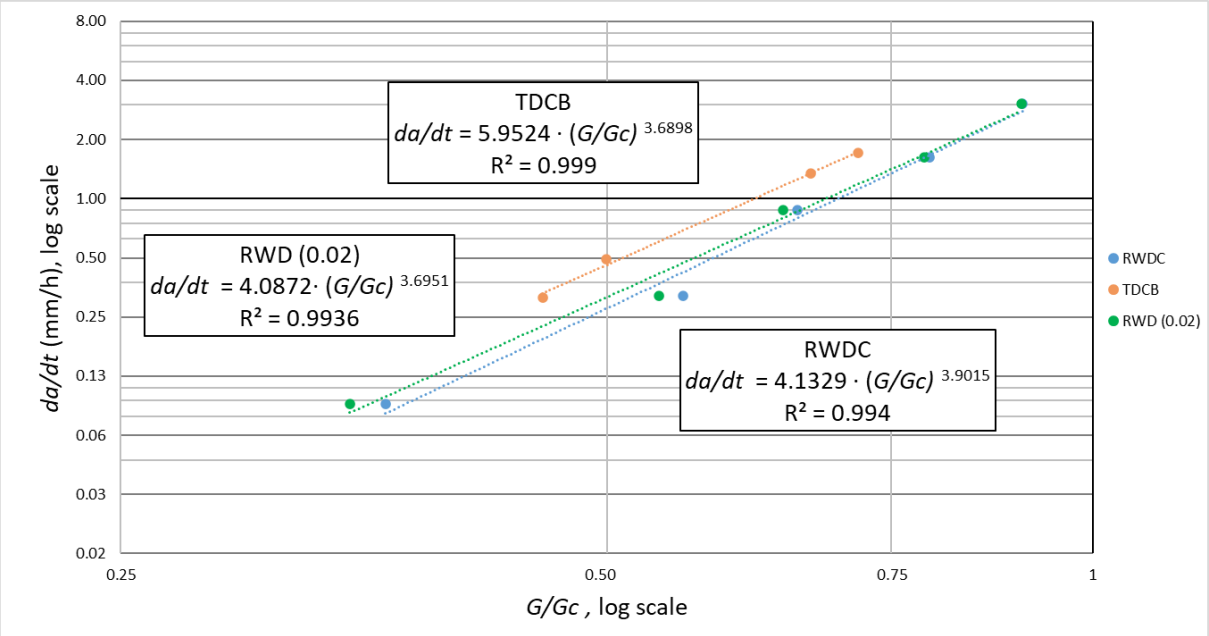

Figure 13. RWDC curve corrected by assuming a friction coefficient of 0.02 in the roller wedge instead of assuming a friction coefficient of zero.

Comparing both test methods, the RWDC method has a significant advantage that crack length measurement is not required during the test, the crack growth rates follow directly from the wedge displacement measurement. Measuring the wedge displacement with a LVDT is a continuous measurement method that is more accurate and gives more information about how the adhesive

behaves over a long time period. To initiate the creep crack growth tests a sharp crack tip must be created, which is done by pre-cracking the specimen. The TDCB specimens require a displacement controlled tensile test machine to pre-crack the specimen before loading it in the TDCB constant load test setup. The RWD test setup can be used with the manual method [15] (pushing the roller wedge in the specimen by turning a threaded bar) to create a pre-crack, which does not require a test machine. In the same test setup then a constant load can be applied to the wedge to immediately start the RWDC test after creating the pre-crack. The specific geometry of the TDCB specimens requires the adherends to be manufactured with a milling machine, while the RWDC method requires simpler DCB-like specimens. The adherends for the DCB-like specimens can be easily cut from a plate or strip which is more affordable than milling. The constant load that needs to be applied to the specimen in the RWDC test setup to have a similar energy release rate at the crack tip as the TDCB is approximately 19% of the weight required for the TDCB constant load test. Resulting in a more practical and safer to use test method.

4.2 Existing fatigue model to simulate creep crack growth in a bonded joint

Fatigue is a durability phenomenon that is already known for a long time and has been extensively researched for metals and composite materials. Therefore, also numerical models have been developed and implemented in commercially available software. For creep crack growth such models are less widely available but the behaviour from the creep crack growth experimental results (Figure 12) show that it also follows a power law behaviour similar as the Paris´ law-like expression for fatigue. Looking at some examples in literature related to fatigue testing or modelling of DCB bonded joints, quite some spread in results of the material parameters can be found. Ranging from 1 to 9 for the power coefficient that determines the slope of the Paris´ law-like expression [43]–[49]. The material parameter found for the slope of the curve for this specific adhesive system is approximately 3.9 (Figure 2). The model parameters of the creep crack growth curve of the RWDC test are implemented in the FEM model of the TDCB constant load test. The geometry and the material properties of the

TDCB adherends in the model result in an energy release rate at the crack tip for different constant loads applied. The constant load applied relating to the energy release rate at the crack tip (Table 4) matches well with what was analytically determined with the ECM data reduction method for the TDCB experimental tests (Table 3). Even though the FEM model is a TDCB specimen, the crack growth rate obtained from the model matches with the creep crack growth rates found in RWDC test results (Figure 12). The assumption is that the VCCT and DC module only follow the Paris´ law-like expression (material parameters from RWDC test) and the energy release rate that is present at the crack tip. In other words, changing the geometry of the adherends will likely change the energy release rate at the crack tip for a certain applied load but it will still follow the same implemented model. However, it should be mentioned that in this model only energy dissipation by forming a crack is considered, other energy dissipating mechanisms are neglected.

The DC module is designed for fatigue simulation and thus works with cycles. The DC module requires an amplitude change and, the start and end value of the amplitude of each cycle needs to be equal [33]. Also, the DC module determines the ΔG for each cycle, which is the input to propagate the crack. This means applying a constant load to the specimen or having a constant amplitude during the simulation is not possible. Because ΔG will be zero, there is no propagation over time, even though an applied load in a quasi-static situation would result in a higher than zero energy release rate at the crack tip. The only option to use this specific DC module in Abaqus to simulate the creep crack growth is to apply an amplitude change within a cycle, as is proposed in section 2.3 (Figure 3). The authors understand that the cyclic behaviour of the FEM model does not represent the reality of the creep crack growth test but are convinced the DC module could be adapted relatively easily. So that the load can be kept constant during the whole simulation and crack propagation takes place following the CCGM as described in section 2.1.

5. Conclusions

A Creep Crack Growth Model (CCGM) is proposed to predict creep crack length based on applied energy release rate. The model parameters are obtained by experimental tests using the RWD creep crack growth (RWDC) test method [9]. The CCGM and the RWDC method are validated against the developed TDCB constant load test method. With an example it is demonstrated that the CCGM can be implemented into an existing commercially available numerical model.

An advantage of using a tapered double cantilever beam (TDCB) specimen is that the load remains constant during propagation regardless of the crack length. When a constant load is applied, the energy release rate corresponding to that load can be determined with the experimental compliance method (ECM) data reduction method. The crack growth rate can be plotted against the energy release rate on a log-log scale. Results of this plot have shown that for this specific tested adhesive system a similar slope is obtained for the CCGM with both the TDCB constant load test and the RWDC test method. Based on these results it can be assumed that the CCGM describes the creep crack growth in the bonded joint. Comparing both test methods, the RWDC method does not require visual crack length measurement, neither a tensile test machine to pre-crack the specimen and the adherends do not have to be milled into a tapered geometry with specific dimensions.

Finite element method (FEM) results of the modelled TDCB specimen demonstrate that existing commercially available fatigue models based on a Paris´ law-like expression can be used to simulate creep crack growth in bonded joints. Entering the experimental material parameters of the CCGM in the direct cyclic (DC) module of the FEM model gives the same results as the RWDC test. This shows that the DC module follows exactly the prescribed CCGM and that the energy release rate controls the crack growth rate. The authors are aware the DC module is designed for fatigue modelling and that the current model in reality does not represent the creep crack growth TDCB constant load test. Because in the DC module the amplitude step within a cycle cannot be excluded to have crack propagation. However, the closing step inside the cycle does not affect the virtual crack closure

technique (VCCT) model that provides the crack growth, thus only considering the results of the last increment of each cycle gives results similar to the creep crack growth results. The authors are optimistic that the DC module could be adapted relatively easily so that a constant load can be applied, and crack propagation takes place following the CCGM. It must be mentioned that this principle only has been demonstrated for this specific adhesive system and using the DC+VCCT modules in Abaqus. Furthermore, it has only be tested on relatively simple straight bonded joints between two similar material types loaded in mode I. Nevertheless, it has been demonstrated that the CCGM can be applied to a different bonded joint geometry and produces similar results.

In conclusion, the durability of bonded joints is a critical aspect of many engineering applications, and a comprehensive understanding of the mechanisms of creep crack growth is crucial for ensuring the safety and reliability of these structures. To achieve this, creep crack growth test methods and FEM models need to be developed to provide tools that engineers can use to improve design and maintenance of bonded joints.

6. Acknowledgements

The work was performed under contract PID2021-127879OB-C21 of the Spanish Government through the Ministerio de Ciencia, Innovacón y Universidades and Grant RYC2021-032171-I funded by MCIN/AEI/ 10.13039/501100011033 and by “European Union NextGenerationEU/PRTR. The authors would like to acknowledge the support for this work by these entities. The first author received additional support through a fellowship grant, IFUdG2021-AE, co-funded by the AMADE research group (GRCT0064) and provided by the Universitat de Girona and Banco Santander. Open Access funding provided thanks to the CRUE-CSIC agreement with Elsevier. The work in this research has been made possible by patent 300352094, PCT/ES2020/070074 made available by IKERLAN, S.COOP. (IKER018) and the Universitat de Girona. Furthermore, the authors like to acknowledge the support from the AMADE research group testing laboratory.

References

[1] L. F. M. Da Silva, A. Öchsner, and R. D. Adams, *Handbook of Adhesion Technology*, 2nd ed. Springer International Publishing AG, 2011. doi: 10.1007/978-3-642-01169-6.

[2] W. Bradley, W. J. Cantwell, and H. H. Kausch, "Viscoelastic Creep Crack Growth: A Review of Fracture Mechanical Analyses," *Mechanics Time-Dependent Materials*, vol. 1, no. 3, pp. 241–268, 1997, doi: 10.1023/A:1009766516429.

[3] C. R. Siviour and J. L. Jordan, "High Strain Rate Mechanics of Polymers: A Review," *Journal of Dynamic Behavior of Materials*, vol. 2, no. 1, pp. 15–32, Mar. 2016, doi: 10.1007/s40870-016-0052-8.

[4] F. Cavezza, M. Boehm, H. Terryn, and T. Hauffman, "A review on adhesively bonded aluminium joints in the automotive industry," *Metals (Basel)*, vol. 10, no. 6, pp. 1–32, 2020, doi: 10.3390/met10060730.

[5] W. J. Broughton and R. D. Mera, "Review of durability test methods and standards for assessing long term performance of adhesive joints," no. May, p. 78, 1997, Accessed: Mar. 09, 2023. [Online]. Available: http://www.adhesivestoolkit.com/Docu-Data/NPLDocuments/PAJ/PAJReports/PAJ3Reports/PAJ3Report1CMMT(A)61.pdf

[6] "ASTM D3762-03(2010) Standard Test Method for Adhesive-Bonded Surface Durability of Aluminum (Wedge Test) (Withdrawn 2019)." ASTM International, p. 5, 2010. [Online]. Available: https://www.astm.org/Standards/D3762.htm

[7] D. O. Adams, K. L. DeVries, and C. Child, "Durability of adhesively bonded joints for aircraft structures," *FAA Joint Advanced Materials and Structures (JAMS) Center of Excellence Technical Review Meeting*, p. 22, 2012, [Online]. Available: http://depts.washington.edu/amtas/events/jams_12/papers/paper-adams_adhesive.pdf

[8] J. Cognard, “Use of the wedge test to estimate the lifetime of an adhesive joint in an aggressive environment,” *Int J Adhes Adhes*, vol. 6, no. 4, pp. 215–220, 1986, doi: 10.1016/0143-7496(86)90008-4.

[9] E. Meulman, J. Renart, L. Carreras, and J. Zurbitu, “A methodology for the experimental characterization of energy release rate-controlled creep crack growth under mode I loading,” *Eng Fract Mech*, vol. 283, no. 109222, Apr. 2023, doi: 10.1016/j.engfracmech.2023.109222.

[10] D. Plausinis and J. K. Spelt, “Application of a new constant G load-jig to creep crack growth in adhesive joints,” *Int J Adhes Adhes*, vol. 15, no. 4, pp. 225–232, 1995, doi: 10.1016/0143-7496(96)83703-1.

[11] D. A. Dillard, J. Z. Wang, and H. Parvatareddy, “A simple constant strain energy release rate loading method for double cantilever beam specimens,” *J Adhes*, vol. 41, no. 1–4, pp. 35–50, Jun. 1993, doi: 10.1080/00218469308026553.

[12] D. R. Lefebvre, D. A. Dillard, and H. F. Brinson, “The development of a modified double-cantilever-beam specimen for measuring the fracture energy of rubber to metal bonds,” *Exp Mech*, vol. 28, no. 1, pp. 38–44, Mar. 1988, doi: 10.1007/BF02328994.

[13] K. Nakamura, Y. Sekiguchi, K. Shimamoto, K. Houjou, H. Akiyama, and C. Sato, “Creep Crack Growth Behavior during Hot Water Immersion of an Epoxy Adhesive Using a Spring-Loaded Double Cantilever Beam Test Method,” *Materials*, vol. 16, no. 2, Jan. 2023, doi: 10.3390/ma16020607.

[14] P. Schrader, C. Schmandt, and S. Marzi, “Mode I creep fracture of rubber-like adhesive joints at constant crack driving force,” *Int J Adhes Adhes*, vol. 113, Mar. 2022, doi: 10.1016/j.ijadhadh.2021.103079.

[15] E. Meulman, J. Renart, L. Carreras, and J. Zurbitu, “Analysis of mode I fracture toughness of adhesively bonded joints by a low friction roller wedge driven quasi-static test,” *Eng Fract Mech*, vol. 271, no. 108619, May 2022, doi: 10.1016/j.engfracmech.2022.108619.

[16] J. Manterola, J. Renart, J. Zurbitu, A. Turon, and I. Urresti, “Mode I fracture characterization of rigid and flexible bonded joints using an advanced Wedge Driven Test,” *Mechanics of Materials*, vol. 148, no. 103534, pp. 1–26, 2020, doi: 10.1016/j.mechmat.2020.103534.

[17] J. Renart, J. Costa, G. Santacruz, S. Lazcano, and E. Gonzalez, “Measuring fracture energy of interfaces under mode I loading with the wedge driven test.,” *Eng Fract Mech*, no. 239, p. 15, 2020, doi: 10.1016/j.engfracmech.2020.107210.

[18] “ISO 25217:2009 - Adhesives — Determination of the mode 1 adhesive fracture energy of structural adhesive joints using double cantilever beam and tapered double cantilever beam specimens.” p. 24, 2009.

[19] B. R. K. Blackman, H. Hadavinia, A. J. Kinloch, M. Paraschi, and J. G. Williams, “The calculation of adhesive fracture energies in mode I: revisiting the tapered double cantilever beam (TDCB) test,” *Eng Fract Mech*, vol. 70, no. 2, pp. 233–248, Jan. 2003, doi: 10.1016/S0013-7944(02)00031-0.

[20] B. R. K. Blackman, A. J. Kinloch, M. Paraschi, and W. S. Teo, “Measuring the mode I adhesive fracture energy, GIc, of structural adhesive joints: The results of an international round-robin,” *Int J Adhes Adhes*, vol. 23, no. 4, pp. 293–305, 2003, doi: 10.1016/S0143-7496(03)00047-2.

[21] B. R. K. Blackman, A. J. Kinloch, F. S. Rodriguez Sanchez, W. S. Teo, and J. G. Williams, “The fracture behaviour of structural adhesives under high rates of testing,” *Eng Fract Mech*, vol. 76, no. 18, pp. 2868–2889, Dec. 2009, doi: 10.1016/j.engfracmech.2009.07.013.

[22] O. Hesebeck, U. Meyer, A. Sondag, and M. Brede, “Investigations on the energy balance in TDCB tests,” *Int J Adhes Adhes*, vol. 67, pp. 94–102, Jun. 2016, doi: 10.1016/j.ijadhadh.2015.12.031.

[23] P. Qiao, J. Wang, and J. F. Davalos, “Tapered beam on elastic foundation model for compliance rate change of TDCB specimen,” *Eng Fract Mech*, vol. 70, no. 2, pp. 339–353, Jan. 2003, doi: 10.1016/S0013-7944(02)00023-1.

[24] W. L. Tsang, “The use of tapered double cantilever beam (TDCB) in investigating fracture properties of particles modified epoxy,” *SN Appl Sci*, vol. 2, no. 4, Apr. 2020, doi: 10.1007/s42452-020-2487-8.

[25] J. M. D. Teixeira, R. D. S. G. Campilho, and F. J. G. da Silva, “Numerical assessment of the Double-Cantilever Beam and Tapered Double-Cantilever Beam tests for the GIC determination of adhesive layers,” *Journal of Adhesion*, vol. 94, no. 11, pp. 951–973, Sep. 2018, doi: 10.1080/00218464.2017.1383905.

[26] S. Marzi, A. Biel, and U. Stigh, “On experimental methods to investigate the effect of layer thickness on the fracture behavior of adhesively bonded joints,” *Int J Adhes Adhes*, vol. 31, no. 8, pp. 840–850, Dec. 2011, doi: 10.1016/j.ijadhadh.2011.08.004.

[27] J. Gómez, C. Barris, Y. Jahani, M. Baena, and L. Torres, “The effect of steady and cyclic environmental conditions on the tensile behaviour of a structural adhesive under sustained loading,” *Compos Struct*, vol. 286, p. 115287, Apr. 2022, doi: 10.1016/j.compstruct.2022.115287.

[28] P. Silva, J. Sena-Cruz, M. Azenha, and G. Escusa, “Experimental investigation on creep behaviour of an epoxy adhesive,” in *SMAR*, 2015.

[29] L. M. Martulli and A. Bernasconi, “An efficient and versatile use of the VCCT for composites delamination growth under fatigue loadings in 3D numerical analysis: The sequential static fatigue algorithm,” *Int J Fatigue*, p. 107493, Dec. 2022, doi: 10.1016/j.ijfatigue.2022.107493.

[30] A. Turon, J. Costa, P. P. Camanho, and C. G. Dávila, “Simulation of delamination in composites under high-cycle fatigue,” *Compos Part A Appl Sci Manuf*, vol. 38, no. 11, pp. 2270–2282, Nov. 2007, doi: 10.1016/j.compositesa.2006.11.009.

[31] L. Carreras *et al.*, “A simulation method for fatigue-driven delamination in layered structures involving non-negligible fracture process zones and arbitrarily shaped crack fronts,” *Compos Part A Appl Sci Manuf*, vol. 122, pp. 107–119, Jul. 2019, doi: 10.1016/j.compositesa.2019.04.026.

[32] H. Khoramishad, A. D. Crocombe, K. B. Katnam, and I. A. Ashcroft, “Predicting fatigue damage in adhesively bonded joints using a cohesive zone model,” *Int J Fatigue*, vol. 32, no. 7, pp. 1146–1158, Jul. 2010, doi: 10.1016/j.ijfatigue.2009.12.013.

[33] “Abaqus Analysis User’s Manual.” Dassault Systemes Simulia, Inc, 2014.

[34] A. Pirondi, G. Giuliese, F. Moroni, A. Bernasconi, and A. Jamil, “Comparative Study of Cohesive Zone and Virtual Crack Closure Techniques for Three-Dimensional Fatigue Debonding,” *J Adhes*, vol. 90, no. 5–6, pp. 457–481, Jun. 2014, doi: 10.1080/00218464.2013.859616.

[35] C. G. Dávila and C. Bisagni, “Fatigue life and damage tolerance of postbuckled composite stiffened structures with initial delamination,” *Compos Struct*, vol. 161, pp. 73–84, Feb. 2017, doi: 10.1016/j.compstruct.2016.11.033.

[36] F. Teimouri, M. Heidari-Rarani, and F. Haji Aboutalebi, “An XFEM-VCCT coupled approach for modeling mode I fatigue delamination in composite laminates under high cycle loading,” *Eng Fract Mech*, vol. 249, p. 107760, May 2021, doi: 10.1016/j.engfracmech.2021.107760.

[37] G. Giuliese, A. Pirondi, and F. Moroni, “A Cohesive Zone Model for Three-dimensional Fatigue Debonding/Delamination,” *Procedia Materials Science*, vol. 3, pp. 1473–1478, 2014, doi: 10.1016/j.mspro.2014.06.238.

[38] J. A. Pascoe, R. C. Alderliesten, and R. Benedictus, “Methods for the prediction of fatigue delamination growth in composites and adhesive bonds – A critical review,” *Eng Fract Mech*, vol. 112–113, pp. 72–96, Nov. 2013, doi: 10.1016/j.engfracmech.2013.10.003.

[39] R. Krueger, “The virtual crack closure technique for modeling interlaminar failure and delamination in advanced composite materials,” in *Numerical Modelling of Failure in Advanced Composite Materials*, Elsevier, 2015, pp. 3–53. doi: 10.1016/B978-0-08-100332-9.00001-3.

[40] R. Krueger, “An Approach to Assess Delamination Propagation Simulation Capabilities in Commercial Finite Element Codes,” 2008. Accessed: Feb. 15, 2023. [Online]. Available: https://ntrs.nasa.gov/citations/20080015439

[41] R. Krueger, “Virtual crack closure technique: History, approach, and applications,” *Appl Mech Rev*, vol. 57, no. 1–6, pp. 109–143, Jan. 2004, doi: 10.1115/1.1595677.

[42] M. L. Benzeggagh and M. Kenane, “Measurement of mixed-mode delamination fracture toughness of unidirectional glass/epoxy composites with mixed-mode bending apparatus,” *Compos Sci Technol*, vol. 56, no. 4, pp. 439–449, 1996, doi: 10.1016/0266-3538(96)00005-X.

[43] I. A. Ashcroft and S. J. Shaw, “Mode I fracture of epoxy bonded composite joints 2. Fatigue loading,” *Int J Adhes Adhes*, vol. 22, no. 2, pp. 151–167, Jan. 2002, doi: 10.1016/S0143-7496(01)00050-1.

[44] M. V. Fernández, M. F. S. F. de Moura, L. F. M. da Silva, and A. T. Marques, “Composite bonded joints under mode I fatigue loading,” *Int J Adhes Adhes*, vol. 31, no. 5, pp. 280–285, 2011, doi: 10.1016/j.ijadhadh.2010.10.003.

[45] A. Pirondi and G. Nicoletto, “Fatigue crack growth in bonded DCB specimens,” *Eng Fract Mech*, vol. 71, no. 4–6, pp. 859–871, 2004, doi: 10.1016/S0013-7944(03)00046-8.

[46] M. F. S. F. de Moura, J. P. M. Gonçalves, and M. V. Fernandez, “Fatigue/fracture characterization of composite bonded joints under mode I, mode II and mixed-mode I+II,” *Compos Struct*, vol. 139, pp. 62–67, Apr. 2016, doi: 10.1016/j.compstruct.2015.11.073.

[47] K. Ishii, “Effect of substrate material on fatigue crack propagation rate of adhesively bonded DCB joints,” *J Adhes Sci Technol*, vol. 25, no. 20, pp. 2775–2787, 2012, doi: 10.1163/016942410X537369.

[48] A. A. M. A. Campos, A. M. P. De Jesus, J. A. F. O. Correia, and J. J. L. Morais, “Fatigue Crack Growth Behavior of Bonded Aluminum Joints,” in *Procedia Engineering*, Elsevier Ltd, 2016, pp. 270–277. doi: 10.1016/j.proeng.2016.08.890.

[49] L. Carreras, J. Renart, A. Turon, J. Costa, Y. Essa, and F. Martin de la Escalera, “An efficient methodology for the experimental characterization of mode II delamination growth under fatigue loading,” *Int J Fatigue*, vol. 95, pp. 185–193, 2017, doi: 10.1016/j.ijfatigue.2016.10.017.

5. General results and discussion

This chapter presents the main results of the work as a whole and discusses them in relation to the proposed objective of the thesis: the development of a method to measure creep crack growth in an adhesively bonded joint by applying a constant energy release rate in mode I. The author of this thesis has tried to make this chapter self-contained, consequently, the reader will find that some figures are reused directly from the previous chapters (articles) with the intention of assisting the reader.

To achieve the main objective of the thesis, the first step is to obtain reliable creep crack growth which requires a test method that can apply a constant energy release rate to the crack tip of a bonded joint. Therefore, a test setup is developed that makes use of a low friction roller wedge. The roller wedge is discussed in section 5.1. Secondly, the mechanisms involved in creep crack growth and how creep crack growth rates are obtained from bonded joints are discussed in section 5.2. Lastly, in section 5.3, the proposed creep crack model is discussed which is obtained from the creep crack growth test results. In the same section it is also discussed that the model can be implemented in an existing FEM model to simulate creep crack growth in bonded joints.

5.1. A Low friction roller wedge test

Wedge friction

Relating to the need for testing with a constant energy release rate, a new test method is developed based on the concept of using a sliding wedge to load a bonded joint in mode I [47], [88]. The friction involved with a sliding wedge in contact with the bonded joint adherends (metal-on-metal) is not easy to determine and it has been shown that it does not stay constant during the test [43]. Friction takes up a significant portion of the total energy introduced to the wedge and needs to be taken into account in the data reduction method. Using rollers can reduce the friction of the wedge significantly. It is assumed that rollers will have a very low friction coefficient so that it can be neglected in the data

reduction to determine the energy release rate [47]. A roller wedge driven (RWD) test method is developed in Chapter 2 that aims to reduce the friction between the roller and specimen to a minimum and to validate if in that case it can indeed be neglected in the data reduction method. This would simplify the data reduction significantly since then only the applied force during the test needs to be measured to determine the applied energy release rate. Experimental results obtained with the RWD test setup have shown that indeed it can be assumed that the friction coefficient of the roller wedge is significantly lower as a sliding wedge (0.02 vs. 0.3 typical for metal-on-metal friction) but that it cannot be neglected in the data reduction. The difference in fracture toughness found between the RWD method and the standardised DCB tests indicates that energy is dissipated in the system and that is likely in the roller wedge. The needle-bearings in the rollers have typically a low friction coefficient ranging from 0.002 – 0.003 [89], which is about a factor 10 lower than the resistance found for the roller wedge. The other part of the friction that is still present could be caused by the roller and specimen surface contact. The specimens received a surface treatment to improve the bond quality by roughing the surface. The resistance (rolling resistance) that the roller wedge experiences is lower for a smooth surface of the adherend compared to a rough surface, regardless of the friction coefficient of the needle-bearing of the roller. It could be possible that if surface and roller conditions are further optimized the total resistance of the roller wedge can be reduced even more and then the dissipated energy could be low enough that it indeed can be neglected. This deserves further investigation.

Fracture toughness

One of the conclusions of Chapter 2 is that the RWD test method could potentially be used to determine the fracture toughness in bonded joints. However, a reliable and accurate analysis of the results is required to adequately determine if the measured spread in the results is related to the test method or due to variation in the material. Especially, in bonded joints, the bonding process is critical for the ultimate bonded joint properties. In this work one type of adhesive is used for the bonded

joints (Araldite 2021-1). It is observed that there is significant variation in the test results for this specific adhesive. The standardised DCB test [41] was used as reference method to determine the fracture toughness of the adhesive, where also variation was found in the test results. Regardless of pre-cracking, there seems to always be a higher initial peak for the energy release rate before a lower more stable energy release rate is found during the later stage of the crack propagation. The same is observed in the RWD test results. It is described in the DCB standard [41] that only the propagation results should be considered in the determination of the fracture toughness (average energy release rate during the crack propagation phase) and not the crack initiation data points. It is not always clear from the test results where the crack initiation takes place exactly, especially if the adhesive shows a high initial peak like, Araldite 2021-1. In that case, one could say that the data points relating to a longer crack length, relatively far away from the assumed crack initiation point, makes it more likely that only crack propagation data points are included in the fracture toughness result. However, there is a limitation for the type of wedge tests considered in this thesis, since the wedge is entered in between the two adherends and at some moment the wedge comes into contact with the adhesive and the test cannot be continued. Taking a more conservative approach for the wedge test, by considering only data points for the fracture toughness calculation when the crack already extended significantly, would reduce the number of available data points significantly. The maximum crack length that can be created in a specimen tested with the RWD test method depends on the diameter of the rollers, the bondline thickness and the stiffness of the adherends. These parameters change the relationship between the opening displacement and the distance between the wedge rollers and the crack tip (crack length *a)*. In other words, for a given stiffness of the adherends a larger opening displacement will increase the crack length. For a certain bonded joint, it could be that a larger roller diameter would be preferable but then it is possible that the simplified roller contact is not applicable anymore (Figure 5-1) [46]. Then, the exact contact point of the roller with the adherend relating to the roller axis needs to be determined and subtracted from the numerical solved crack length, which

makes the data reduction more complex and more susceptible to errors in the determination of the energy release rate.

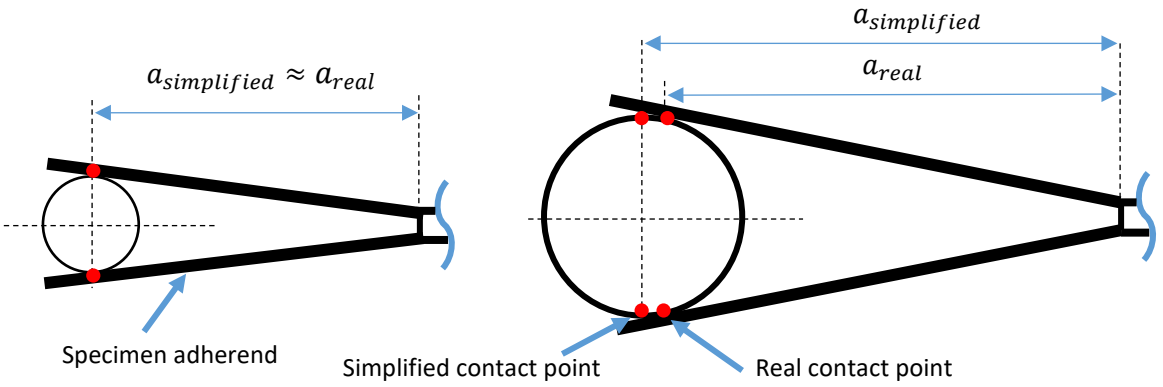

Figure 5-1. A roller wedge entered in a specimen with the real and simplified contact points indicated. For a smaller diameter roller, the simplified and real contact point can be considered equal and therefore crack length a can be assumed from the centre of the roller (the simplified contact point).

RWD manual method

The RWD test rig was originally conceived to be used for durability testing, i.e. without a test machine and in a climatic chamber. Based on this idea, a modification of the RWD was designed to apply the displacement manually, called the RWD manual method. A threaded bar is turned around with a wrench so that the threaded bar pushes the roller wedge into the specimen. Since the load required to fracture the tested adhesive is low it can be performed by hand. However, controlling the displacement of the wedge using the RWD manual test method is not easy. Firstly, the angular rotation, and as a result the wedge displacement rate, is not completely constant during the test. The human hand can rotate the bar with a certain degree of precision but will never be as constant as a machine. Secondly, the displacement rate of the wedge can only be determined after the test has finished and is not predefined like in the test machine. In chapter 2 the results of the RWD test from the testing machine and applying the displacement manually are compared. The wedge displacement rate applied manually was on average almost a factor 8 higher than with the test machine. With the RWD manual method it was noticed that the determined fracture toughness is higher than the RWD

method that uses the test machine. Based on these results it is assumed that the adhesive used in this work is rate sensitive. This could also indicate that a significant amount of energy is dissipated in this adhesive by mechanisms like, for example viscosity. In this work the bulk adhesive is not characterized. Therefore, testing at relatively high rates with this specific adhesive makes the energy release rate results obtained unreliable. Regardless of the rate sensitivity of the adhesive, the RWD manual method can still be used to pre-crack the specimen for durability testing. For the RWD creep crack growth (RWDC) test a constant energy release rate is applied to the specimen by placing a weight on top of the wedge. Thus, the load on the wedge will remain constant during the test while the crack is propagating. At the same time the wedge displacement is measured during the test to be able to obtain creep crack growth rates. This makes the RWD rig practical in use since, the specimen is clamped into the test setup, pre-cracked. And, without removing the wedge, the threaded bar used for pre-cracking the specimen is replaced with a weight to immediately start the creep crack growth test.

5.2. Creep crack growth

Fracture surface transition

The crack growth rate from the creep test is relatively low compared to the static test. It has been observed that the fracture surface undergoes a transition from cohesive to adhesive failure when creep crack growth takes place. This seems not to be a complete cohesive or adhesive failure but rather a mix of both depending on the crack growth rate. The lower the creep crack growth rate the higher fraction of adhesive failure is present. The transition of failure mode is likely related to the rate and a time dependent mechanism (which are connected in some way, since time influences the rate) that is active in the adhesive in front of the crack tip. There the adhesive gets stressed before a crack is formed. Araldite 2021-1 is a toughened adhesive. The rubber particles in the adhesive, that increase the toughness also promote the forming of voids when the adhesive is stressed. Between the voids the polymer chains align and form fibrils [90]–[93]. It can be imagined that the properties of the

adhesive change if there is more time available for the adhesive to realign polymer chains and to relax stresses in the adhesive in front of the crack tip. The exact mechanism is not clear from this work and not part of the scope of this thesis. However, it was visually noticed during the experimental tests that the colour of the adhesive changes from greyish to white (Figure 5-2). The voids and fibrilization of the adhesive changes the refractive index of the material and therefore the colour changes when this specific material gets stressed. This has been reported as whiting or craze forming [93], [94].

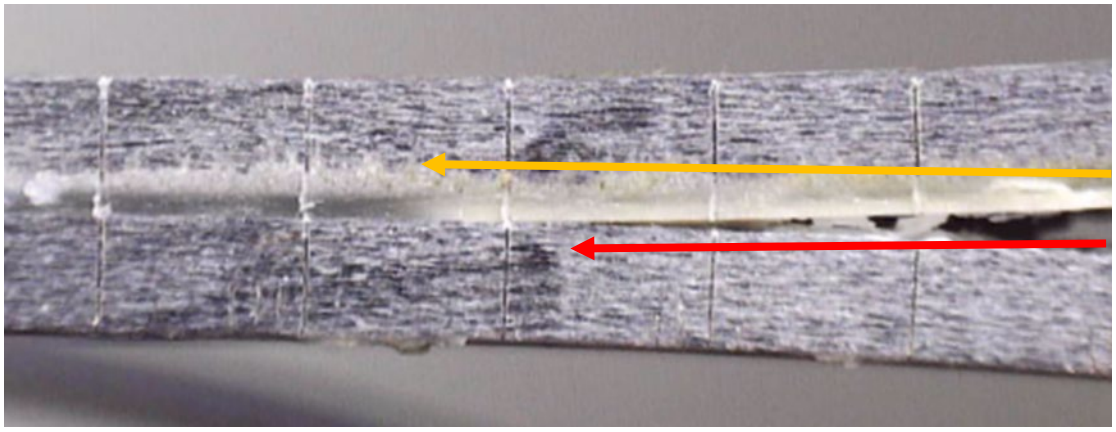

Figure 5-2. example of crazing in Specimen RWD-C_05 with whitened adhesive ahead of the crack tip. The yellow arrow indicates the distance the whitened area had passed through the adhesive and the red arrow the crack tip. [95] *(Figure 8 in article of chapter 3)*.

Transitory phase

In the creep crack growth tests an energy release rate below the fracture toughness of the adhesive is applied to the crack tip. According to the Griffith's criterion, it is assumed that under static conditions crack propagation will not take place. The results from the creep crack growth tests show something different. After a certain amount of time suddenly creep crack growth initiates. This transitory time is likely related to the time it takes for the adhesive to completely develop the craze zone. It seems that the amount of energy release rate applied to the crack tip influences the duration of the transitory phase (Figure 5-3). Not enough experimental test data is available to find a clear correlation, but there appears to be a trend that the lower the energy release rate applied the longer the duration of transitory phase. All the specimens tested for creep crack growth were pre-cracked. One would say that therefore the craze zone should already have been developed. However, pre-

cracking is done quasi-statically by displacement control and relatively high rates compared to creep crack growth rates. It is stated that the displacement of the wedge equals the crack growth. This means also the craze zone is developed at the same rate not allowing the time dependent mechanism to develop the craze zone in the way it would if a constant load or i.e. constant energy release rate would be applied to the specimen.

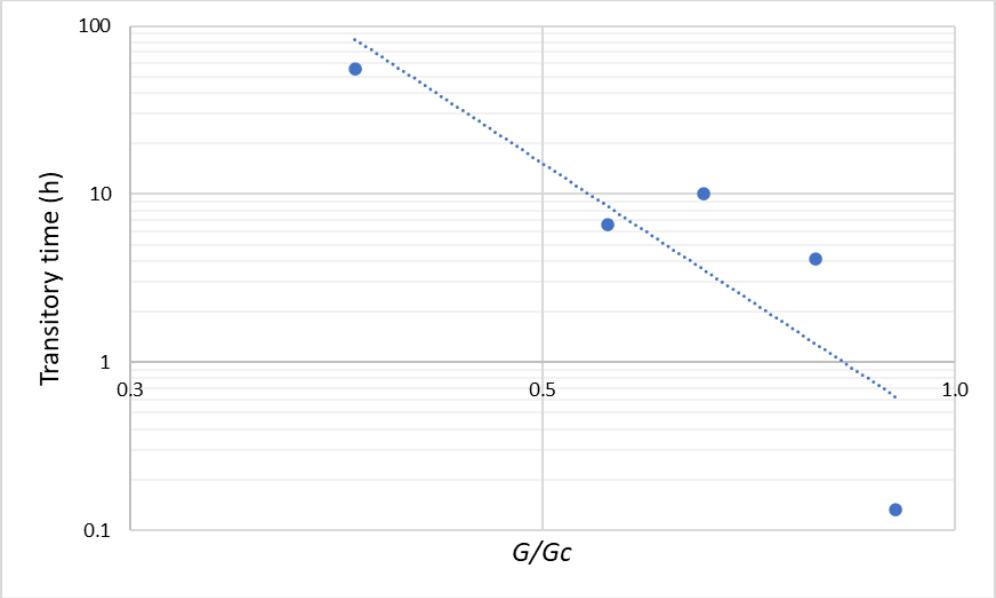

Figure 5-3. Transitory time in hours found for specimens RWD-C_01 to RWD-C_05 against the normalized applied energy release rate [95]*(Figure 11 in article of chapter 3)*.

The average creep crack growth rate

With quasi-static testing and the visual measurement method the assumption that the wedge displacement equals the crack length is validated for the adhesive system, Araldite 2021-1. The available data show that on average the wedge indeed follows the crack length increase in the propagation phase. However, for any specific moment in time this does not have to be the case. Because in the creep crack growth test the continuous wedge displacement data (LVDT) shows that for the tested adhesive the crack growths in a step-like manner. Nevertheless, we are in this case interested in the expected crack length over a longer period of time. If an average crack growth rate is determined by taking the linear trendline of the LVDT crack growth data it follows a similar trendline as found with a visual measurement, which is discontinuous (Figure 5-4). Photos are taken at a certain

time interval, displacement and crack length can be measured in the photos by using a reference length and measuring the number of pixels. Accuracy of this measuring system can be questioned but over larger time periods the average trendlines match quite well. Therefore, the assumption that wedge displacement equals the crack length can be applied for the RWDC method. Therefore, the slope found for the linear trendline is considered as the average creep crack growth rate for the steady-state crack propagation phase.

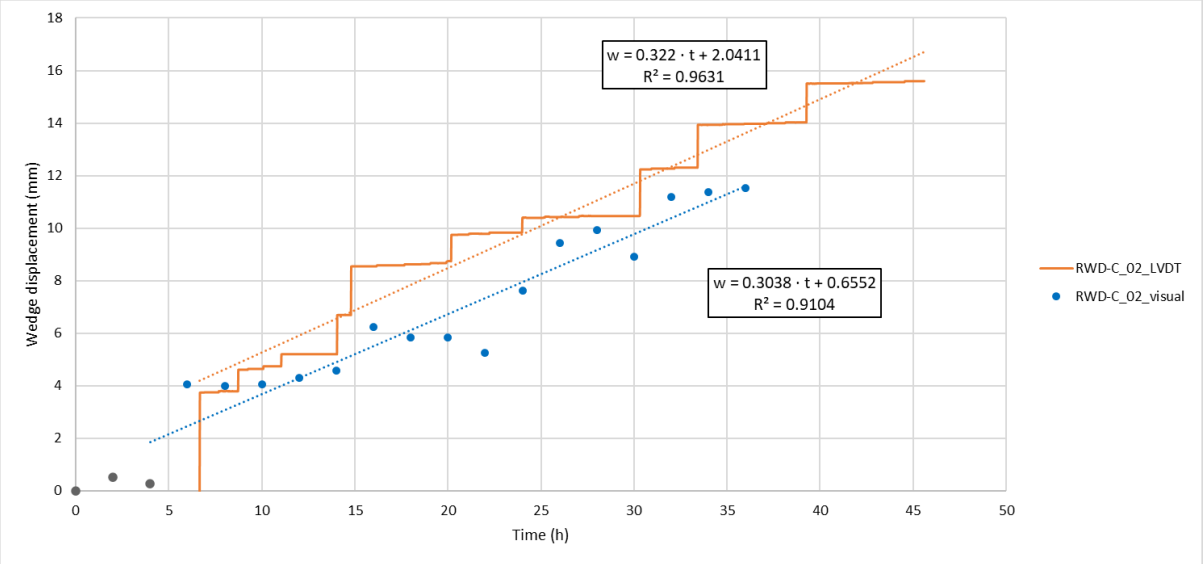

Figure 5-4. Wedge displacement (w) in millimeters against time (t) in hours of specimen RWD-C_02 measured with the visual measurement method and the LVDT [95]*(Figure 4 in article of chapter 3)*.

5.3. Creep crack growth models

When a constant load is applied to the specimen in the RWD test setup, the energy release rate at the crack tip can be determined. By plotting the energy release rate (normalized with the fracture toughness) and the average creep crack growth rate on a graph a point is found. If we repeat this procedure for different values of the energy release rate and we present them on the graph (log-log scale), a log-linear trendline is found, which is described by a Paris´ law-like equation proposed in this work as the Creep Crack Growth Model (CCGM). The model could be a useful tool for engineers to be able to predict expected crack length when a certain energy release rate is applied to a bonded joint. The proposed CCGM is based on the test results of the RWDC method.

A priori, the same behaviour would be expected to occur with other similar tests such as creep crack growth test based on the DCB. Indeed, it is possible to take a DCB specimen and apply a constant load to it by means of a weight hanging from the bottom adherend. In theory, the instantaneous energy release rate and corresponding crack growth rate can be found for this type of test. However, for the used adhesive in this experimental campaign it would not be possible. As pointed out before, this specific adhesive has a transitory phase. With an DCB specimen, the energy release rate changes constantly during crack propagation, and it is very difficult to distinguish if the measured crack growth rate is from the steady-state crack propagation or influenced by the transitory phase. Using a modified version of the DCB, such as the Tapered Double Cantilever Beam (TDCB) specimen has proven to be a better option, since the compliance rate is constant for a TDCB specimen and therefore the energy release rate and the steady-state crack growth rate are constant when a constant load is applied. It was observed that the slope of the CCGM of both the RWDC and TDCB constant load are very similar (Figure 5-5). Although, there was an offset found between the two methods. By correcting the RWDC results by the possible friction coefficient of the roller wedge (0.02), the results improved for the slope but only slightly for the offset. That means over the tested range the expected creep crack growth rate is lower for a bonded joint tested with the RWDC method compared to the TDCB constant load test.

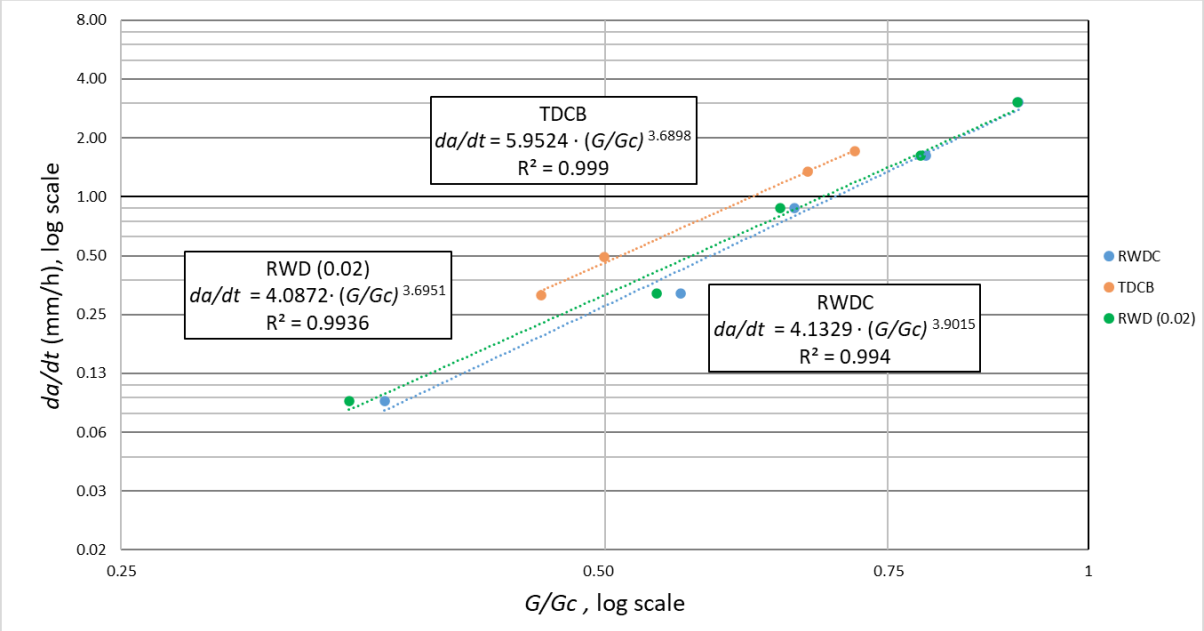

Figure 5-5: Friction coefficient correction of 0.02 for the roller compared to the zero friction roller wedge results and the TDCB [96] *(Figure 13 in article of chapter 4).*

As discussed, spread in specimens tested in this work is observed for both the TDCB and DCB quasi-static tests. Some variation in test results might be expected when conducting experimental tests on adhesively bonded joints. Comparing it to more well known and developed fatigue experimental test methods it seems that also spread like this can be found in fatigue test data. Sometimes the spread between similar specimens tested is almost a decade difference for the crack growth rate [97].

The threshold energy release rate

Besides obtaining the creep crack growth rate for a specific energy release rate it could also be interesting to know at which energy release rate there is no creep crack growth. This is similar to what is obtained from fatigue testing and known as the threshold energy release rate (G_{th}) [15]. In the log-log da/dN vs G curve, G_{th} can be identified as a vertical asymptote, meaning that below this energy release rate no fatigue crack growth takes place (Figure 5-6).

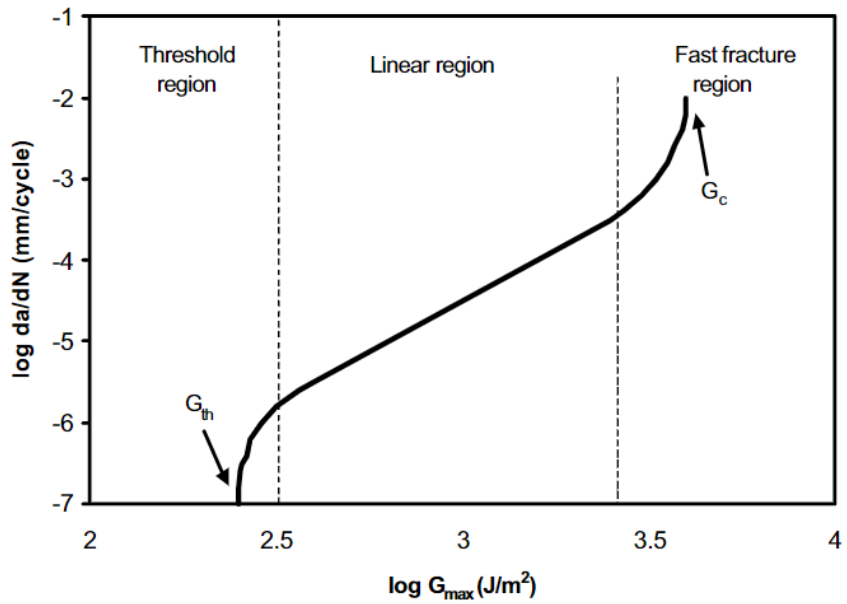

Figure 5-6. Example from literature where the threshold energy release rate (G_{th}) describes a vertical asymptote, where below no crack growth takes place [15].

The lowest G/G_c for which crack propagation took place in the RWDC test campaign is 0.36. Some specimens have been tested at lower levels ranging from 0.26 to 0.34, but there was no clear crack propagation observed. For practical reasons the tests had to be stopped at some moment (approximately 30 days of testing). It could have been possible that the energy release rate was below the G_{th} or that the specimens where in the transitory phase. If the possible trend observed in Figure 5-3 is correct it can be seen that the transitory time increases dramatically when G/G_c is below 0.3. With the current available data, it cannot be stated accurately what is the G_{th} of the adhesive. The RWDC method could likely provide an estimation of the G_{th} if more tests were performed at lower G/G_c values, but it will take a long time to perform these tests. If the tested adhesive does not exhibit a transitory time before the steady-state creep crack growth phase, then a stationary wedge test like, the Boeing Wedge test [23], is probably a better candidate to find a more accurate G_{th} value in a faster manner. In this test, energy release rate constantly decreases until crack arrest is reached. The energy release rate at that point can be determined and considered as G_{th}. For design purposes this value can be interesting in case a bonded joint should never experience creep crack growth in its service lifetime. However, this approach is rather conservative.

It has been demonstrated that the CCGM shows similarities with fatigue testing in terms of crack growth rate, the author would like to demonstrate that the proposed model can be implemented in an existing commercially available fatigue model. To do so the direct cyclic (DC) model and virtual crack closing technique (VCCT) in Abaqus are used. The TDCB specimen were used for validation purposes of the creep crack growth method but can also be used in the Abaqus model. The creep crack growth model fitted to data from the RWDC tests is implemented in a TDCB FEM model. The idea is that the proposed model describes the creep crack growth rate as a function of the energy release rate, therefore changing the specimen geometry will change the energy release rate at the crack tip for a certain applied load but not the relationship described by the CCGM. The TDCB specimen is created in Abaqus as a simple 2D model with plane strain elements. The adhesive is represented by the VCCT row of paired nodes that release when the crack tip node pair reaches the fracture toughness. The model obtained from the RWD creep crack growth results is implemented in the DC module. The FEM results follow the results of the RWDC results because it follows the implemented CCGM (Figure 5-7).

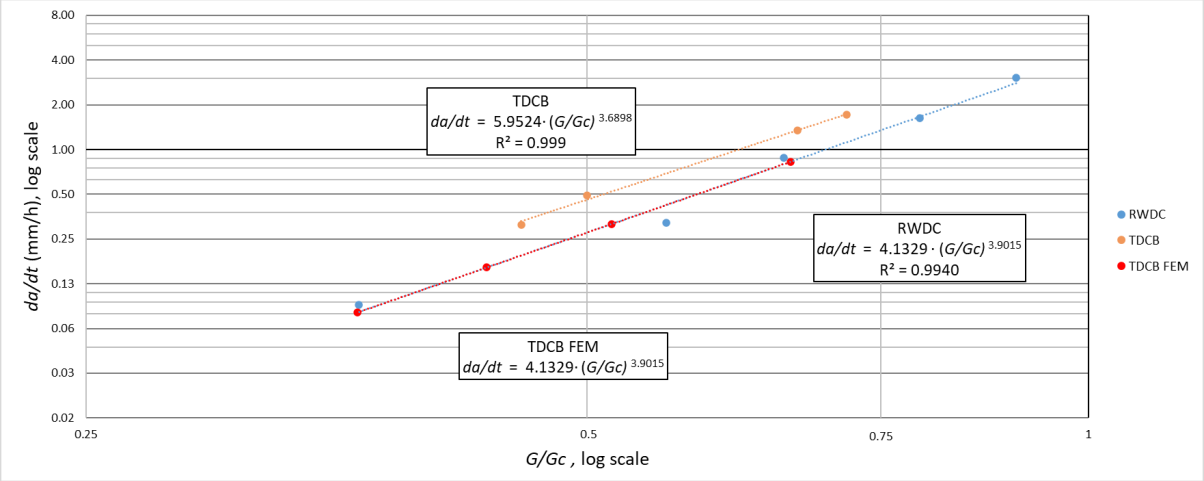

Figure 5-7. Creep crack growth rate against normalised energy release rate on a log-log scale with the data of the RWDC tests, constant load TDCB tests and the TDCB FEM model [96] *(Figure 12 in article of chapter 4)*.

In principle the DC module is designed for fatigue simulation and requires an amplitude change to have crack propagation in the FEM model. The CCGM uses the envelope of the energy release rate determined by the VCCT at the most open position of the specimen arms. Thus, the results are not affected by the cyclic movement of the arms. A user subroutine could be developed to make a module for creep crack growth simulation where the applied constant energy release rate drives the crack growth like in the CCGM instead of the ΔG as for fatigue simulation.

6. Concluding remarks

6.1. Conclusions

The work presented in this thesis contributes to the development of a new method to measure mode I creep crack growth in an adhesively bonded joint. The measurement is achieved by the design of roller wedge driven (RWD) test setup where a constant load can be applied to the wedge during the whole propagation phase. As a result, the energy release rate remains constant at the crack tip and creep crack growth curves can be easily obtained from the experimental results. Because besides a constant energy release rate, a moving roller wedge makes it possible to determine the creep crack growth rate directly from the displacement of the wedge. Since on average the crack length increase equals the wedge displacement, which can be easily measured with a Linear Variable Displacement Transducer (LVDT) connected to the wedge. It has been demonstrated that this assumption is correct for the tested specimens in this campaign.

The RWD manual test method is proposed to make a quick and affordable estimation of the fracture toughness of a specimen. The displacement rate is difficult to control with this method and can only be used with non-rate sensitive adhesives. However, this method is still useful for pre-cracking a specimen just prior initiation of the creep crack growth test and to obtain an estimation of the fracture toughness of the bonded joint.

The roller wedge reduces the friction between the wedge and the specimen significantly. Nevertheless, the results have shown that the friction coefficient is not low enough that it can be completely neglected in the data reduction method to determine the energy release rate. The friction needs to be reduced even further to be able to use the RWD test method to determine the energy release rate accurately.

The bonded joints in this work show a transitory phase at the initiation of the creep crack growth test. There seems to be relation between the duration of the transitory time and the energy release rate,

but the exact relationship cannot be determined with the current available test results. Likely it takes time to completely develop the zone in front of the crack tip before creep crack growth starts. Although a crazing zone in front of the crack tip is already formed during the quasi-static pre-cracking of the specimen. It is observed that the bonded joints have a complete cohesive failure mode for quasi-static test rates and then transitions to adhesive failure in the creep crack growth test. It seems that creep crack growth rate determines the ratio between cohesive and adhesive failure, because the lower the creep crack growth the higher the ratio of adhesive failure is observed. This behaviour could be different if, for instance, a different surface treatment is applied, because adhesive failure is influenced by the ability of the adhesive to bond to the adherend surface.

Some specimens were tested at low energy release rates but did not show clear crack propagation in the timeframe that they were tested. It is unclear if the specimens where still in the transitory phase before crack initiation or below the threshold energy release rate. Because of the duration of the creep crack growth test and the application of a specific constant energy release rate, the RWD creep crack growth (RWDC) test method is not optimal to find an exact value for threshold energy release rate. A test method like, the Boeing Wedge test, where the energy release rate decreases until there is crack arrest (equals the threshold energy release rate) is a better candidate. Although designing based on the threshold energy release rate is a conservative approach and likely results in over dimensioned bonded joints. Especially in the aeronautical industry the designs should be optimized to reduce the weight of the structure as much as possible.

The proposed creep crack growth model (CCGM) derived from the test results of the RWDC test results is validated against tapered double cantilever beam (TDCB) specimens of the same materials loaded with a constant weight. The results show that regardless of using a specimen with a different geometry and loading it in a different way, the TDCB results are similar as the RWDC results. Indicating that the CCGM can describe the creep crack growth rate in a general bonded joint. Comparing both methods,

the TDCB test method still requires visual crack growth measuring, a tensile test machine to pre-crack the specimens and the adherends have to be milled into a tapered geometry with specific dimensions.

It is demonstrated that the CCGM can be implemented in existing commercially available finite element models. The direct cyclic (DC) module in Abaqus is designed for fatigue simulating but since the CCGM is a Paris´ law-like expression it can be directly implemented. Taking a frequency of 1hz makes that da/dN can be interpreted as da/dt (in seconds). The opening and closing of the specimen in the simulation cannot be avoided in the DC module to have crack propagation but it is not affecting the crack behaviour of the virtual crack closure technique (VCCT), since the envelope of the energy release rate is used. As a result, the simulation produces the creep crack growth rate in the bonded joint as described by the implemented CCGM.

To sum up, the durability of bonded joints is an essential factor in various structures. A thorough comprehension of the processes involved in the propagation of cracks due to the creep mechanism is necessary to guarantee the reliability and safety of these structures. To accomplish this, there is a need to create creep crack growth testing methods and finite element models that can serve as resources for engineers to enhance the design of bonded joints.

6.2. Perspectives and future work

The work of this PhD project contributes to the development of methods and models for creep crack growth in bonded joints. Some limitations of the current methods/models and interesting topics for future work were identified during the PhD project. These will be addressed below:

- It was clear from the RWD quasi-static test results that even though the friction of the roller wedge is low, it cannot be completely ignored for the data reduction. Different type of adherend surfaces and roller combination could be tested to determine if the friction is

related to the specimen or the roller wedge itself. If the latter, it might be possible to obtain a general correction factor for the friction parameter in the data reduction.

- Optimizing the roller diameter relating to the specimen (adherend and adhesive type) could provide a larger testing range compared to the current roller and specimen configuration in this work. With a larger crack propagation range a more conservative approach could be used when determining the fracture toughness by only considering data points that are not close to the assumed crack initiation point. As a result, likely less spread in the test data will be measured and more accurate material properties can be obtained.
- In industry there is a growing demand for bonded joints with flexible adhesives. Likely the roller wedge diameter has to be increased significantly to accommodate the large elastic deformation of the adhesive before fracture occurs. The wedge can be provided with larger diameter rollers but in the data reduction method this should be considered, since the assumed simplified contact point between the roller and the adherend does not apply anymore and it influences the calculated corrected crack length.
- The number of specimens available to demonstrate the RWD manual test method was limited. For the tested specimens it was observed that the adhesive (Araldite 2021-1) is rate sensitive. With the RWD manual test method it is difficult to control and predetermine the wedge displacement rate and is therefore not suitable for rate sensitive adhesives. The test method deserves to be tested more extensively with non-rate sensitive adhesives to demonstrate it can be used to quickly determine the fracture toughness of a bonded joint in an affordable way.
- It was noted in the creep crack growth tests that there is a possible relationship between the duration of the transitory phase and the applied energy release rate. More testing is required to determine the exact relationship. It would also be interesting to test bonded joints with different types of adhesives to investigate if other types of adhesives also show a transitory phase like Araldite 2021-1.

- Likely the transitory phase is related to a time dependent mechanism in the fracture process zone (FPZ). In bonded joints the FPZ can be relatively large and therefore maybe takes more time to develop. More profound research could be done to better understand the role of the development of the FPZ in creep crack growth behaviour in adhesively bonded joints. The FPZ zone in creep crack growth tests as a function of the energy release rate deserves further investigation.
- Even though the RWD creep crack growth method is not suitable to find an exact threshold energy release rate it is still interesting to do longer tests at low energy release rate levels. In this work some specimens tested at low energy release rates did not show clear crack propagation, but the tests were stopped after a certain time period for practical reasons. Maybe the applied energy release rate was below the threshold, or the specimen was still in the transitory phase and crack propagation had not initiated yet. Doing some long term tests at low energy release rates would be interesting to obtain a more extensive creep crack growth model.
- It was demonstrated that an existing commercially available finite element model can be used to simulate creep crack growth in a bonded joint. However, the model is designed for fatigue and therefore the model needs an amplitude to propagate the crack, even though the energy release rate at the crack tip should propagate the crack in the specimen is constantly in an open loaded position like in a creep crack growth test. A modification of the existing fatigue model could be made in a user-subroutine to have a more realistic representation of the creep crack growth test.
- The next step would be to simulate and validate more complex bonded joints for creep crack growth. The proposed creep crack growth model was obtained for mode I testing of bonded joints. The same principle could be extended to characterise creep crack growth behaviour of bonded joints in mode II and mixed mode. Other test setups need to be developed to

introduce a constant energy release rate to the crack tip. However, before that step, relevant specimens for more complex bonded joints should be defined.

- As was described in the introduction, besides the factor time, it is known that adhesively bonded joints are negatively affected by humidity and elevated temperatures. The RWD test setup is relatively small and doesn´t need heavy weights to introduce a load to have crack growth. Therefore, the RWD creep crack growth method is suitable to be performed in a climate chamber where relative humidity and temperature can be controlled. This makes it possible to test bonded joints under different environmental conditions while being stressed similar to what a bonded joint in a structural element would experience during its service life.

References

[1] R. J. Good, “On the Definition of Adhesion,” *J Adhes*, vol. 8, no. 1, pp. 1–9, Jan. 1976, doi: 10.1080/00218467608075066.

[2] S. Ebnesajjad, *Adhesive Technology Handbook*, 2nd ed. Wiliam Andrew, 2008.

[3] L. F. M. Da Silva, A. Öchsner, and R. D. Adams, *Handbook of Adhesion Technology*, 2nd ed. Springer International Publishing AG, 2011. doi: 10.1007/978-3-642-01169-6.

[4] C. V. Katsiropoulos, A. N. Chamos, K. I. Tserpes, and S. G. Pantelakis, “Fracture toughness and shear behavior of composite bonded joints based on a novel aerospace adhesive,” *Compos B Eng*, vol. 43, no. 2, pp. 240–248, Mar. 2012, doi: 10.1016/j.compositesb.2011.07.010.

[5] 3M, “3M adhesives - bonded parts car.” https://www.3m.com/3M/en_US/collision-repair-us/featured-products/structural-adhesives/ (accessed Mar. 20, 2023).

[6] A. J. Kinloch, *Durability of structural adhesives*. Springer Netherlands, 1983.

[7] M. Costa, G. Viana, L. F. M. da Silva, and R. D. S. G. Campilho, “Effect of humidity on the mechanical properties of adhesively bonded aluminium joints,” *Proceedings of the Institution of Mechanical Engineers, Part L: Journal of Materials: Design and Applications*, vol. 232, no. 9, pp. 733–742, 2018, doi: 10.1177/1464420716645263.

[8] X. Zhao, X. Wang, Z. Wu, and Z. Zhu, “Fatigue behavior and failure mechanism of basalt FRP composites under long-term cyclic loads,” *Int J Fatigue*, vol. 88, pp. 58–67, Jul. 2016, doi: 10.1016/j.ijfatigue.2016.03.004.

[9] M. Nakada and Y. Miyano, “Accelerated testing for long-term fatigue strength of various FRP laminates for marine use,” *Compos Sci Technol*, vol. 69, no. 6, pp. 805–813, May 2009, doi: 10.1016/j.compscitech.2008.02.030.

[10] H. Mivehchi and A. Varvani-Farahani, “The effect of temperature on fatigue strength and cumulative fatigue damage of FRP composites,” *Procedia Eng*, vol. 2, no. 1, pp. 2011–2020, Apr. 2010, doi: 10.1016/j.proeng.2010.03.216.

[11] T. P. Philippidis and T. T. Assimakopoulou, “Strength degradation due to fatigue-induced matrix cracking in FRP composites: An acoustic emission predictive model,” *Compos Sci Technol*, vol. 68, no. 15–16, pp. 3272–3277, Dec. 2008, doi: 10.1016/j.compscitech.2008.08.020.

[12] S. Sarkani, G. Michaelov, D. P. Kihl, and D. L. Bonanni, “Comparative Study of Nonlinear Damage Accumulation Models in Stochastic Fatigue of FRP Laminates,” *Journal of Structural Engineering*, vol. 127, no. 3, pp. 314–322, Mar. 2001, doi: 10.1061/(ASCE)0733-9445(2001)127:3(314).

[13] A. Pirondi and G. Nicoletto, “Fatigue crack growth in bonded DCB specimens,” *Eng Fract Mech*, vol. 71, no. 4–6, pp. 859–871, 2004, doi: 10.1016/S0013-7944(03)00046-8.

[14] A. A. M. A. Campos, A. M. P. De Jesus, J. A. F. O. Correia, and J. J. L. Morais, “Fatigue Crack Growth Behavior of Bonded Aluminum Joints,” in *Procedia Engineering*, Elsevier Ltd, 2016, pp. 270–277. doi: 10.1016/j.proeng.2016.08.890.

[15] I. A. Ashcroft and S. J. Shaw, “Mode I fracture of epoxy bonded composite joints 2. Fatigue loading,” *Int J Adhes Adhes*, vol. 22, no. 2, pp. 151–167, Jan. 2002, doi: 10.1016/S0143-7496(01)00050-1.

[16] G. M. Silva de Oliveira Viana, “Development of a Cohesive Zone Model for Adhesive Joints that Includes Environment Degradation,” 2018.

[17] W. Conshohocken, “Standard Test Method Practice for Effect of Moisture and Temperature on Adhesive Bonds 1,” *Test*, vol. 90, no. Reapproved, pp. 1–3, 1995, doi: 10.1520/D1151-00R13.2.

[18] ASTM, “ASTM D1183-03(2019) - Standard Practices for Resistance of Adhesives to Cyclic Laboratory Aging Conditions.” ASTM International, 2019. doi: 10.1520/D1183-03R19.

[19] J. Manterola, J. Zurbitu, J. Renart, A. Turon, and I. Urresti, “Durability study of flexible bonded joints under stress,” *Polym Test*, vol. 88, no. April, p. 106570, 2020, [Online]. Available: https://doi.org/10.1016/j.polymertesting.2020.106570

[20] W. Broughton, *Adhesives in Marine Engineering*, First edit. Woodhead publishing, 2012, pp. 99–154. doi: 10.1533/9780857096159.2.99.

[21] J. Cognard *et al.*, “Testing Adhesive Joints: Best Practices,” in *Testing Adhesive Joints: Best Practices*, D. Silva, Dillard, Blackman, and Adams, Eds., First.Wiley-VCH Verlag GmbH & Co. KGaA, 2012.

[22] J. Bijen, *Durability of engineering structures*. 2003. doi: 10.1533/9781855738560.

[23] R. D. Adams, J. W. Cowap, G. Farquharson, G. M. Margary, and D. Vaughn, “The relative merits of the Boeing wedge test and the double cantilever beam test for assessing the durability of adhesively bonded joints, with particular reference to the use of fracture mechanics,” *Int J Adhes Adhes*, vol. 29, no. 6, pp. 609–620, 2009, doi: 10.1016/j.ijadhadh.2009.02.010.

[24] S. Abdel-Monsef, J. Renart, L. Carreras, P. Maimí, and A. Turon, “Effect of environmental conditioning on pure mode I fracture behaviour of adhesively bonded joints,” *Theoretical and Applied Fracture Mechanics*, vol. 110, p. 102826, 2020, doi: 10.1016/j.tafmec.2020.102826.

[25] D. A. Ashcroft and D. Briskham, “Designing adhesive joints for fatigue and creep load conditions,” *Advances in Structural Adhesive Bonding*, pp. 469–515, 2010, doi: 10.1533/9781845698058.4.469.

[26] N. I. Malinin, “Creep of polymer materials in structural elements,” *Journal of Applied Mechanics and Technical Physics*, vol. 11, pp. 294–309, 1970, doi: 10.1007/BF00908111.

[27] G. Jhin, S. Azari, A. Ameli, N. V. Datla, M. Papini, and J. K. Spelt, “Crack growth rate and crack path in adhesively bonded joints: Comparison of creep, fatigue and fracture,” *Int J Adhes Adhes*, vol. 46, pp. 74–84, Oct. 2013, doi: 10.1016/j.ijadhadh.2013.05.009.

[28] W. Bradley, W. J. Cantwell, and H. H. Kausch, “Viscoelastic Creep Crack Growth: A Review of Fracture Mechanical Analyses,” *Mechanics Time-Dependent Materials*, vol. 1, no. 3, pp. 241–268, 1997, doi: 10.1023/A:1009766516429.

[29] M. L. Cerrada, “Introduction to the Viscoelastic Response in Polymers,” *Thermal Analysis. Fundamentals and Applications to Material Characterization*, pp. 167–182, 2005, [Online]. Available: https://ruc.udc.es/dspace/handle/2183/11487

[30] N. F. Mott, “LXXVIII. A theory of work-hardening of metals II: Flow without slip-lines, recovery and creep,” *The London, Edinburgh, and Dublin Philosophical Magazine and Journal of Science*, vol. 44, no. 354, pp. 742–765, Jul. 1953, doi: 10.1080/14786440708521052.

[31] M. E. Kassner and T. A. Hayes, “Creep cavitation in metals,” *Int J Plast*, vol. 19, no. 10, pp. 1715–1748, Oct. 2003, doi: 10.1016/S0749-6419(02)00111-0.

[32] X. Han *et al.*, “Improved creep resistance of high entropy transition metal carbides,” *J Eur Ceram Soc*, vol. 40, no. 7, pp. 2709–2715, Jul. 2020, doi: 10.1016/j.jeurceramsoc.2019.12.036.

[33] T. Matsunaga, T. Kameyama, S. Ueda, and E. Sato, “Grain boundary sliding during ambient-temperature creep in hexagonal close-packed metals,” *Philosophical Magazine*, vol. 90, no. 30, pp. 4041–4054, Oct. 2010, doi: 10.1080/14786435.2010.502883.

[34] R. A. Queiroz, E. M. Sampaio, V. J. Cortines, and N. R. Rohem, “Study on the creep behavior of bonded metallic joints,” *Applied Adhesion Science*, vol. 2, no. 1, pp. 1–12, 2014, doi: 10.1186/2196-4351-2-8.

[35] C. de Zeeuw *et al.*, “Creep behaviour of steel bonded joints under hygrothermal conditions,” *Int J Adhes Adhes*, vol. 91, no. February, pp. 54–63, 2019, doi: 10.1016/j.ijadhadh.2019.03.002.

[36] W. Luo, C. Wang, R. Zhao, X. Tang, and Y. Tomita, “Creep behavior of poly(methyl methacrylate) with growing damage,” *Materials Science and Engineering A*, vol. 483–484, no. 1-2 C, pp. 580–582, 2008, doi: 10.1016/j.msea.2006.07.176.

[37] Z. Gao, W. Liu, Q. H. Li, and Z. F. Yue, “Creep life assessment craze damage evolution of polyethylene methacrylate,” *Advances in Polymer Technology*, vol. 37, no. 8, pp. 3619–3628, 2018, doi: 10.1002/adv.22146.

[38] P. Schrader, C. Schmandt, and S. Marzi, “Mode I creep fracture of rubber-like adhesive joints at constant crack driving force,” *Int J Adhes Adhes*, vol. 113, Mar. 2022, doi: 10.1016/j.ijadhadh.2021.103079.

[39] Y. Saito, M. Yoda, and S. Imamura, “Creep crack growth in polypropylene film with various crack lengths at diverse stresses and temperatures,” *Int J Fract*, vol. 143, no. 1, pp. 113–118, 2007, doi: 10.1007/s10704-006-9046-1.

[40] ASTM D5528-01, “Standard test method for mode I interlaminar fracture toughness of unidirectional fiber-reinforced polymer matrix composites,” *American Standard of Testing Methods*, vol. 03, no. Reapproved 2007, pp. 1–12, 2014, doi: 10.1520/D5528-13.2.

[41] “ISO 25217:2009 - Adhesives — Determination of the mode 1 adhesive fracture energy of structural adhesive joints using double cantilever beam and tapered double cantilever beam specimens.” p. 24, 2009.

[42] A. J. Paris and P. C. Paris, “Instantaneous evaluation of J and C,” *Int J Fract*, vol. 38, no. 1, pp. 19–21, 1988, doi: 10.1007/BF00034281.

[43] J. Manterola, J. Renart, J. Zurbitu, A. Turon, and I. Urresti, “Mode I fracture characterization of rigid and flexible bonded joints using an advanced Wedge Driven Test,” *Mechanics of Materials*, vol. 148, no. 103534, pp. 1–26, 2020, doi: 10.1016/j.mechmat.2020.103534.

[44] N. Brown, D. Adams, and L. Devries, “Test method development for environmental durability of bonded composite joints.” The University of Utah, p. 30, 2013.

[45] D. A. Dillard, D. J. Pohlit, G. C. Jacob, J. M. Starbuck, and R. K. Kapania, “On the use of a driven wedge test to acquire dynamic fracture energies of bonded beam specimens,” *Journal of Adhesion*, vol. 87, no. 4, pp. 395–423, 2011, doi: 10.1080/00218464.2011.562125.

[46] J. Renart, J. Costa, G. Santacruz, S. Lazcano, and E. Gonzalez, “Measuring fracture energy of interfaces under mode I loading with the wedge driven test.,” *Eng Fract Mech*, no. 239, p. 15, 2020, doi: 10.1016/j.engfracmech.2020.107210.

[47] A. L. Glessner, M. T. Takemori, M. A. Vallance, and S. K. Gifford, “Mode I interlaminar fracture toughness of ud cf composites using a novel wedge-driven delamination design,” *Composite Materials: Fatigue and Fracture*, vol. 2, pp. 181–200, 1989, doi: 10.1520/STP10416S.

[48] R. Mansour, M. Kannan, G. N. Morscher, F. Abdi, C. Godines, and S. Dormohammadi, “The wedge-loaded double cantilever beam test: A friction based method for measuring

interlaminar fracutre properties in ceramic matrix composites," in *Advances in High Temperature Ceramic Matrix Composites and Materials for Sustainable Development*, M. Singh, T. Ohji, S. Dong, D. Koch, K. Shimamura, B. Clauss, B. Heidenreich, and J. Akedo, Eds., First edit.2017, pp. 273–282. doi: 10.1002/9781119407270.

[49] D. Adams, H. McCartin, and Z. Sievert, "Development of Environmental Durability Test Methods for Composite Bonded Joints," *JAMS 2018 Technical Review*. The Univeristy of Utah, p. 31, 2018.

[50] "ASTM D3762-03(2010) Standard Test Method for Adhesive-Bonded Surface Durability of Aluminum (Wedge Test) (Withdrawn 2019)." ASTM International, p. 5, 2010. [Online]. Available: https://www.astm.org/Standards/D3762.htm

[51] D. O. Adams, K. L. DeVries, and C. Child, "Durability of adhesively bonded joints for aircraft structures," *FAA Joint Advanced Materials and Structures (JAMS) Center of Excellence Technical Review Meeting*, p. 22, 2012, [Online]. Available: http://depts.washington.edu/amtas/events/jams_12/papers/paper-adams_adhesive.pdf

[52] D. Plausinis and J. K. Spelt, "Designing for time-dependent crack growth in adhesive joints," *Int J Adhes Adhes*, vol. 15, no. 3, pp. 143–154, 1995, doi: 10.1016/0143-7496(95)91625-G.

[53] D. Plausinis and J. K. Spelt, "Application of a new constant G load-jig to creep crack growth in adhesive joints," *Int J Adhes Adhes*, vol. 15, no. 4, pp. 225–232, 1995, doi: 10.1016/0143-7496(96)83703-1.

[54] D. A. Dillard, J. Z. Wang, and H. Parvatareddy, "A simple constant strain energy release rate loading method for double cantilever beam specimens," *J Adhes*, vol. 41, no. 1–4, pp. 35–50, Jun. 1993, doi: 10.1080/00218469308026553.

[55] D. R. Lefebvre, D. A. Dillard, and H. F. Brinson, “The development of a modified double-cantilever-beam specimen for measuring the fracture energy of rubber to metal bonds,” *Exp Mech*, vol. 28, no. 1, pp. 38–44, Mar. 1988, doi: 10.1007/BF02328994.

[56] K. Nakamura, Y. Sekiguchi, K. Shimamoto, K. Houjou, H. Akiyama, and C. Sato, “Creep Crack Growth Behavior during Hot Water Immersion of an Epoxy Adhesive Using a Spring-Loaded Double Cantilever Beam Test Method,” *Materials*, vol. 16, no. 2, Jan. 2023, doi: 10.3390/ma16020607.

[57] B. F. Sørensen, K. Jørgensen, T. K. Jacobsen, and R. C. Østergaard, “DCB-specimen loaded with uneven bending moments,” *Int J Fract*, vol. 141, no. 1–2, pp. 163–176, 2006, doi: 10.1007/s10704-006-0071-x.

[58] E. Lindgaard and B. L. V. Bak, “Experimental characterization of delamination in off-axis GFRP laminates during mode I loading,” *Compos Struct*, vol. 220, pp. 953–960, Jul. 2019, doi: 10.1016/j.compstruct.2019.04.022.

[59] B. R. K. Blackman, H. Hadavinia, A. J. Kinloch, M. Paraschi, and J. G. Williams, “The calculation of adhesive fracture energies in mode I: revisiting the tapered double cantilever beam (TDCB) test,” *Eng Fract Mech*, vol. 70, no. 2, pp. 233–248, Jan. 2003, doi: 10.1016/S0013-7944(02)00031-0.

[60] B. R. K. Blackman, A. J. Kinloch, M. Paraschi, and W. S. Teo, “Measuring the mode I adhesive fracture energy, GIc, of structural adhesive joints: The results of an international round-robin,” *Int J Adhes Adhes*, vol. 23, no. 4, pp. 293–305, 2003, doi: 10.1016/S0143-7496(03)00047-2.

[61] B. R. K. Blackman, A. J. Kinloch, F. S. Rodriguez Sanchez, W. S. Teo, and J. G. Williams, “The fracture behaviour of structural adhesives under high rates of testing,” *Eng Fract*

Mech, vol. 76, no. 18, pp. 2868–2889, Dec. 2009, doi: 10.1016/j.engfracmech.2009.07.013.

[62] O. Hesebeck, U. Meyer, A. Sondag, and M. Brede, "Investigations on the energy balance in TDCB tests," *Int J Adhes Adhes*, vol. 67, pp. 94–102, Jun. 2016, doi: 10.1016/j.ijadhadh.2015.12.031.

[63] P. Qiao, J. Wang, and J. F. Davalos, "Tapered beam on elastic foundation model for compliance rate change of TDCB specimen," *Eng Fract Mech*, vol. 70, no. 2, pp. 339–353, Jan. 2003, doi: 10.1016/S0013-7944(02)00023-1.

[64] W. L. Tsang, "The use of tapered double cantilever beam (TDCB) in investigating fracture properties of particles modified epoxy," *SN Appl Sci*, vol. 2, no. 4, Apr. 2020, doi: 10.1007/s42452-020-2487-8.

[65] J. M. D. Teixeira, R. D. S. G. Campilho, and F. J. G. da Silva, "Numerical assessment of the Double-Cantilever Beam and Tapered Double-Cantilever Beam tests for the GIC determination of adhesive layers," *Journal of Adhesion*, vol. 94, no. 11, pp. 951–973, Sep. 2018, doi: 10.1080/00218464.2017.1383905.

[66] S. Marzi, A. Biel, and U. Stigh, "On experimental methods to investigate the effect of layer thickness on the fracture behavior of adhesively bonded joints," *Int J Adhes Adhes*, vol. 31, no. 8, pp. 840–850, Dec. 2011, doi: 10.1016/j.ijadhadh.2011.08.004.

[67] M. A. S. Sadigh, B. Paygozar, L. F. M. da Silva, and F. V. Tahami, "Creep deformation simulation of adhesively bonded joints at different temperature levels using a modified power-law model," *Polym Test*, vol. 79, Oct. 2019, doi: 10.1016/j.polymertesting.2019.106087.

[68] P. Perzyna, "Thermodynamic Theory of Viscoplasticity," 1971, pp. 313–354. doi: 10.1016/S0065-2156(08)70345-4.

[69] A. Corigliano and M. Ricci, “Rate-dependent interface models: formulation and numerical applications,” *Int J Solids Struct*, vol. 38, no. 4, pp. 547–576, Jan. 2001, doi: 10.1016/S0020-7683(00)00088-3.

[70] G. Giambanco and G. Fileccia Scimemi, “Mixed mode failure analysis of bonded joints with rate-dependent interface models,” *Int J Numer Methods Eng*, vol. 67, no. 8, pp. 1160–1192, Aug. 2006, doi: 10.1002/nme.1671.

[71] H. Khoramishad, A. D. Crocombe, K. B. Katnam, and I. A. Ashcroft, “Predicting fatigue damage in adhesively bonded joints using a cohesive zone model,” *Int J Fatigue*, vol. 32, no. 7, pp. 1146–1158, Jul. 2010, doi: 10.1016/j.ijfatigue.2009.12.013.

[72] G. Marannano, A. Pasta, and A. Giallanza, “A model for predicting the mixed-mode fatigue crack growth in a bonded joint,” *Fatigue Fract Eng Mater Struct*, vol. 37, no. 4, pp. 380–390, Apr. 2014, doi: 10.1111/ffe.12121.

[73] H. Khoramishad, A. D. Crocombe, K. B. Katnam, and I. A. Ashcroft, “Predicting fatigue damage in adhesively bonded joints using a cohesive zone model,” *Int J Fatigue*, vol. 32, no. 7, pp. 1146–1158, Jul. 2010, doi: 10.1016/j.ijfatigue.2009.12.013.

[74] A. Pirondi and F. Moroni, “Simulating fatigue failure in bonded composite joints using a modified cohesive zone model,” in *Composite Joints and Connections*, Elsevier, 2011, pp. 363–398. doi: 10.1533/9780857094926.2.363.

[75] M. F. S. F. de Moura and J. P. M. Gonçalves, “Cohesive zone model for high-cycle fatigue of adhesively bonded joints under mode I loading,” *Int J Solids Struct*, vol. 51, no. 5, pp. 1123–1131, Mar. 2014, doi: 10.1016/j.ijsolstr.2013.12.009.

[76] P. Paris and F. Erdogan, “A critical analysis of crack propagation laws,” *Journal of Fluids Engineering, Transactions of the ASME*, vol. 85, no. 4, pp. 528–533, 1963, doi: 10.1115/1.3656900.

[77] G. Jhin, S. Azari, A. Ameli, N. V. Datla, M. Papini, and J. K. Spelt, “Crack growth rate and crack path in adhesively bonded joints: Comparison of creep, fatigue and fracture,” *Int J Adhes Adhes*, vol. 46, pp. 74–84, Oct. 2013, doi: 10.1016/j.ijadhadh.2013.05.009.

[78] L. M. Martulli and A. Bernasconi, “An efficient and versatile use of the VCCT for composites delamination growth under fatigue loadings in 3D numerical analysis: The sequential static fatigue algorithm,” *Int J Fatigue*, p. 107493, Dec. 2022, doi: 10.1016/j.ijfatigue.2022.107493.

[79] A. Turon, J. Costa, P. P. Camanho, and C. G. Dávila, “Simulation of delamination in composites under high-cycle fatigue,” *Compos Part A Appl Sci Manuf*, vol. 38, no. 11, pp. 2270–2282, Nov. 2007, doi: 10.1016/j.compositesa.2006.11.009.

[80] L. Carreras *et al.*, “A simulation method for fatigue-driven delamination in layered structures involving non-negligible fracture process zones and arbitrarily shaped crack fronts,” *Compos Part A Appl Sci Manuf*, vol. 122, pp. 107–119, Jul. 2019, doi: 10.1016/j.compositesa.2019.04.026.

[81] “Abaqus Analysis User’s Manual.” Dassault Systemes Simulia, Inc, 2014.

[82] R. Krueger, “The virtual crack closure technique for modeling interlaminar failure and delamination in advanced composite materials,” in *Numerical Modelling of Failure in Advanced Composite Materials*, Elsevier, 2015, pp. 3–53. doi: 10.1016/B978-0-08-100332-9.00001-3.

[83] R. Krueger, “An Approach to Assess Delamination Propagation Simulation Capabilities in Commercial Finite Element Codes,” 2008. Accessed: Feb. 15, 2023. [Online]. Available: https://ntrs.nasa.gov/citations/20080015439

[84] R. Krueger, “Virtual crack closure technique: History, approach, and applications,” *Appl Mech Rev*, vol. 57, no. 1–6, pp. 109–143, Jan. 2004, doi: 10.1115/1.1595677.

[85] A. Pirondi, G. Giuliese, F. Moroni, A. Bernasconi, and A. Jamil, “Comparative Study of Cohesive Zone and Virtual Crack Closure Techniques for Three-Dimensional Fatigue Debonding,” *J Adhes*, vol. 90, no. 5–6, pp. 457–481, Jun. 2014, doi: 10.1080/00218464.2013.859616.

[86] C. G. Dávila and C. Bisagni, “Fatigue life and damage tolerance of postbuckled composite stiffened structures with initial delamination,” *Compos Struct*, vol. 161, pp. 73–84, Feb. 2017, doi: 10.1016/j.compstruct.2016.11.033.

[87] F. Teimouri, M. Heidari-Rarani, and F. Haji Aboutalebi, “An XFEM-VCCT coupled approach for modeling mode I fatigue delamination in composite laminates under high cycle loading,” *Eng Fract Mech*, vol. 249, p. 107760, May 2021, doi: 10.1016/j.engfracmech.2021.107760.

[88] J. Manterola Najera, J. Zurbitu Gonzalez, M. J. Cabello Ulloa, I. Urresti Ugarteburu, J. Renart Canalias, and A. Turon Travesa, “Procedimiento y aparato para la determinación de la tasa de liberacion de energia de una probeta,” 300352094, 2020

[89] JTEKT, “Frictional coefficient (Basic Bearing Knowledge),” 2023. https://koyo.jtekt.co.jp/en/support/bearing-knowledge/8-4000.html#:~:text=For%20plain%20bearings%2C%20the%20value,it%20is%200.1%20to%200.2. (accessed Mar. 27, 2023).

[90] E. J. Kramer and L. L. Berger, “Fundamental processes of craze growth and fracture,” in *Crazing in Polymers Vol. 2*, Berlin, Heidelberg: Springer Berlin Heidelberg, 1990, pp. 1–68. doi: 10.1007/BFb0018018.

[91] M. G. A. Tijssens, E. van der Giessen, and L. J. Sluys, “Simulation of mode I crack growth in polymers by crazing,” *Int J Solids Struct*, vol. 37, no. 48–50, pp. 7307–7327, Nov. 2000, doi: 10.1016/S0020-7683(00)00200-6.

[92] M. Konstantakopoulou, A. Deligianni, and G. Kotsikos, “Failure of dissimilar material bonded joints,” *Physical Sciences Reviews*, vol. 1, no. 3. De Gruyter, 2019. doi: 10.1515/psr-2015-0013.

[93] G. H. Michler and F. J. Baltá-Calleja, *Mechanical properties of polymers based on nanostructure and morphology*. 2005. doi: 10.1201/9781420027136.

[94] S. Lampman, *Characterization and Failure Analysis of Plastics*. ASM International, 2003.

[95] E. Meulman, J. Renart, L. Carreras, and J. Zurbitu, “A methodology for the experimental characterization of energy release rate-controlled creep crack growth under mode I loading,” *Eng Fract Mech*, vol. 283, no. 109222, Apr. 2023, doi: 10.1016/j.engfracmech.2023.109222.

[96] E. Meulman, J. Renart, L. Carreras, and J. Zurbitu, “Analysis of creep crack growth in bonded joints based on a Paris’ law-like approach (submitted for revision),” 2023.

[97] L. Carreras, B. L. V. Bak, S. M. Jensen, C. Lequesne, H. Xiong, and E. Lindgaard, “Benchmark test for mode I fatigue-driven delamination in GFRP composite laminates: Experimental results and simulation with the inter-laminar damage model implemented in SAMCEF,” *Compos B Eng*, vol. 253, p. 110529, Mar. 2023, doi: 10.1016/j.compositesb.2023.110529.